Aula 3

Identificação de Argilominerais por Difração de Raios X (DRX)

PMT 5846 – Ciência e Tecnologia de Argilas

Prof. Antonio Carlos Vieira Coelho

Departamento de Engenharia Metalúrgica e de Materiais

EPUSP - 2020

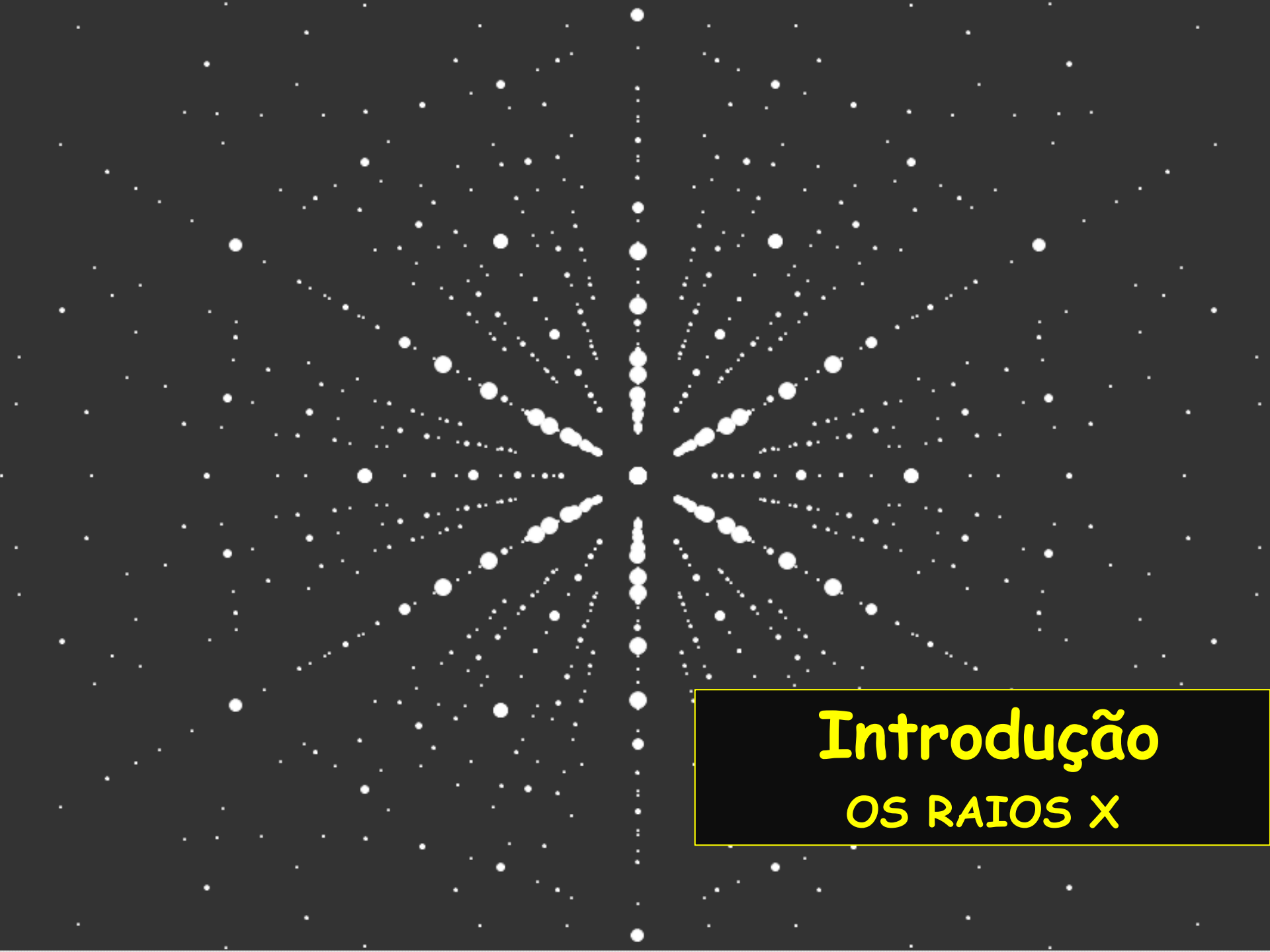

Introdução

OS RAIOS X

O Espectro Eletromagnético

Os raios X são radiações eletromagnéticas similares à luz, porém com um comprimento de onda muito menor

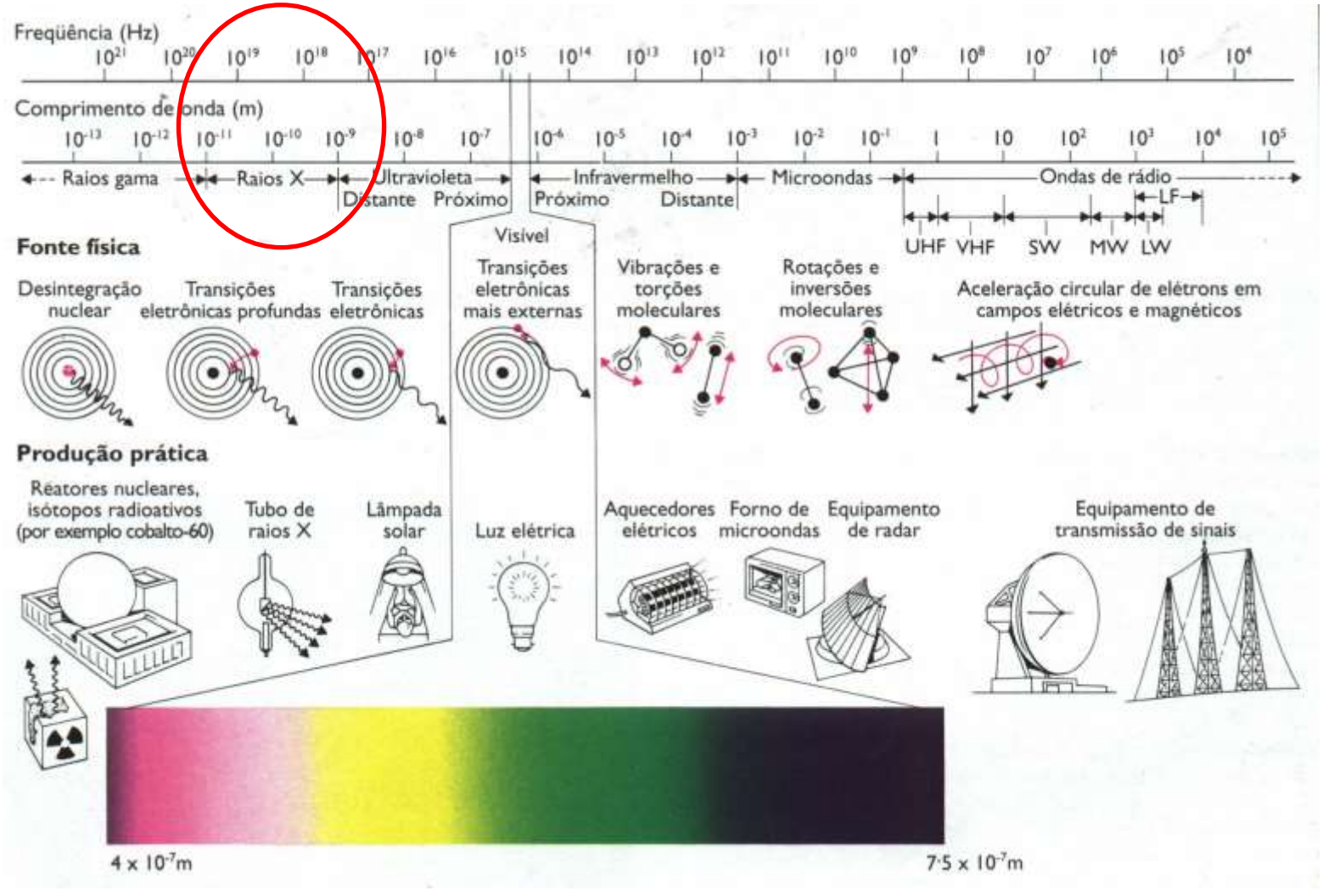

Um pouco de História... Os raios X

Rœntgen

- Wilhelm Conrad Röntgen (1845-1923) discovered X-rays on November 8, 1895, at the University of Wurzburg in Germany. X-rays are still called Röntgenstrahlen in Europe.
- Röntgen used electrons to bombard inert gas in tubes, and discovered that nearby photographic plates had been exposed by some sort of unknown ("X") radiation.
- He demonstrated that X-rays travel in straight lines and are very penetrative, traversing all materials to varying degrees.
- He received the first Nobel Prize in Physics in 1901 for his discovery, donating the prize money (then about $40,000) to the University of Wurzburg.

W. Rontgen and his first X-ray photograph of a human shows the hand of his wife with the ring she was wearing.

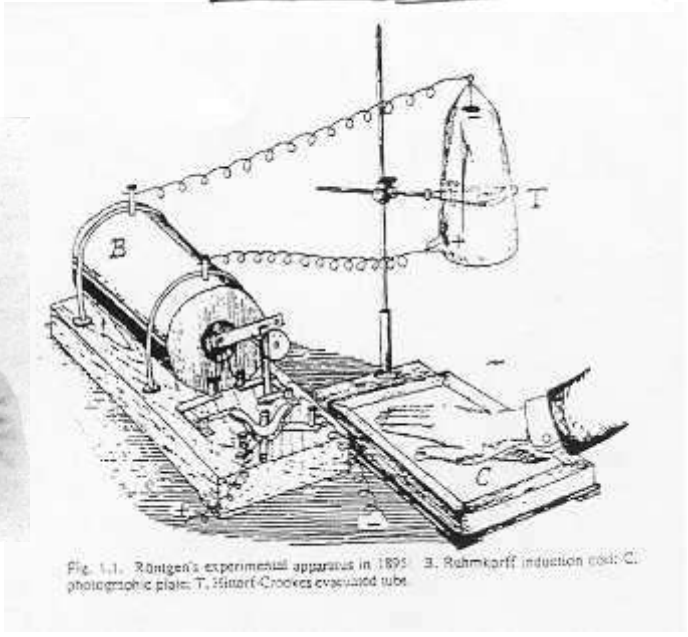

Fig. 1.1. Röntgen's experimental apparatus in 1895. B, Ruhmkorff induction coil; C, photographic plate; T, Hittorf-Crookes evacuated tube.

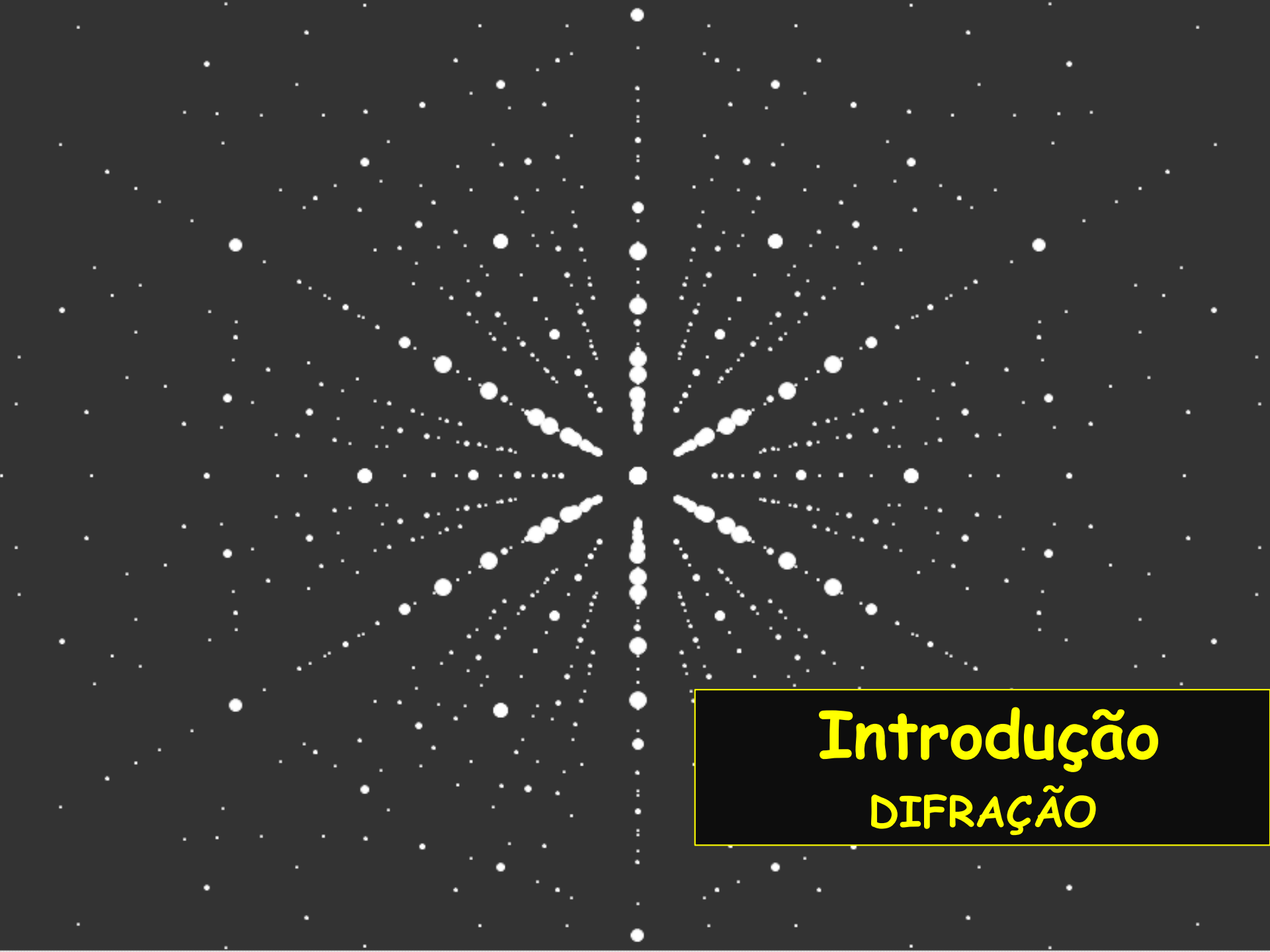

Introdução

DIFRAÇÃO

Difração

- Passagem de ondas pela borda de uma barreira ou através de uma ou mais aberturas que provoca, em geral, um alargamento do comprimento de onda e interferência das frentes de onda, que criam regiões de maior ou menor intensidade.
  - As ondas podem ser eletromagnéticas, de som ou aquelas associadas a partículas atômicas e subatômicas, e a barreira pode ser formada por fendas ópticas ou mesmo átomos numa rede cristalina.

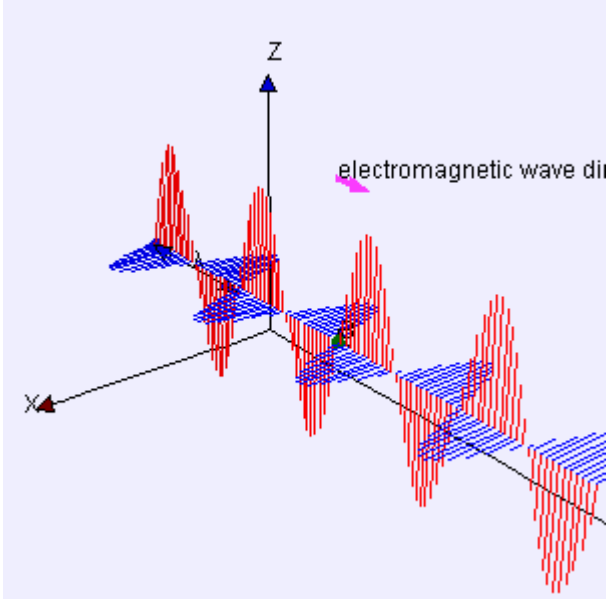

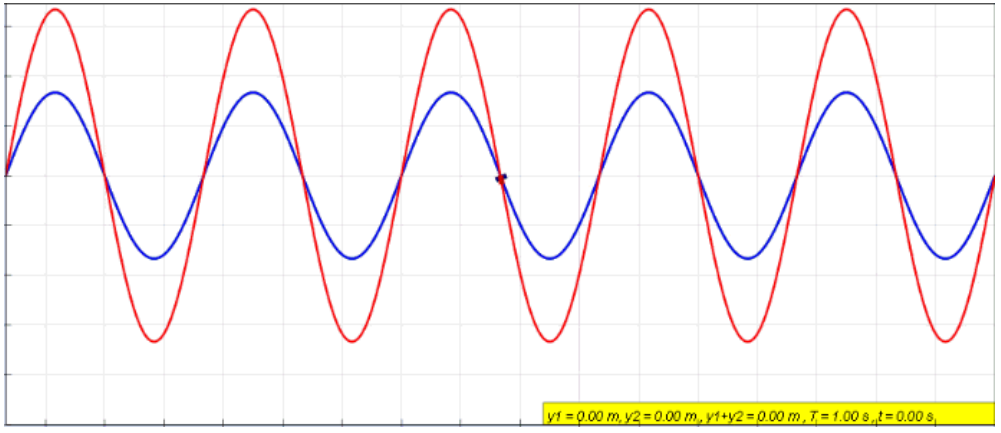

Interferências de Ondas: Construtiva e Destrutiva

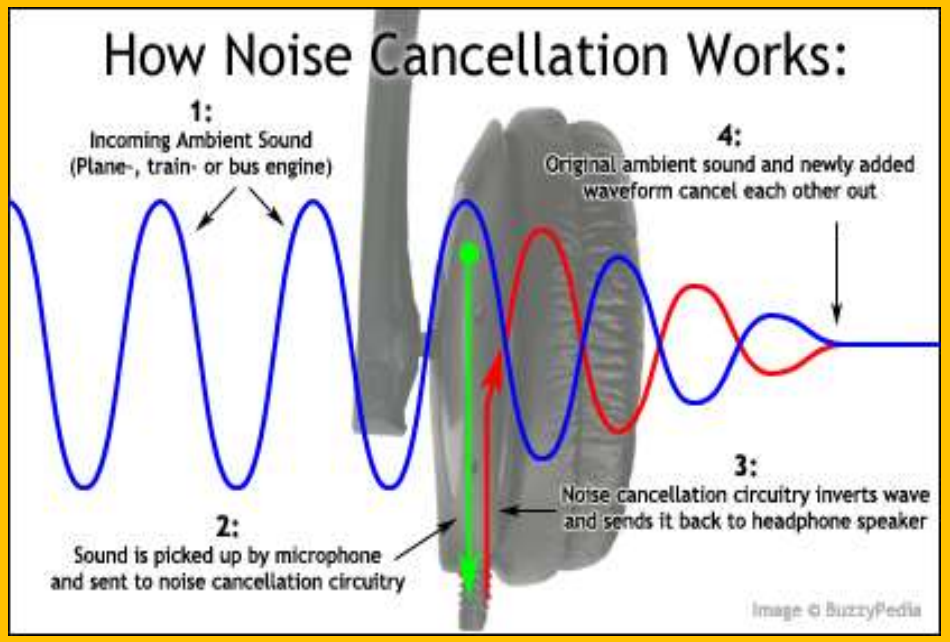

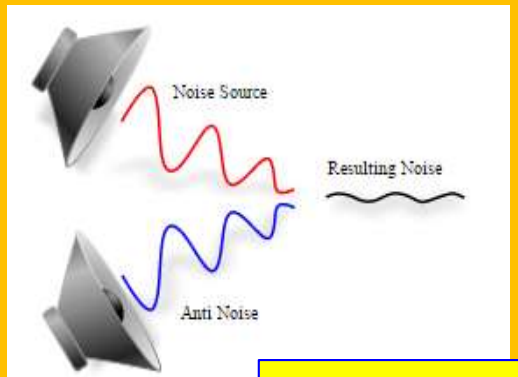

Interferência Destrutiva

*...nos sites abaixo, você **ouvir** interferências de onda...*

http://www.szynalski.com/tone-generator

https://www.youtube.com/watch?v=V8W4Djz6jnY

...difração de raios X... Max von Laue

- German physicist Max von Laue (1879 – 1960) won the Nobel Prize in 1914, for his work measuring the wavelength of x-rays by their diffraction through the atoms of a crystal.
- This discovery originated when he was discussing problems related to the passage of waves of light through a periodic, crystalline arrangement of particles. The idea then came to him that the much shorter electromagnetic rays, which X-rays were supposed to be, would cause in such a medium some kind of diffraction or interference phenomena and that a crystal would provide such a medium.
- Although his colleagues Sommerfeld, W. Wien and others raised objections to the idea, W. Friedrich, one of Sommerfeld's assistants and P. Knipping tested it out experimentally and, after some failures, succeeded in proving it to be correct.
- Von Laue worked out the mathematical formulation of it and the discovery was published in 1912. It established the fact that X-rays are electromagnetic in nature and it opened the way to the later work of Sir William and Sir Lawrence Bragg. Subsequently von Laue made other contributions to this subject .

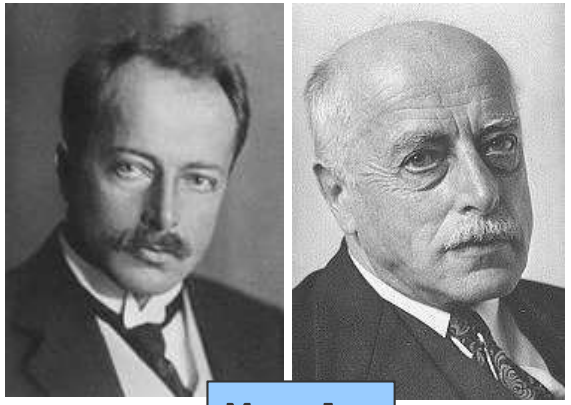

Max von Laue

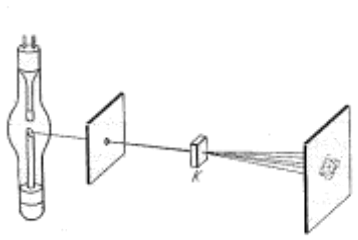

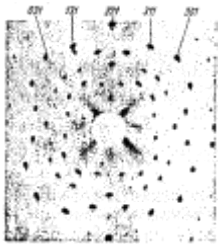

...difração de raios X... Max von Laue

- As the Nazis came to power in Germany, von Laue openly criticized the governmental stance against "Jewish physics" (i.e., Einstein), and remained in contact with otherwise-isolated Jewish colleagues. During World War II he refused to work on the Nazi program to develop nuclear weapons, and instead wrote a respected book on the history of physics.
- Still, as one of the leading physicists in Germany, he was among the scientists taken into custody after the war and was imprisoned for almost a year at Farm Hill in England. During his incarceration he wrote a paper on the absorption of X-rays.
- He was an early and enthusiastic adapter of the automobile and had a reputation for driving at fast speeds. He was seriously injured in a collision with a motorcycle in Berlin on 7 April 1960 in which the cyclist was killed, and von Laue died of his injuries about two weeks later.

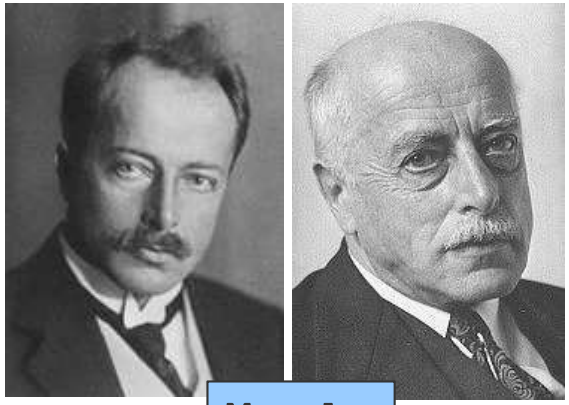

Max von Laue

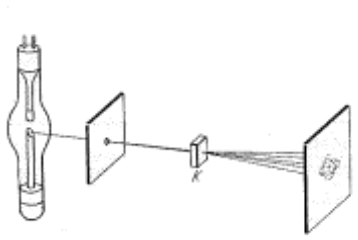

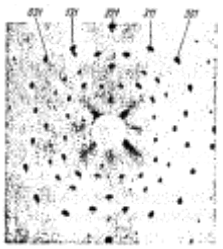

...difração de raios X... os Bragg

- In 1913, William Lawrence Bragg (1890-1971) observed the first X-ray spectrum, examining the L lines produced from platinum using an NaCl crystal.
- W.L. Bragg confirmed that X-rays produced ionization and also could be diffracted by a regular crystal: the wave-particle duality.
- The older Bragg – William Henry Bragg (1862-1942) – developed developed an X-ray detector that when coupled with the younger Bragg's diffracting crystal is the basis of all X-ray spectrometry.
- The Braggs received the Nobel Prize in 1915 for their work.

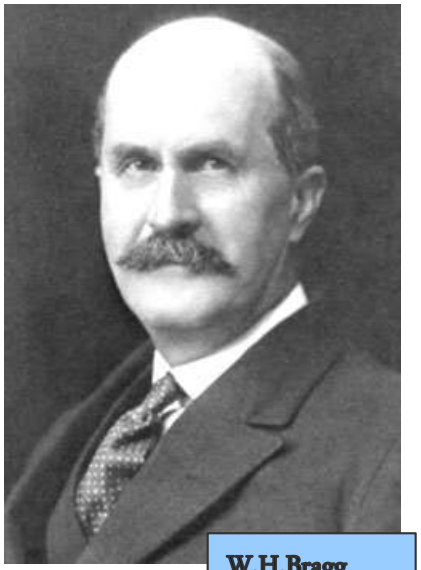
W.H.Bragg


W.L.Bragg

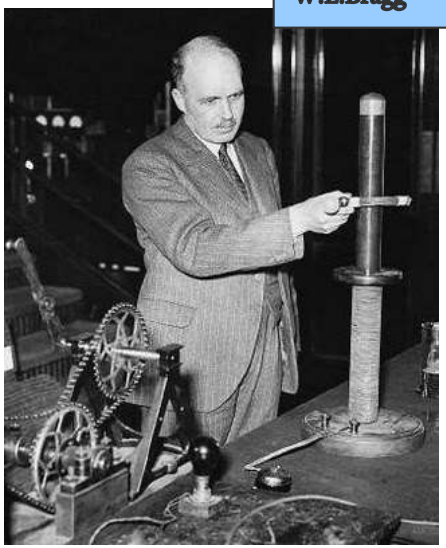

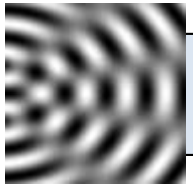

Difração – Cristais !

Diffraction occurs when light is scattered by a periodic array with long-range order, producing constructive interference at specific angles.

- The atoms in a crystal are arranged in a periodic array and thus can diffract light.
- The wavelength of X rays are similar to the distance between atoms.
- **The scattering of X-rays from atoms produces a diffraction pattern, which contains information about the atomic arrangement within the crystal**

- Amorphous materials like glass do not have a periodic array with long-range order, so they do not produce a diffraction pattern

The diffraction pattern is a product of the unique crystal structure of a material

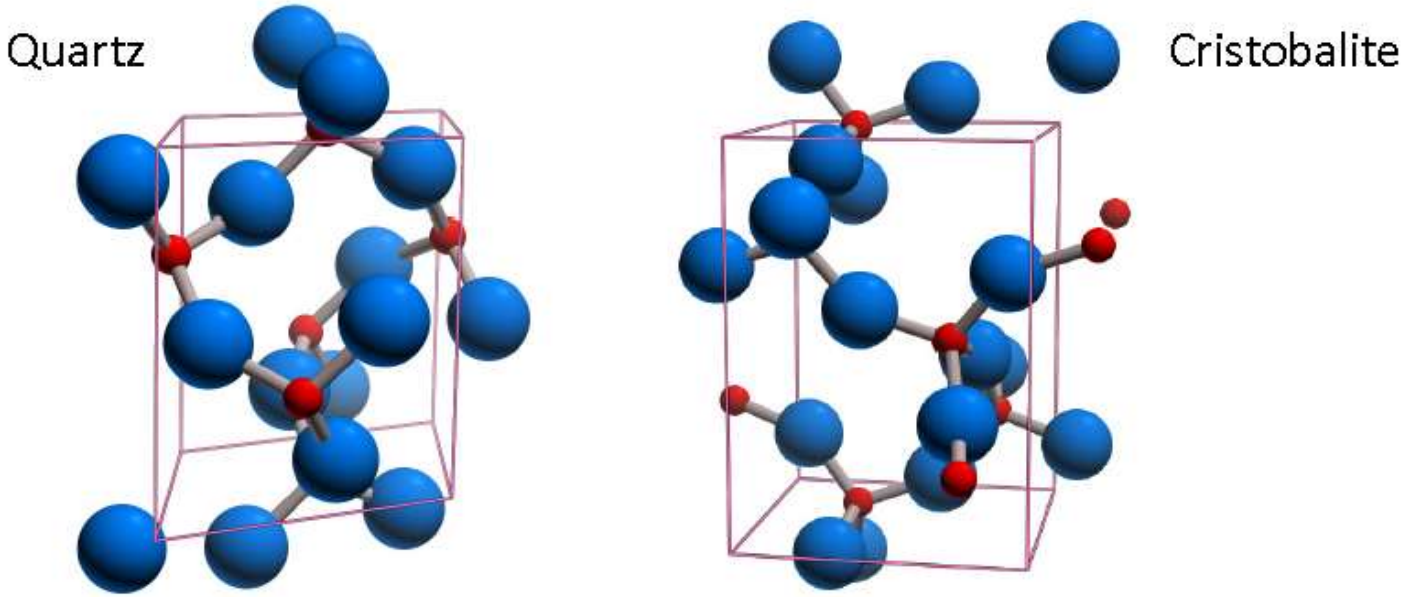

- The crystal structure describes the atomic arrangement of a material.
- When the atoms are arranged differently, a different diffraction pattern is produced (ie quartz vs cristobalite)

The figure below compares the X-ray diffraction patterns from 3 different forms of SiO_2

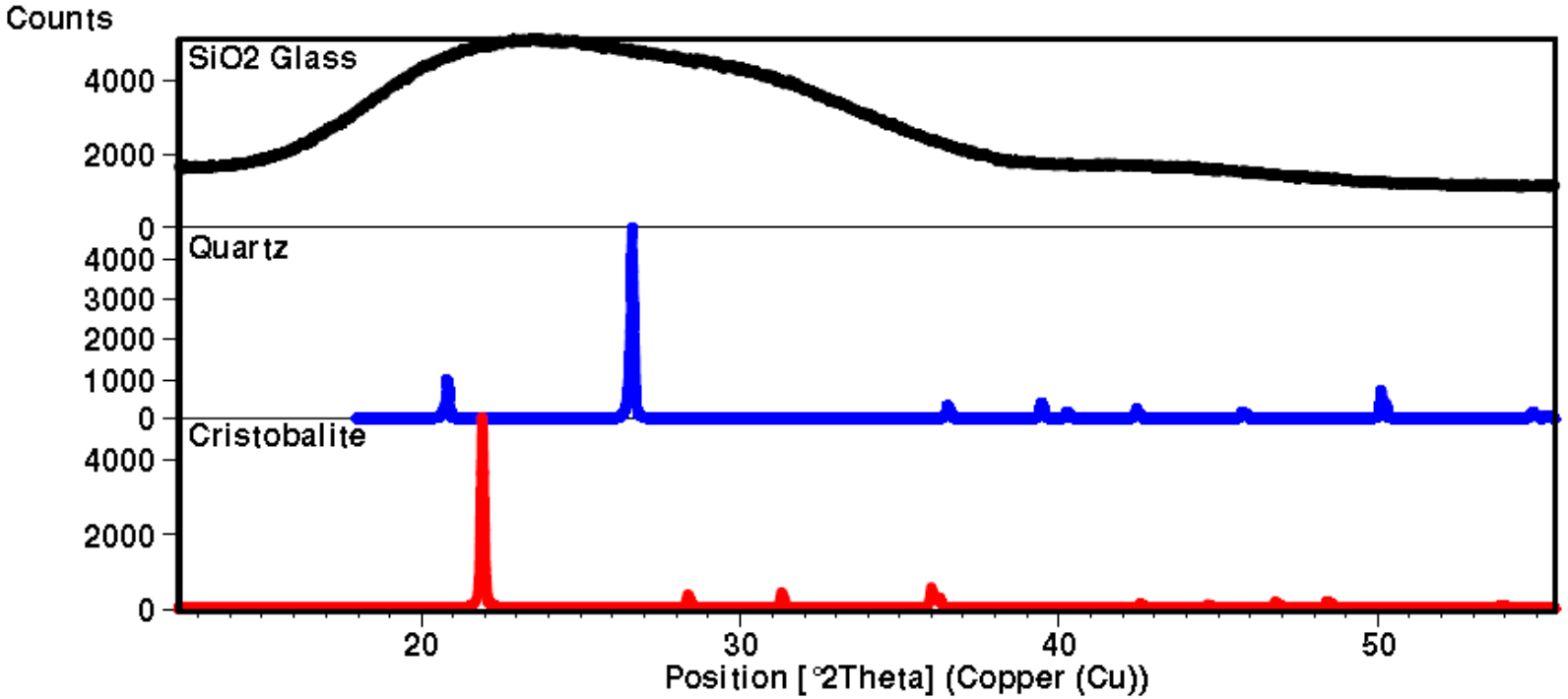

- These three phases of SiO_2 are chemically identical
- Quartz and cristobalite have two different crystal structures
  - The Si and O atoms are arranged differently, but both have structures with long-range atomic order
  - The difference in their crystal structure is reflected in their different diffraction patterns
- The amorphous glass does not have long-range atomic order and therefore produces only broad scattering peaks

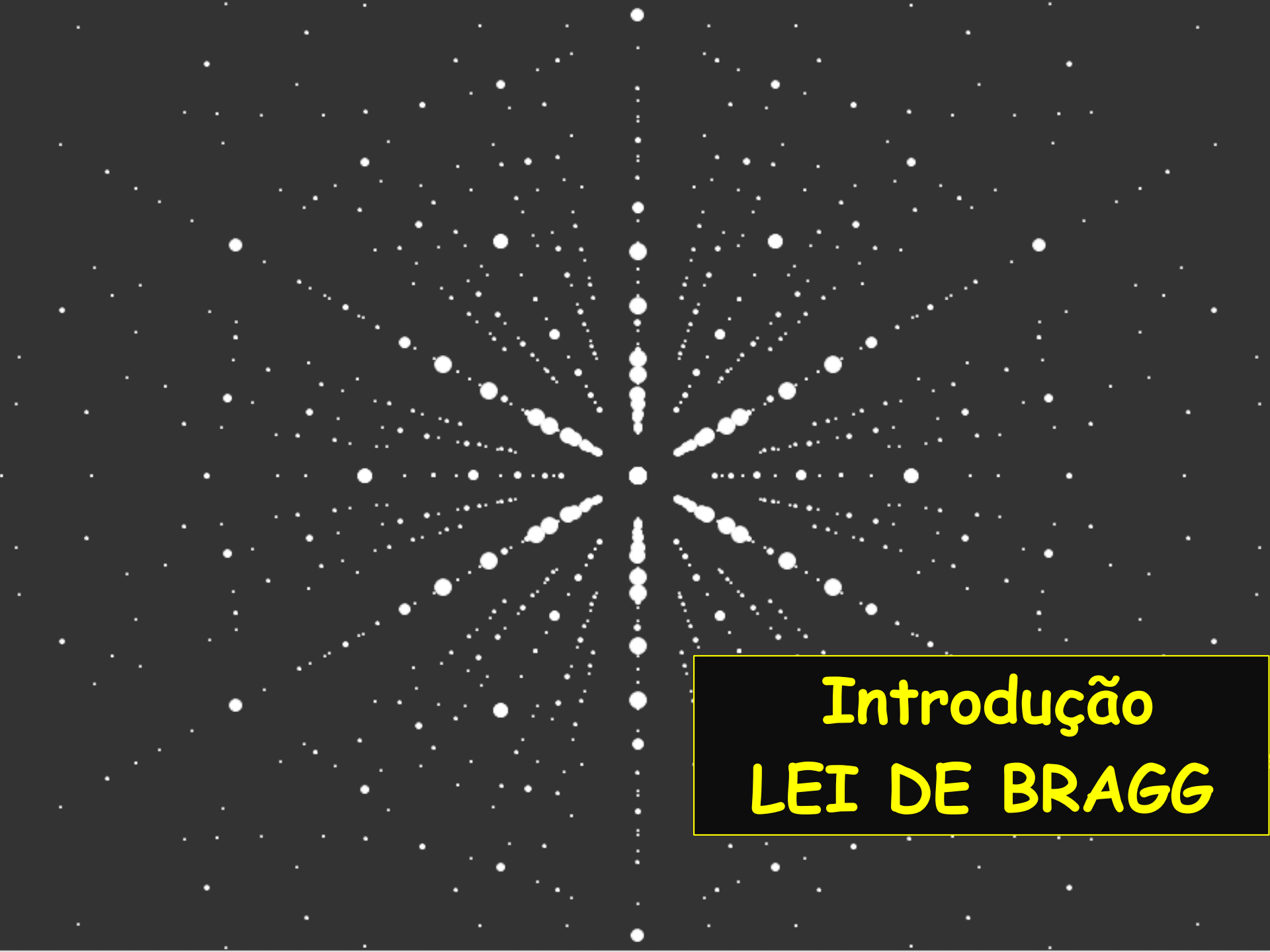

Introdução
LEI DE BRAGG

A curva de DRX de um material é resultado de sua estrutura cristalina

Lei de Bragg

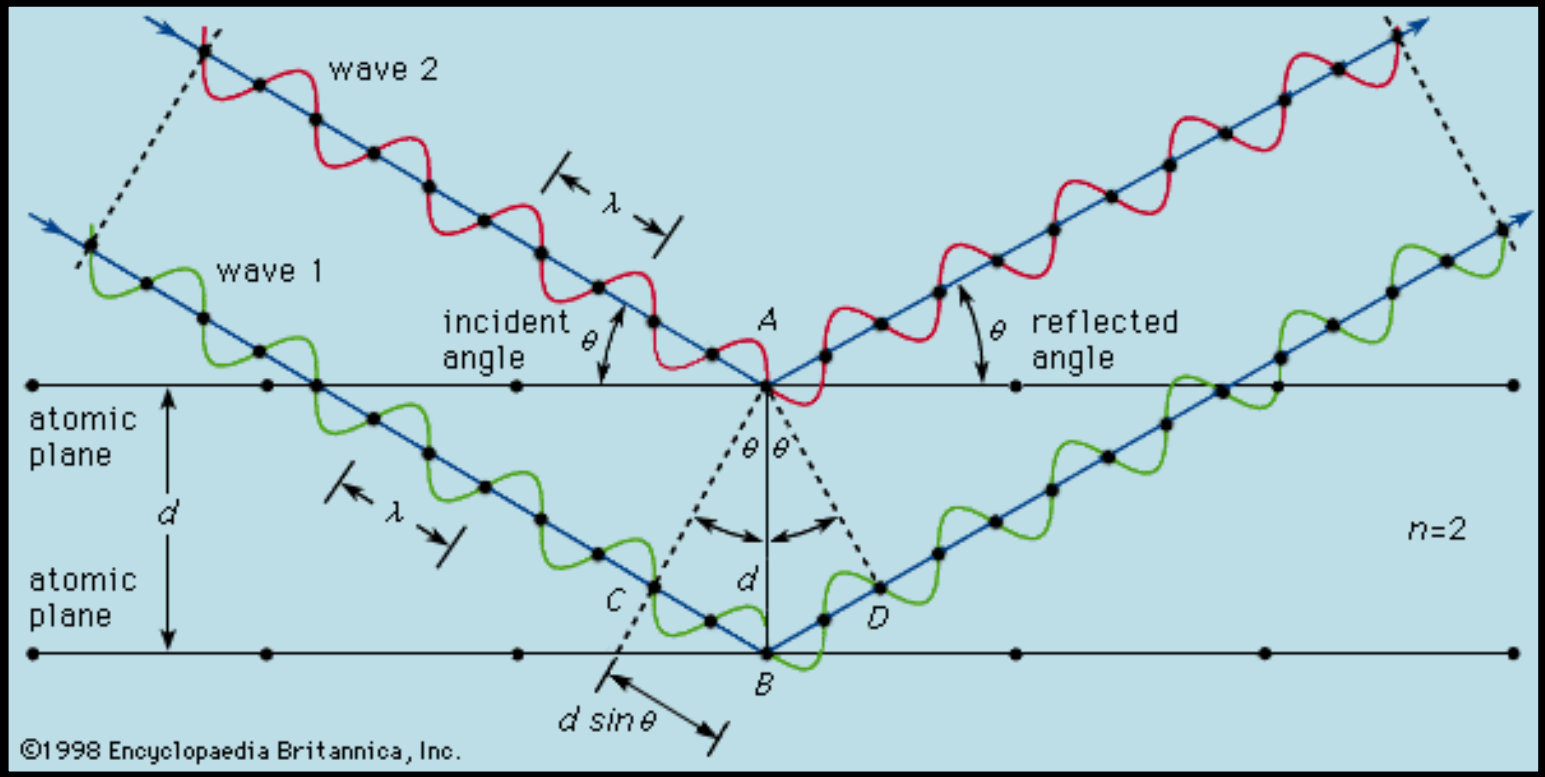

BRAGG LAW

$$2d(\sin\theta) = \lambda_o$$

where:

d = lattice interplanar spacing of the crystal

θ = x-ray incidence angle (Bragg angle)

λ = wavelength of the characteristic x-rays

Lei de Bragg *(1)*

Diffraction of x-rays by planes of atoms (A–A′ and B–B′).

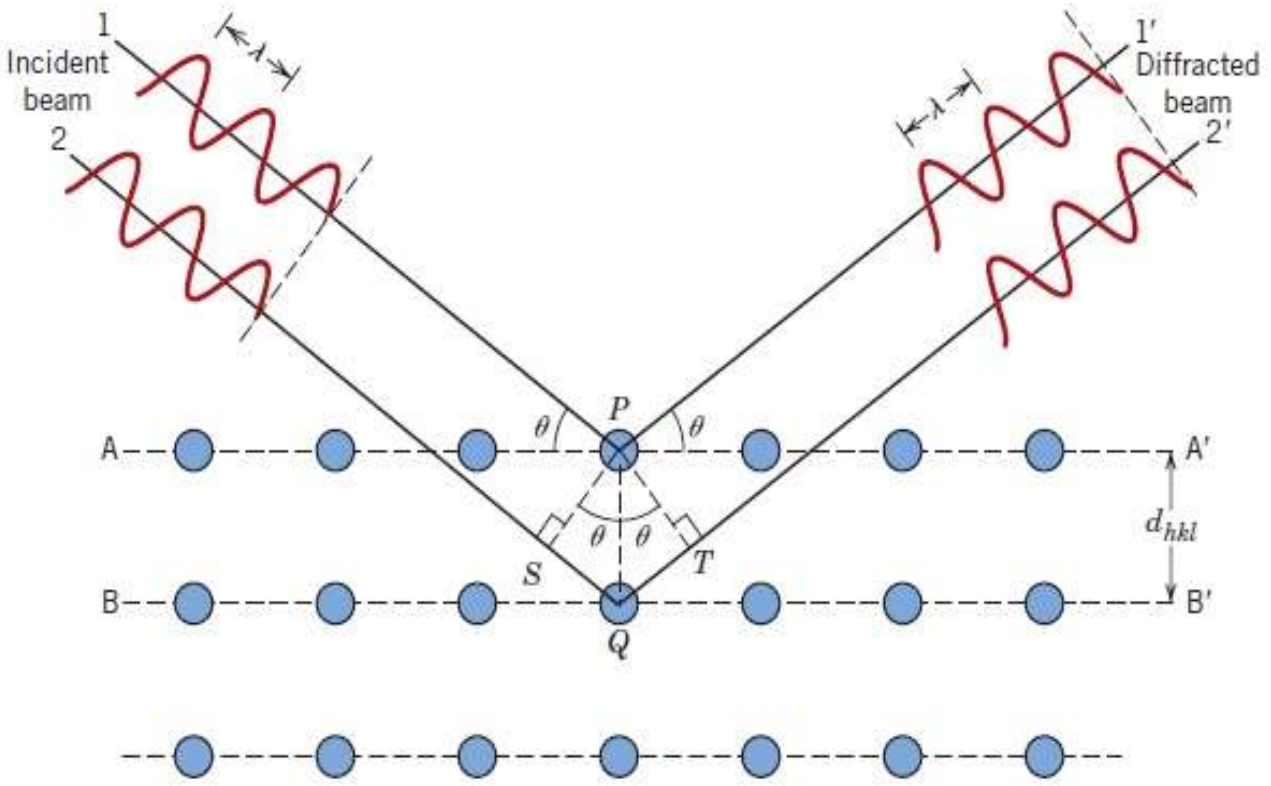

- A lei de Bragg foi apresentada pela primeira vez por W.L. Bragg (filho de W.H. Bragg, ambos cristalógrafos) num trabalho apresentado à Cambridge Philosophical Society no final de 1912.
- A discussão da lei será feita a partir da figura acima.

Lei de Bragg *(2)*

- Consideremos os raios 1 e 2, caminhando em fase segundo a frente de onda X-X', e incidindo num cristal, que tem um conjunto de planos representado pelas "fileiras" de átomos AA' e BB'. O ângulo de incidência é θ .
- Para que seja observada a difração (ou seja, para que haja interferência construtiva) , os raios emergentes do cristal 1' e 2', que deixam o cristal segundo o mesmo ângulo θ devem estar em fase.

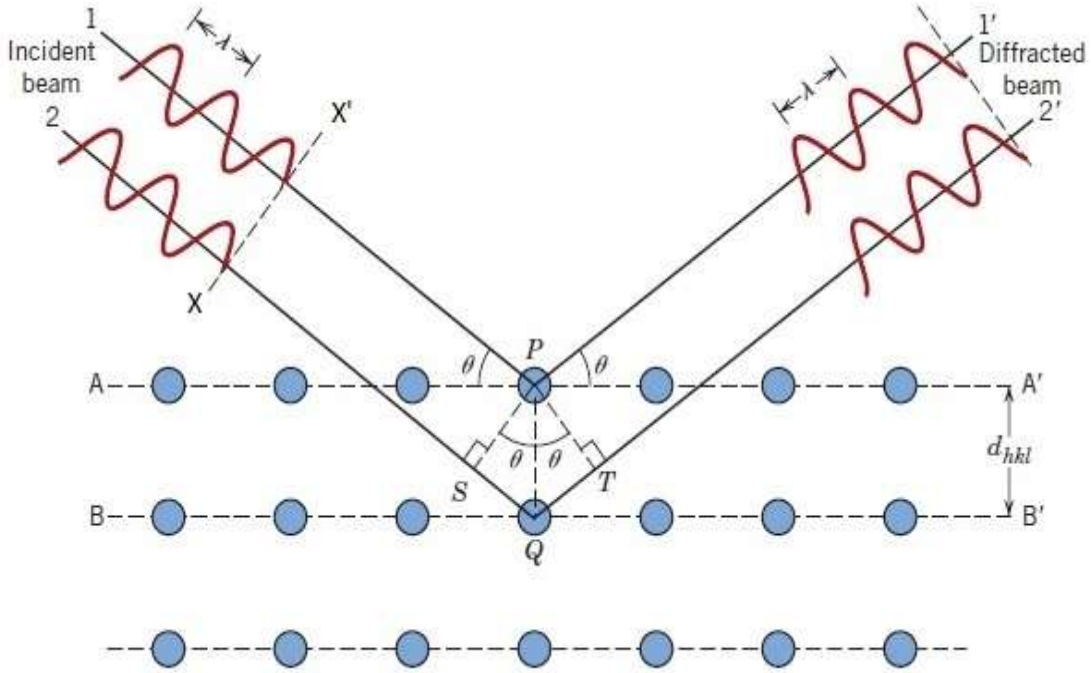

- Observemos o que ocorre com os raios 1 e 2. Os raios 1 e 2 chegam em fase quando a frente de onda X-X' chega em PS.
- O raio 1 interage com o átomo P do cristal e é espalhado; assumamos que ele sai do cristal por uma trajetória que segue o mesmo ângulo θ → esse é o raio 1'.

Lei de Bragg *(3)*

- O raio 2, em fase com o raio 1 até OS, não interage com nenhum átomo do plano AA' → ele segue o segmento SQ e interage com o átomo Q no plano BB'.
- Depois de interagir com o átomo Q, o raio 2 é espalhado; assumamos que ele sai do cristal por uma trajetória que segue o mesmo ângulo θ → esse é o raio 2'.
- Para poderem ser detectados por um detector posicionado em YY', 1' e 2' devem estar interferindo construtivamente.

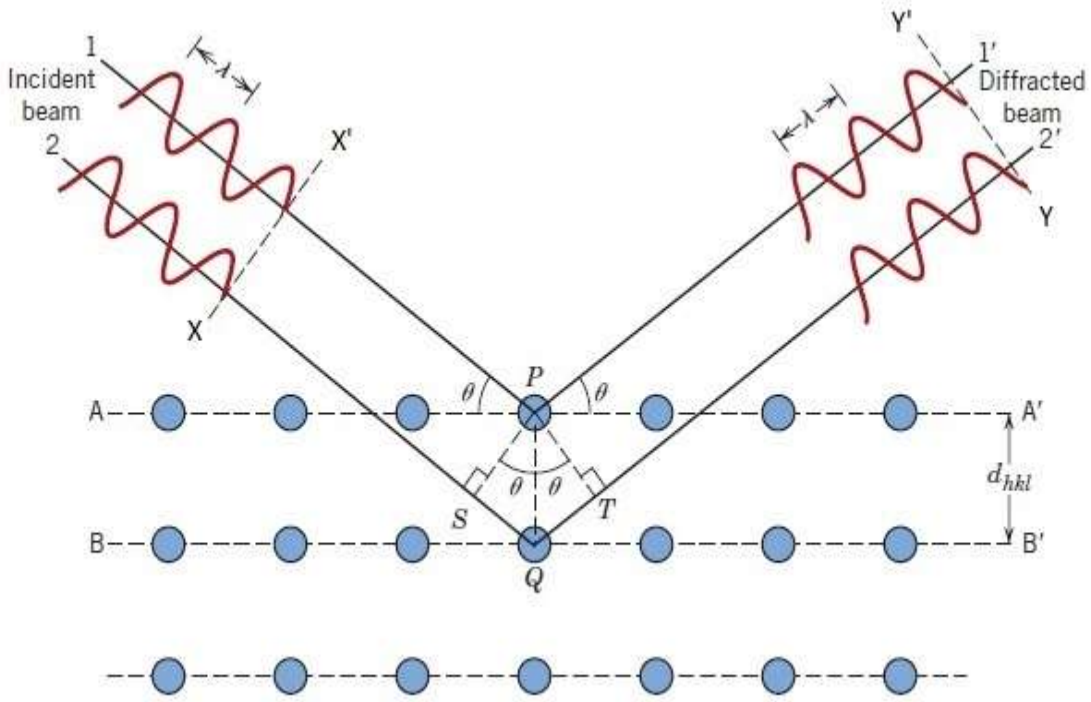

- Para estarem em condição de interferência construtiva em YY', os raios 1' e 2' devem estar em fase. Para estarem em fase em YY', eles devem necessariamente estar em fase em PT.

Lei de Bragg *(4)*

- Ora, a condição para que os raios 1 e 2, que estavam em fase em PS, estejam em fase em PT (agora como 1’ e 2’), é que a distância [SQ + QT], percorrida pelo raio 2, seja igual a um número inteiro de comprimentos de onda.
- Se os ângulos de incidência e de saída são iguais a θ, por meio de considerações geométricas, pode-se chegar a que o ângulos SPQ e QPT são iguais entre si e iguais a θ.

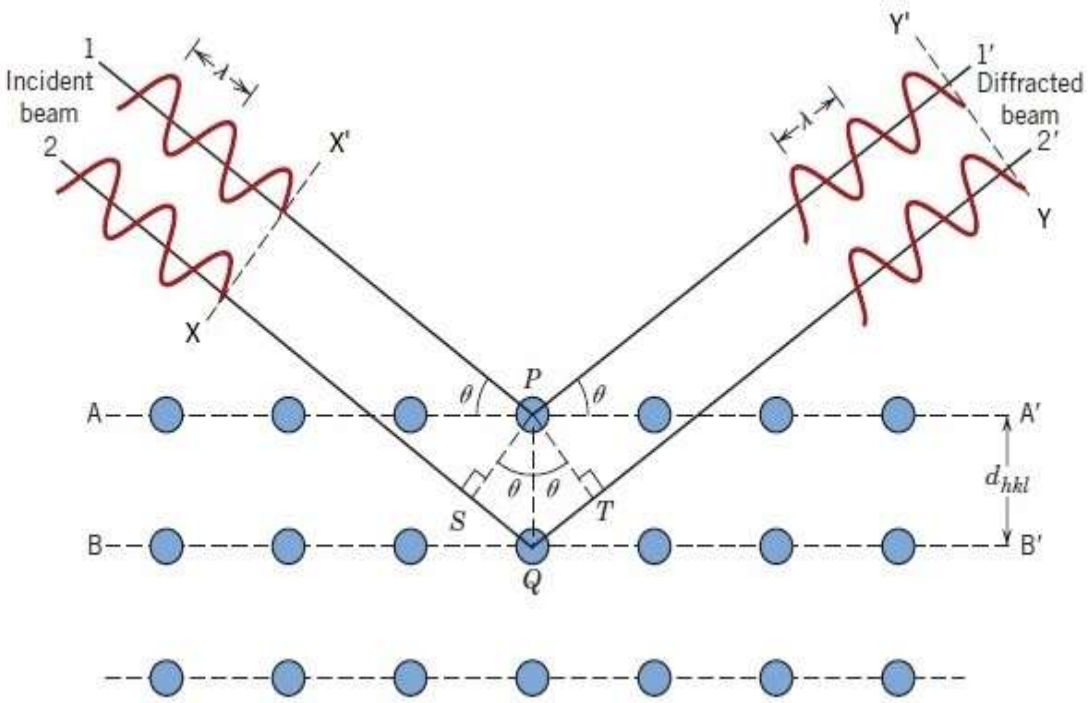

- Também por meio de considerações geométricas, pode-se chegar a que as distâncias [SQ] e [QT] são iguais, e que [SQ] = [QT] = d_{hkl} sen θ.
- d_{hkl} é a distância que separa os planos AA’ e BB’ na figura → essa é a distância que separa planos (hkl) paralelos na estrutura cristalina.
  - ***(hkl) são os índices de Miller desses planos***.

Lei de Bragg *(5)*

- Bom, depois de todas essas considerações, agora chegamos à **lei de Bragg**:
- A soma dos segmentos [SQ] e [QT] deve ser igual a um número inteiro de comprimentos de onda (λ).

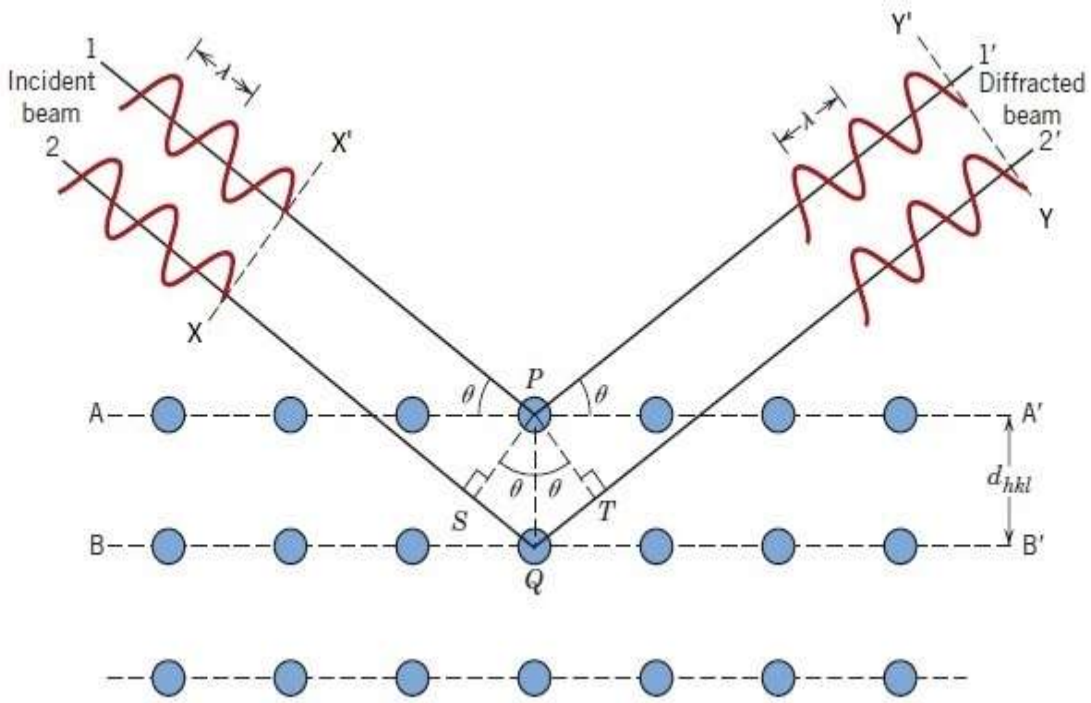

$$n\lambda = \overline{SQ} + \overline{QT}$$

$$n\lambda = d_{hkl}\,\mathrm{sen}\,\theta + d_{hkl}\,\mathrm{sen}\,\theta = 2d_{hkl}\,\mathrm{sen}\,\theta$$

$$n\lambda = 2d_{hkl}\,\mathrm{sen}\,\theta$$

DIFRATÔMETRO DE RAIOS X

MÉTODO DO PÓ

Difratômetro de Raios X

Schematic diagram of an x-ray diffractometer; T = x-ray source, S = specimen, C = detector, and O = the axis around which the specimen and detector rotate.

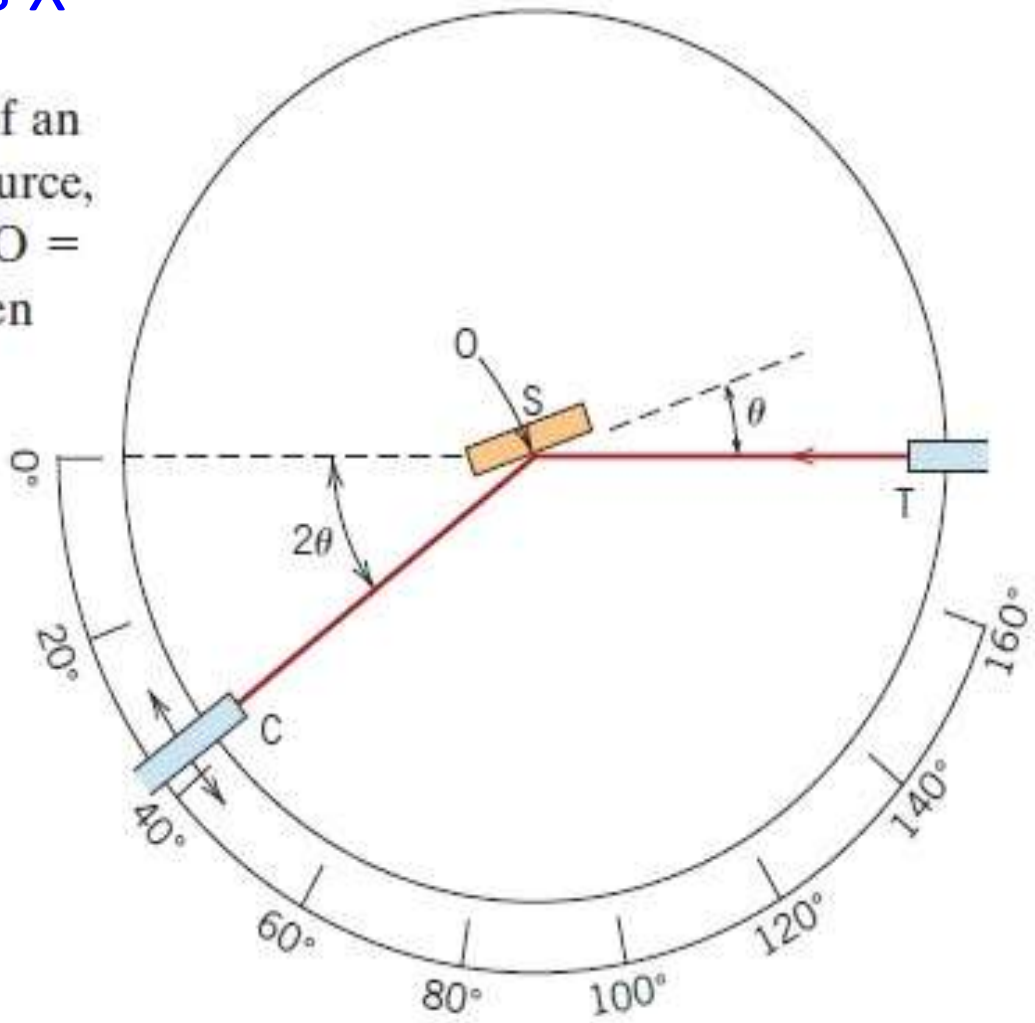

- Os primeiros equipamentos tinham essa configuração.
- A fonte **T**, pesada, era mantida fixa.
- O detector **C** se move ao longo de uma circunferência na qual estão inscritos **C** e **T**, com uma velocidade angular 2θ/tempo.
- Para manter um arranjo no qual a amostra analisada está posicionada sempre no mesmo ângulo a cada tempo com **T** e **C**, o suporte da amostra de move.
- Enquanto **C** se move a uma velocidade 2θ/tempo, o suporte da amostra se move a uma velocidade θ/tempo.
- Dessa forma, os ângulos entre **C** e **S**, e entre **T** e **S** são sempre iguais a todo instante, e iguais a θ.

- O conjunto mecânico que realiza a movimentação precisa de fonte e detector chama-se **goniômetro**.
- O resultado desse arranjo experimental é a curva de difração (também chamada de difratograma).
- Quando um determinado ângulo θ atende à lei de Bragg para um determinado conjunto de planos (hkl) do material analisado, existe interferência construtiva e um sinal é registrado na curva de difração.
- A cada conjunto de planos paralelos para o qual a lei de Bragg é atendida em um ângulo **2θ** registrado pelo equipamento, corresponde um pico na curva de difração.
- *Atenção: a cada ângulo 2θ determinado pelo equipamento, corresponde um ângulo θ que deve ser utilizado na lei de Bragg para determinação do valor de d_{hkl} !!*
- A curva de difração é uma curva que relaciona o **ângulo 2θ** à intensidade de sinal lida pelo detector.

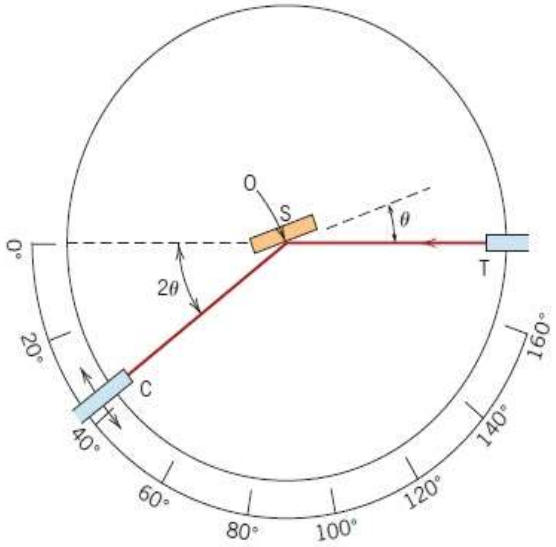

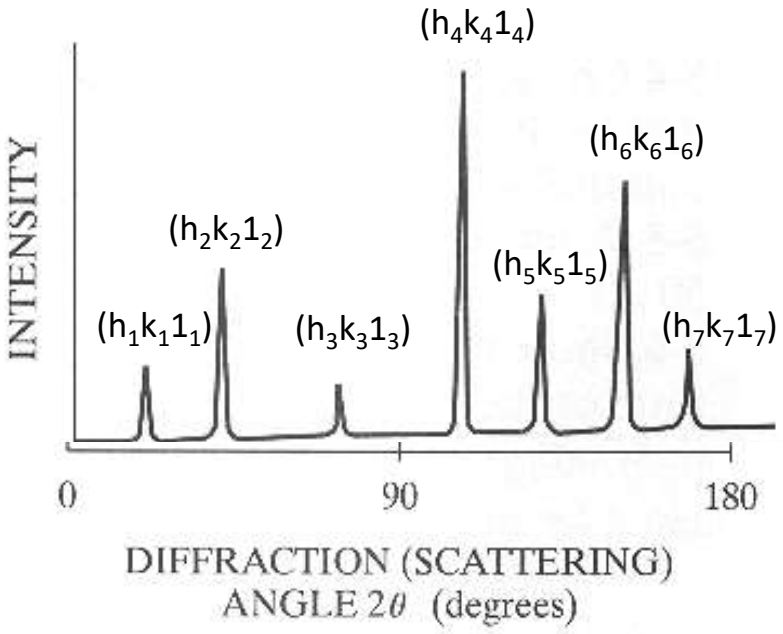

- Os equipamentos atuais já contam com fontes e detectores móveis.
- Ambos (**C** e **T**) se movimentam com velocidade θ/tempo.
- No entanto, as curvas de difração continuam a ser apresentadas em ângulos 2θ contra intensidade de sinal identificado pelo detector.

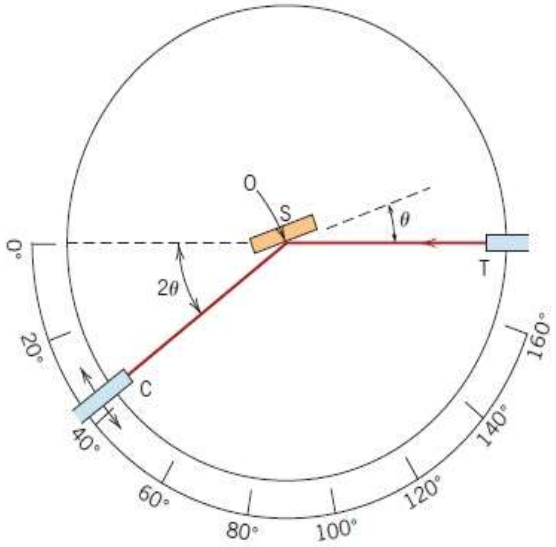

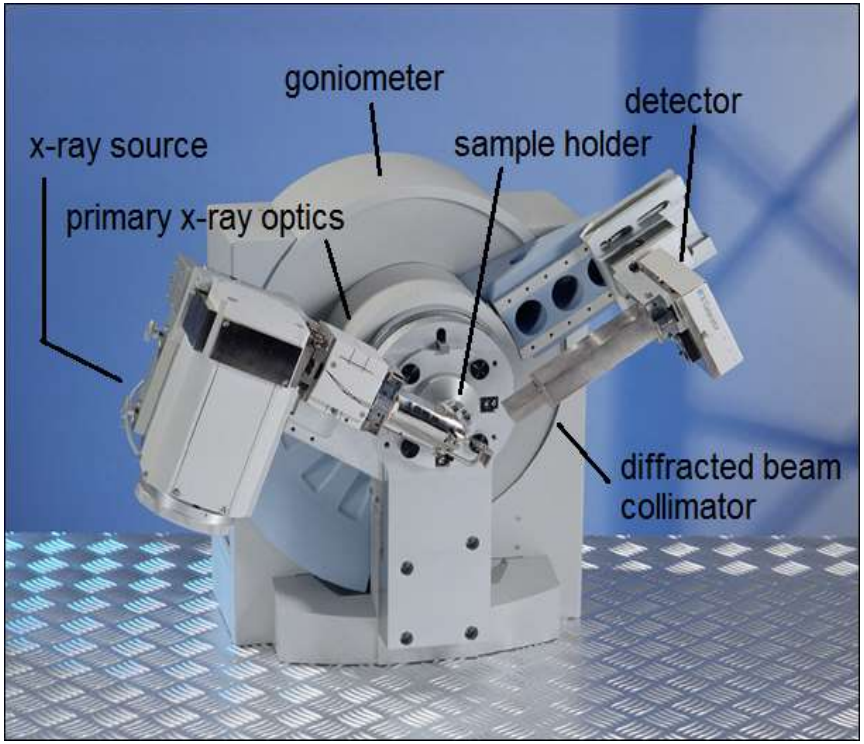

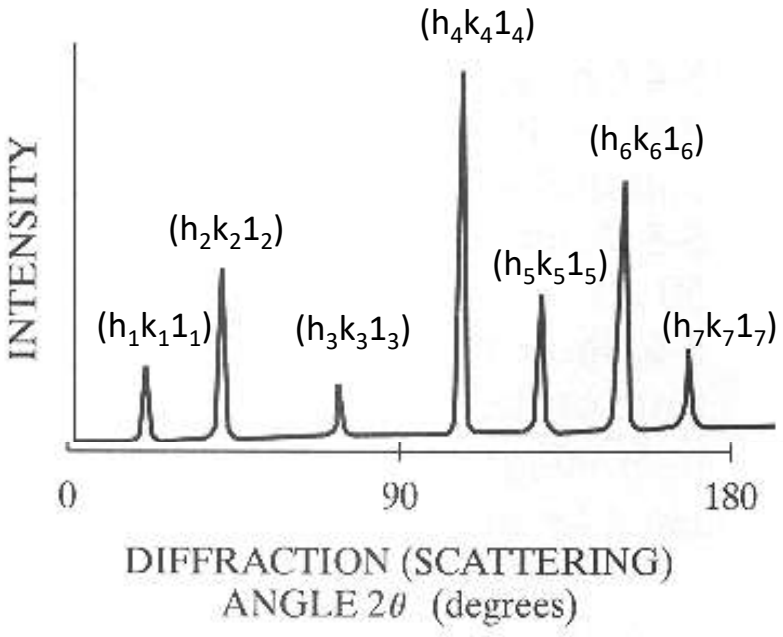

Difratômetro de pó clássico

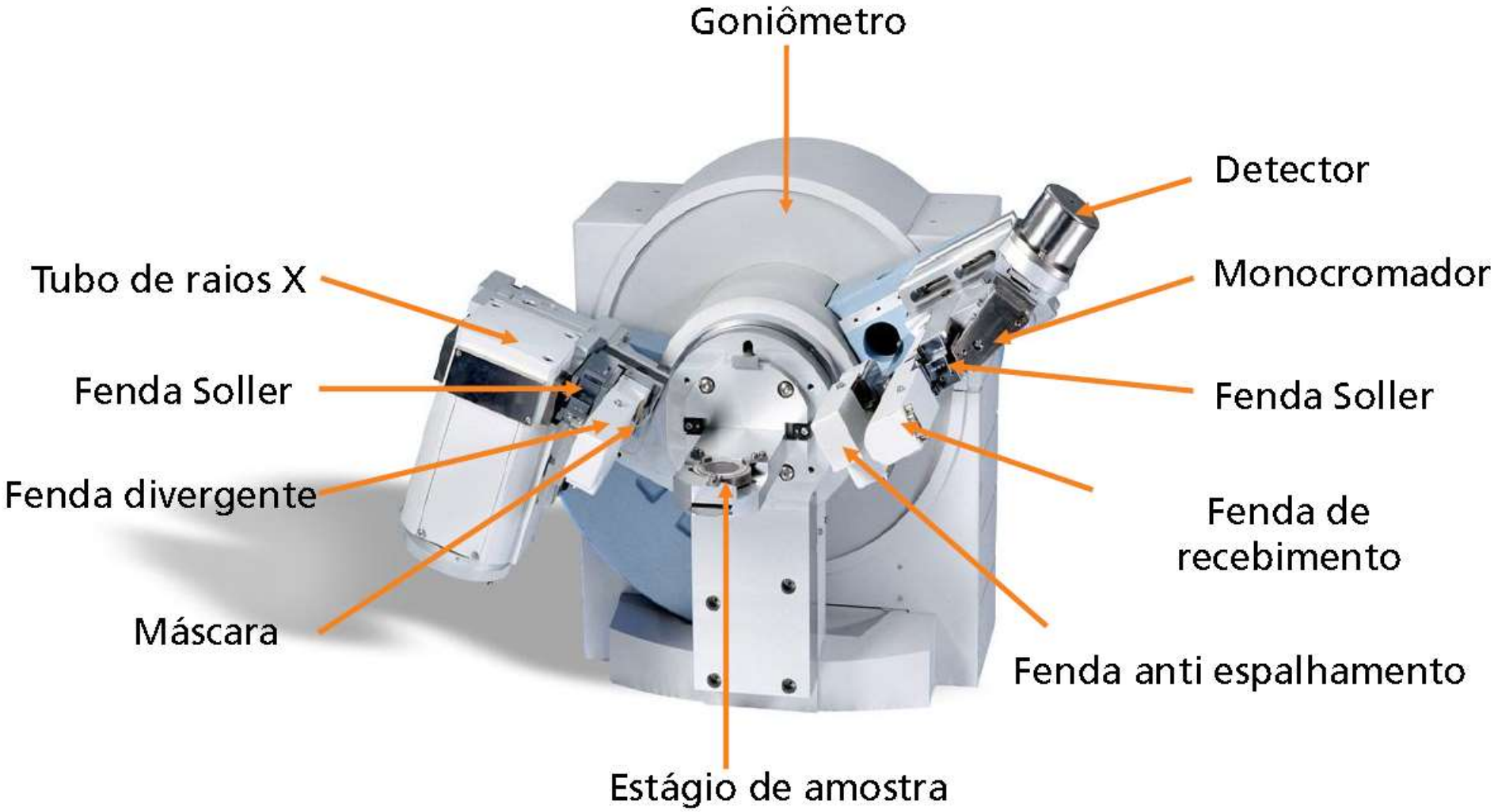

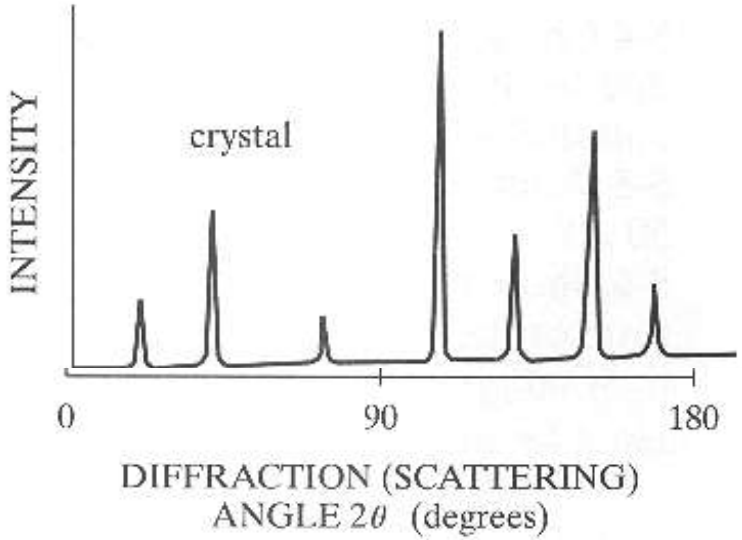

Difratograma esquemático de um sólido cristalino.

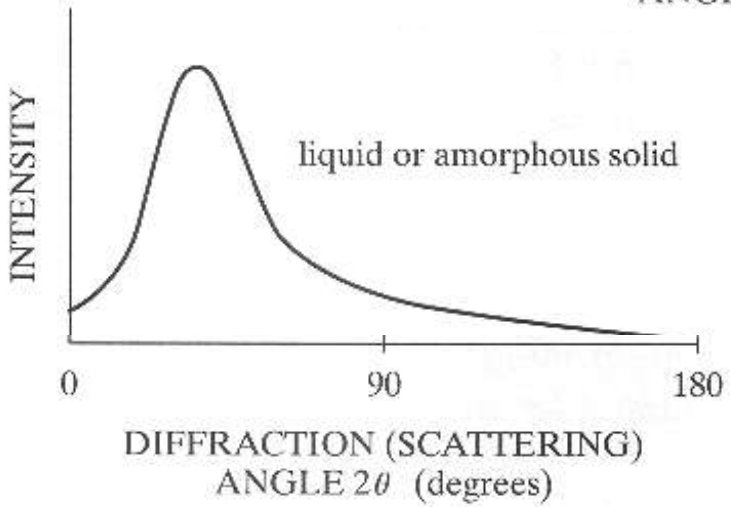

Gráfico de intensidade de raios X em função da variação de 2θ para um sólido amorfo ou para um líquido.

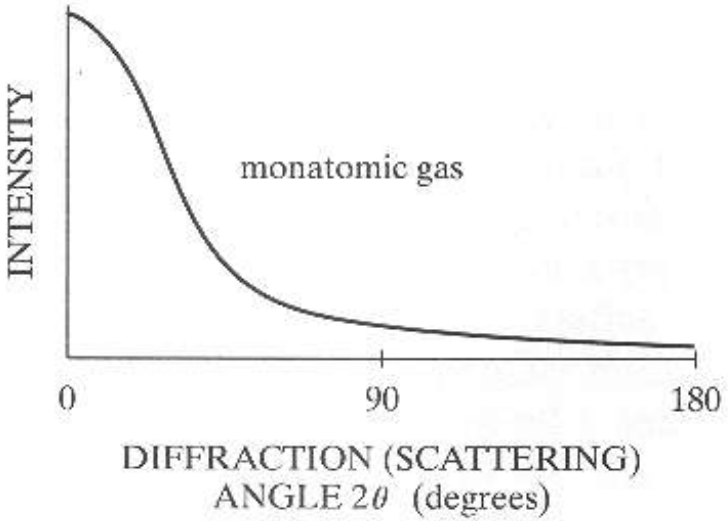

Gráfico de intensidade de raios X em função da variação de 2θ para um gás monoatômico.

SiO_2 – Curvas de Difração: Quartzo *(cristalino)* e Vidro *(amorfo)*

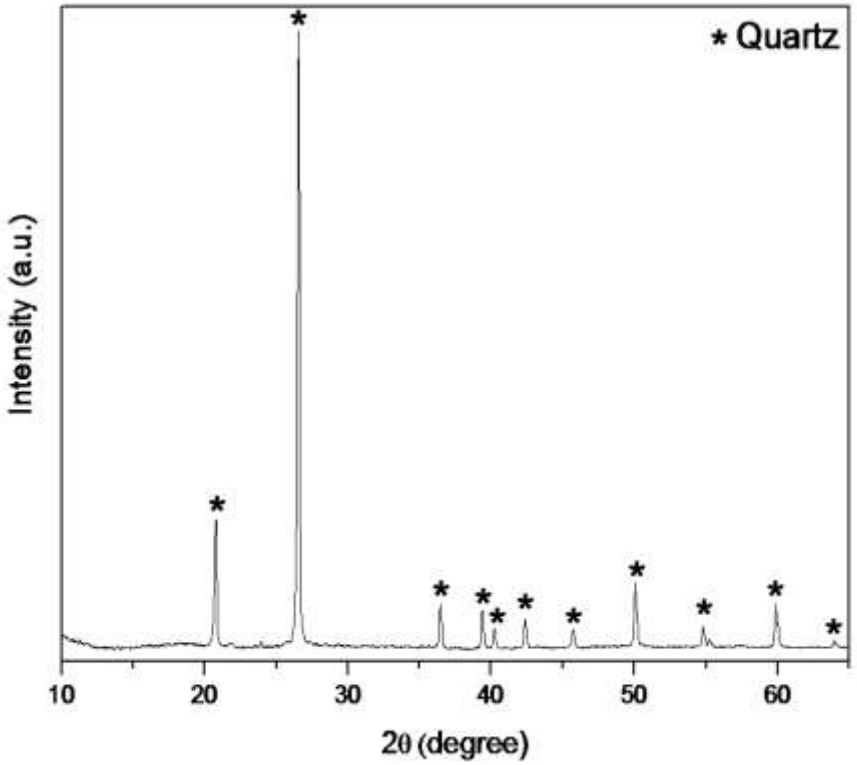

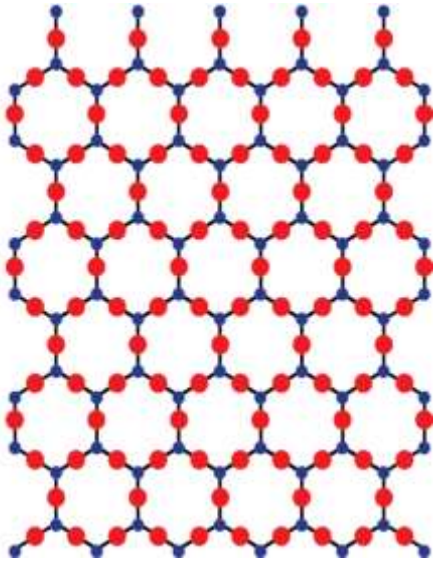

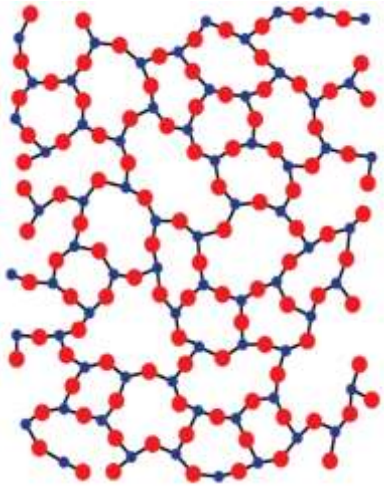

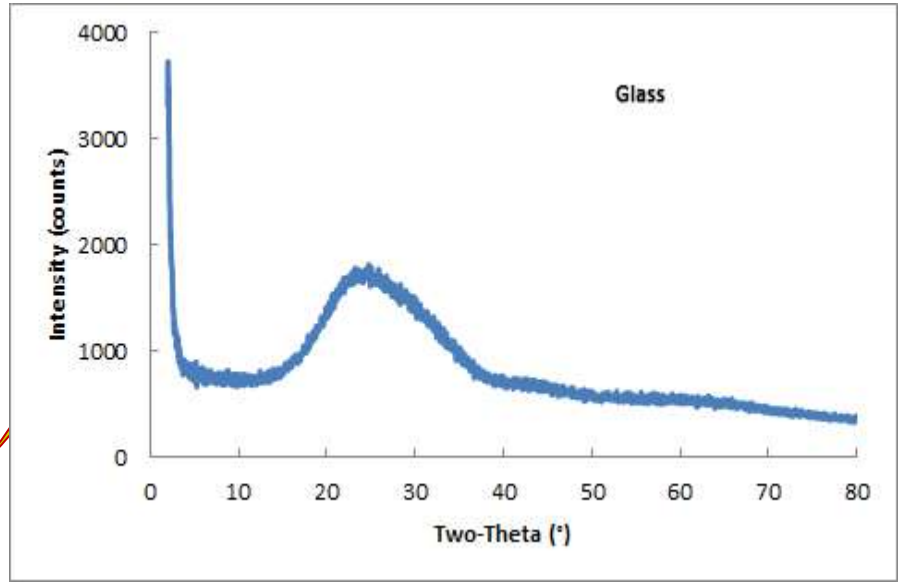

...em resumo

Diffraction peaks are associated with planes of atoms

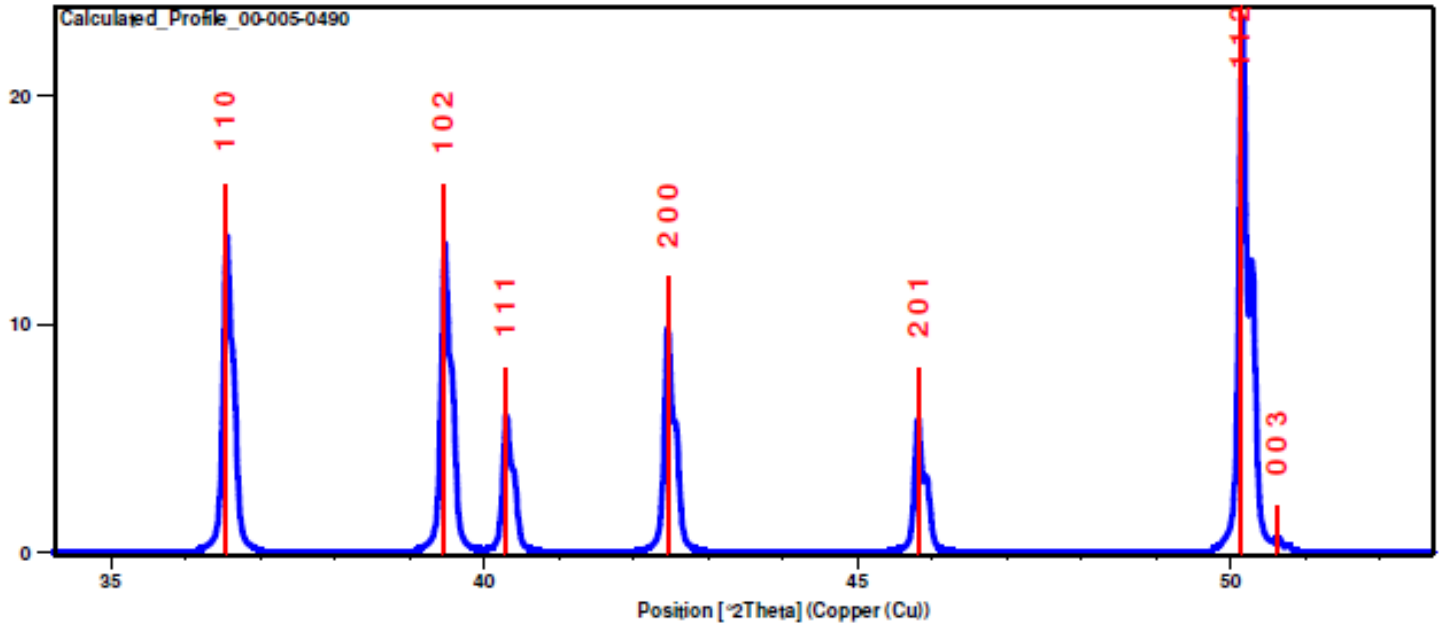

- Miller indices (hkl) are used to identify different planes of atoms
- Observed diffraction peaks can be related to planes of atoms to assist in analyzing the atomic structure and microstructure of a sample

Difração pelo método do pó *(Powder XRD)*

A single crystal specimen in a Bragg-Brentano diffractometer would produce only one family of peaks in the diffraction pattern.

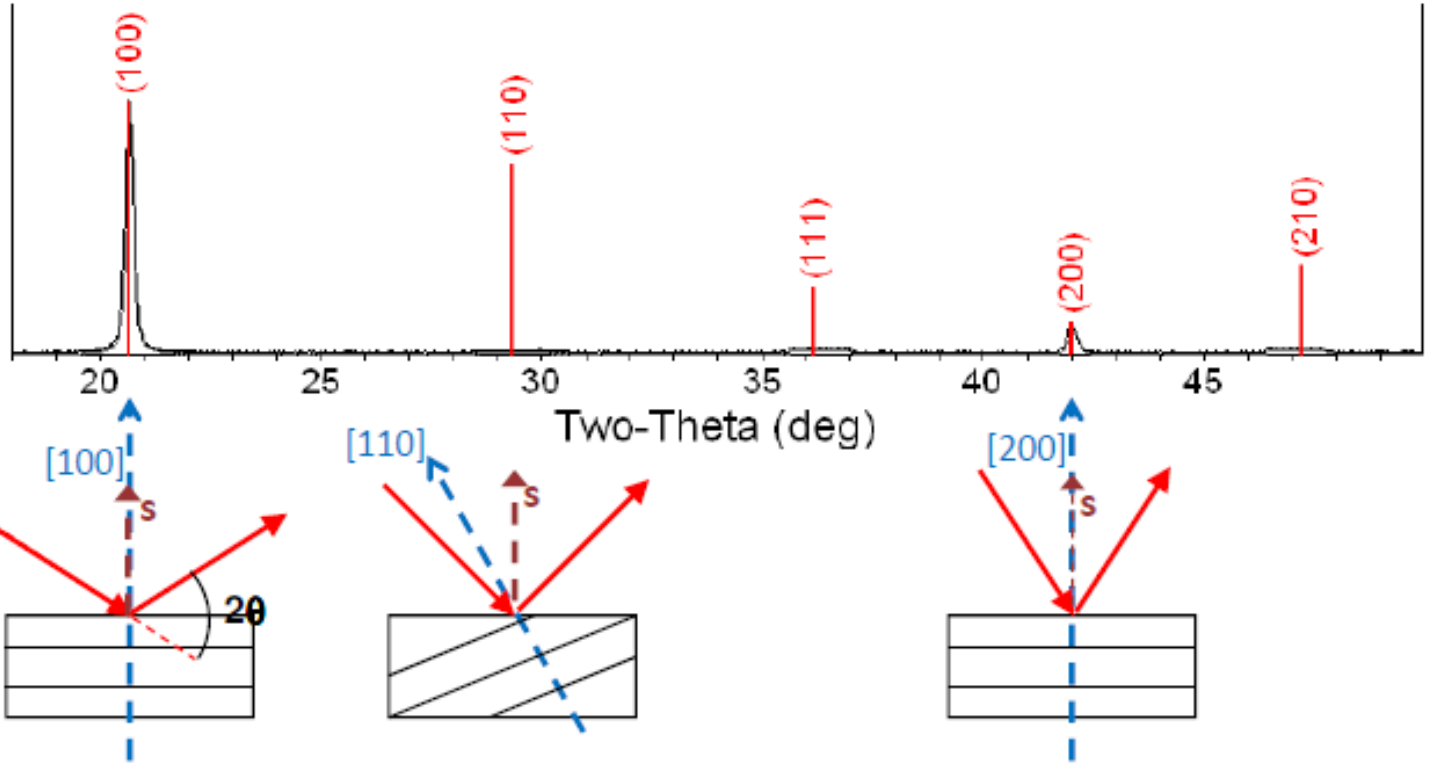

At 20.6 °2θ, Bragg's law fulfilled for the (100) planes, producing a diffraction peak.

The (110) planes would diffract at 29.3 °2θ; however, they are not properly aligned to produce a diffraction peak (the perpendicular to those planes does not bisect the incident and diffracted beams). Only background is observed.

The (200) planes are parallel to the (100) planes. Therefore, they also diffract for this crystal. Since d_{200} is ½ d_{100}, they appear at 42 °2θ.

Difração pelo método do pó *(Powder XRD)*

A polycrystalline sample should contain thousands of crystallites. Therefore, all possible diffraction peaks should be observed.

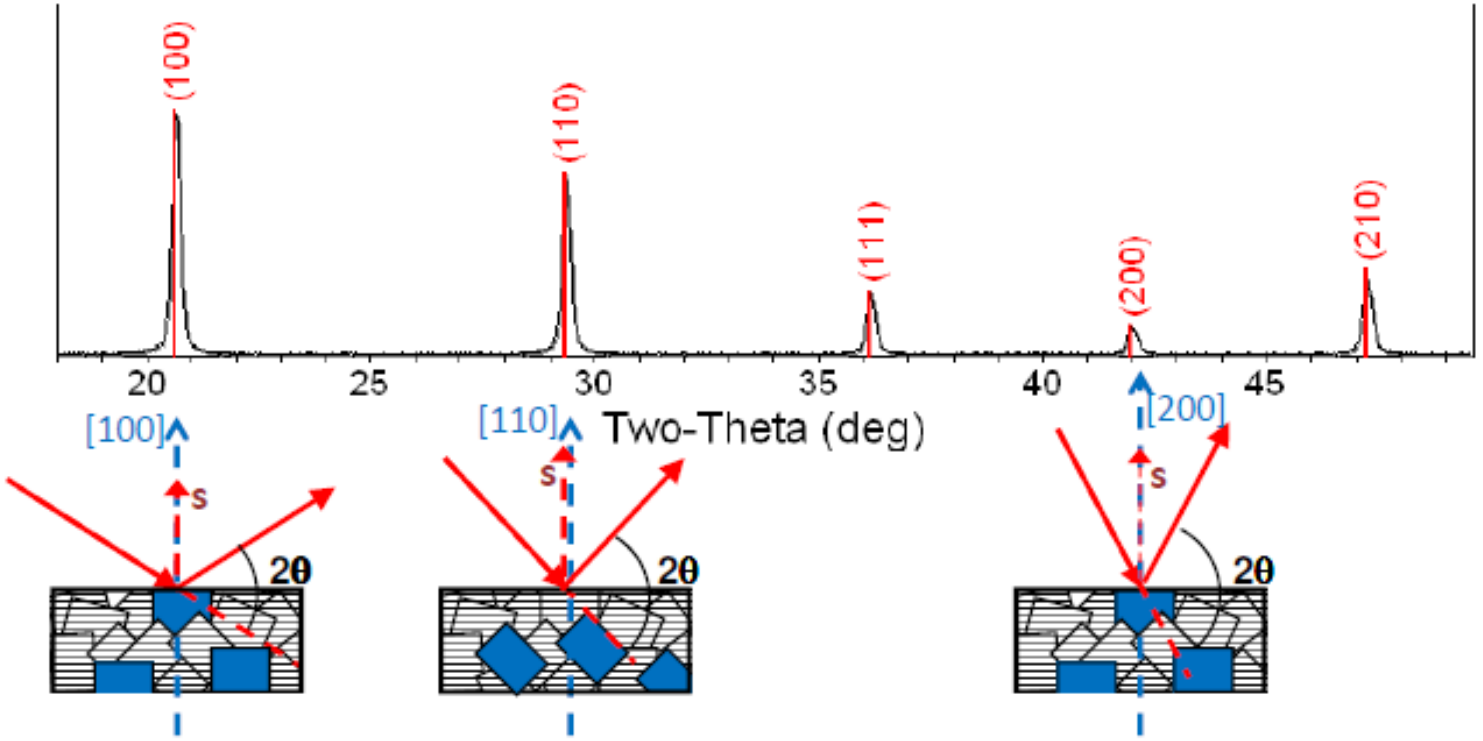

- For every set of planes, there will be a small percentage of crystallites that are properly oriented to diffract (the plane perpendicular bisects the incident and diffracted beams).
- Basic assumptions of powder diffraction are that for every set of planes there is an equal number of crystallites that will diffract and that there is a statistically relevant number of crystallites, not just one or two.

Difração pelo método do pó *(Powder XRD)*

Powder diffraction is more aptly named polycrystalline diffraction

- Samples can be powder, sintered pellets, coatings on substrates, engine blocks...
- The ideal "powder" sample contains tens of thousands of randomly oriented crystallites
  - Every diffraction peak is the product of X-rays scattering from an equal number of crystallites
  - Only a small fraction of the crystallites in the specimen actually contribute to the measured diffraction pattern
    - XRPD is a somewhat inefficient measurement technique
- Irradiating a larger volume of material can help ensure that a statistically relevant number of grains contribute to the diffraction pattern
  - Small sample quantities pose a problem because the sample size limits the number of crystallites that can contribute to the measurement

Difração pelo método do pó *(Powder XRD)*

Powder diffraction data consists of a record of photon intensity versus detector angle 2θ.

- Diffraction data can be reduced to a list of peak positions and intensities
  - Each d_{hkl} corresponds to a **family** of atomic planes {hkl}
  - individual planes cannot be resolved- this is a limitation of powder diffraction versus single crystal diffraction

Raw Data

Position [°2θ]	Intensity [cts]
25.2000	372.0000
25.2400	460.0000
25.2800	576.0000
25.3200	752.0000
25.3600	1088.0000
25.4000	1488.0000
25.4400	1892.0000
25.4800	2104.0000
25.5200	1720.0000
25.5600	1216.0000
25.6000	732.0000
25.6400	456.0000
25.6800	380.0000
25.7200	328.0000

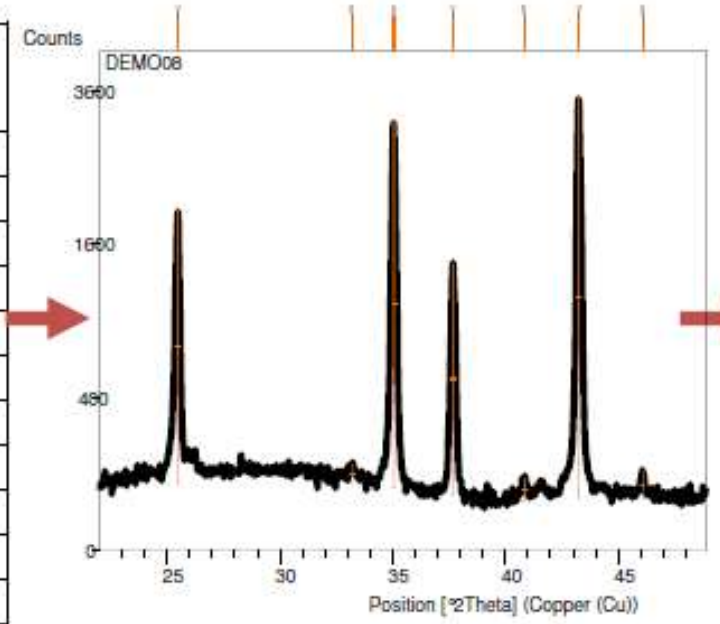

Reduced dI list

hkl	d_{hkl} (Å)	Relative Intensity (%)
{012}	3.4935	49.8
{104}	2.5583	85.8
{110}	2.3852	36.1
{006}	2.1701	1.9
{113}	2.0903	100.0
{202}	1.9680	1.4

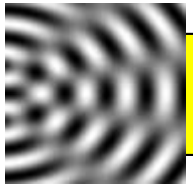

Difração pelo método do pó *(Powder XRD)*

POWDER DIFFRACTION

Peak positions determined by size and shape of unit cell
(d-spacings and systematic absences)

Peak intensities determined by the atomic number and position of the various atoms within the unit cell

Peak widths determined by instrument parameters, temperature, and crystal size, strain, and inhomogeneities

Para que serve a DRX ?

- A Difração de Raios X **(DRX)** é uma importante ferramenta que pode ser empregada para:
  - *Identificar fases cristalinas* por comparação com dados obtidos a partir de fases conhecidas.
  - Obter informações a respeito de *tamanho de domínio cristalino* e de outros *parâmetros estruturais* *(por exemplo: tensão residual; orientação de cristais)*.
  - Obter informações a respeito de mudanças em parâmetros de rede de estruturas conhecidas.
  - *Determinação da estrutura cristalina* *(parâmetro de rede, grupo espacial e coordenadas atômicas)* de materiais cristalinos desconhecidos.

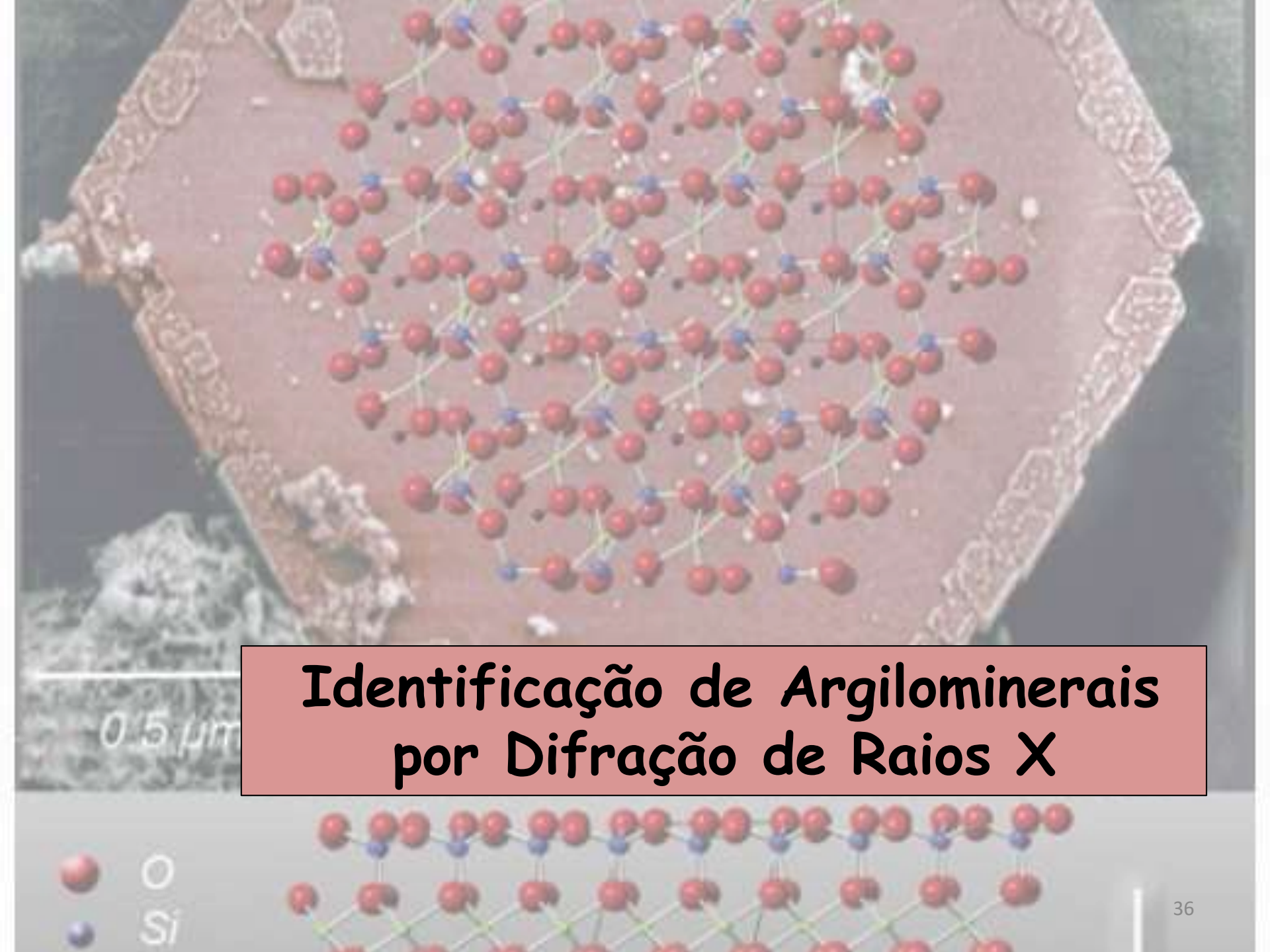

Identificação de Argilominerais por Difração de Raios X

Identificação de Argilominerais por DRX

- Os argilominerais são classificados em **grupos** e **subgrupos**.
- A difração de raios-X (DRX) pode ser empregada para classificar os argilominerais a partir da determinação da **reflexão (00ℓ)** obtida a partir de uma ou várias amostras (orientadas e/ou desorientadas), preparadas de uma ou mais de uma das cinco formas seguintes:
  - Amostra saturada de umidade (em equilíbrio com umidade relativa, por exemplo, de 70%);
  - Amostra seca ao ar (ou secas a 110ºC);
  - Amostra saturada com etilenoglicol;
  - Amostra aquecida a 300ºC;
  - Amostra aquecida a 550ºC.
- Sub-grupos de minerais di- ou tri-octaédricos podem ser diferenciados a partir da **reflexão (060)** :
  - O **parâmetro b** é maior para argilominerais trioctaédricos do que para dioctaédricos, e essa diferença aparece claramente em reflexões observáveis em ângulos 2θ elevados como é o caso da **reflexão (060)**.
- Em alguns casos, apenas o resultado de análises de DRX é capaz de produzir uma identificação dos argilominerais presentes em uma amostra.
- Em outros casos, especialmente se a concentração em argilominerais for pequena, pode ser necessário o uso de técnicas auxiliares (por exemplo: análise química; espectroscopia IR; microscopias eletrônicas; análise térmicas).

Argilominerais : Grupos por Reflexões Basais

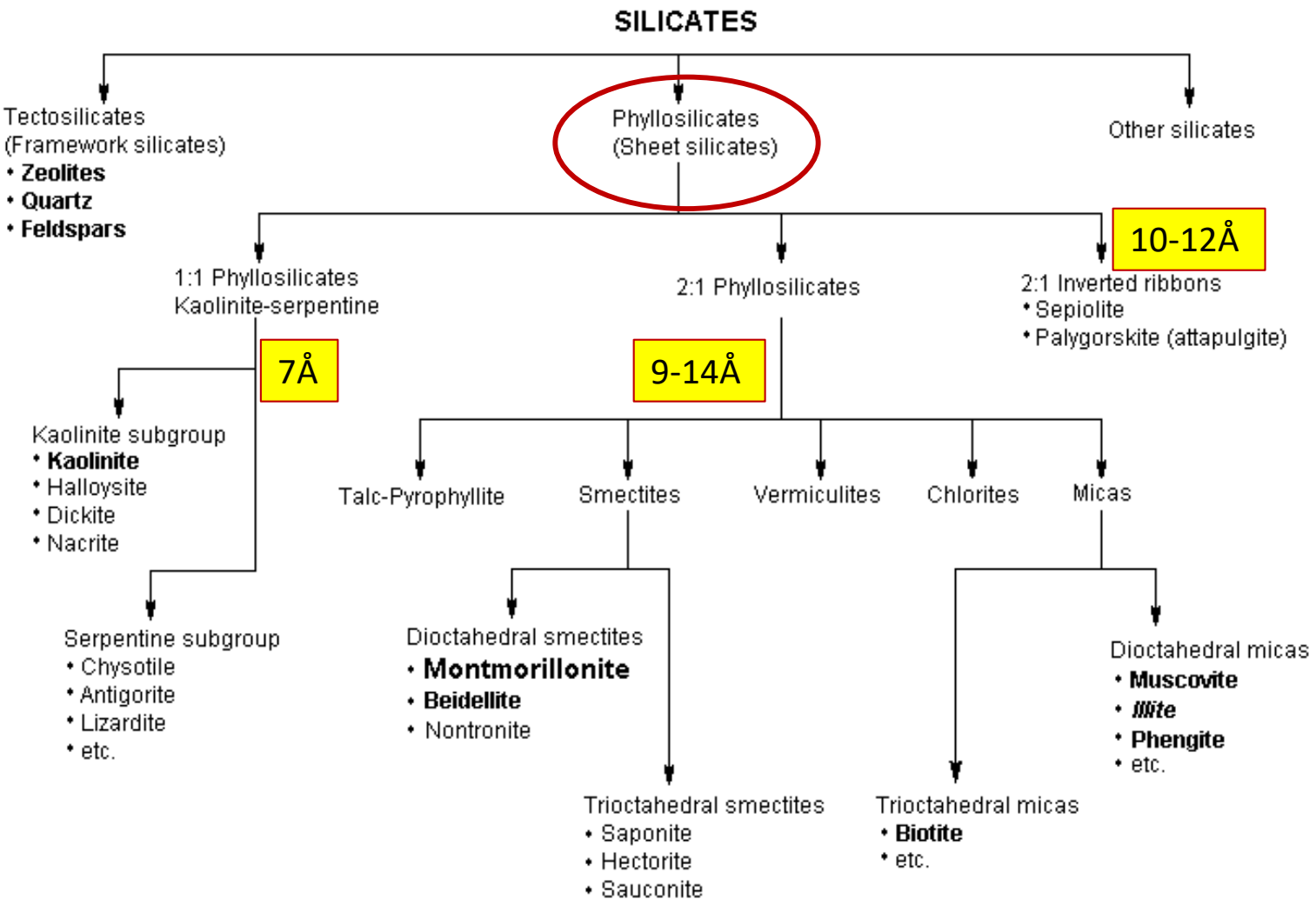

Caracterização de Argilominerais : **Reflexão Basal**

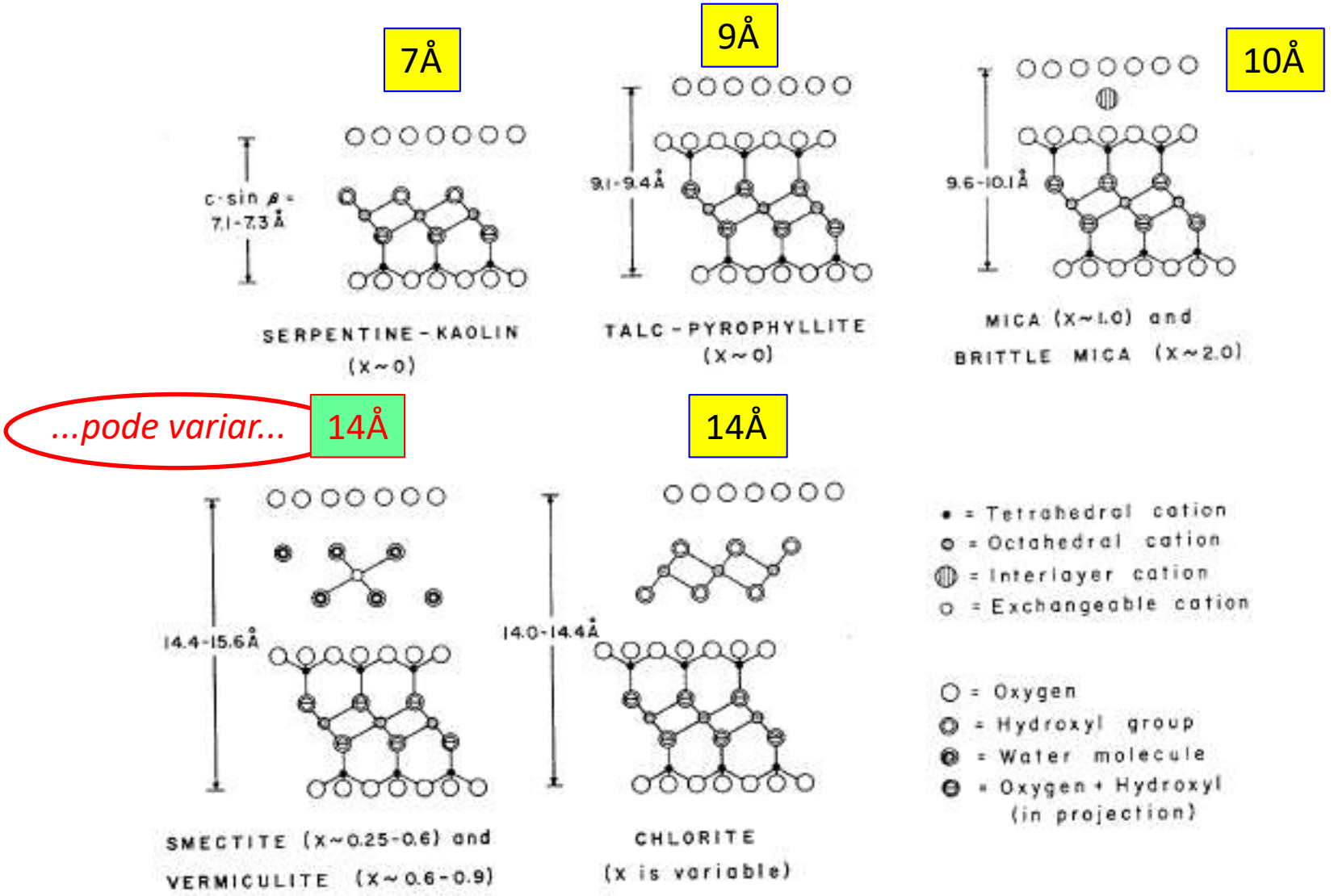

FIG. 1.2. [010] view of structures of major clay mineral groups. Layer charge per formula unit = X.

Argilominerais : Sub-Grupos por Reflexão (060)

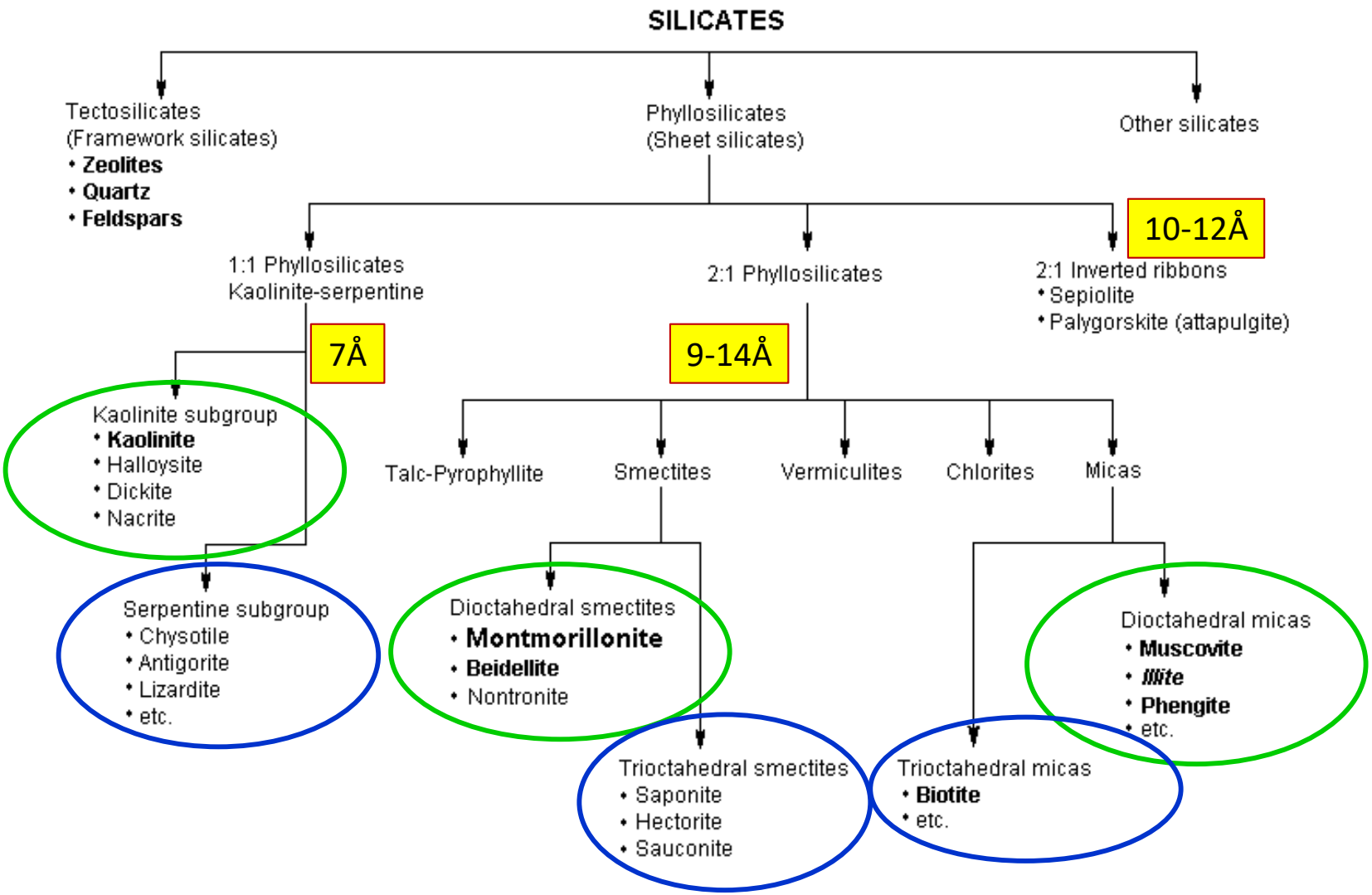

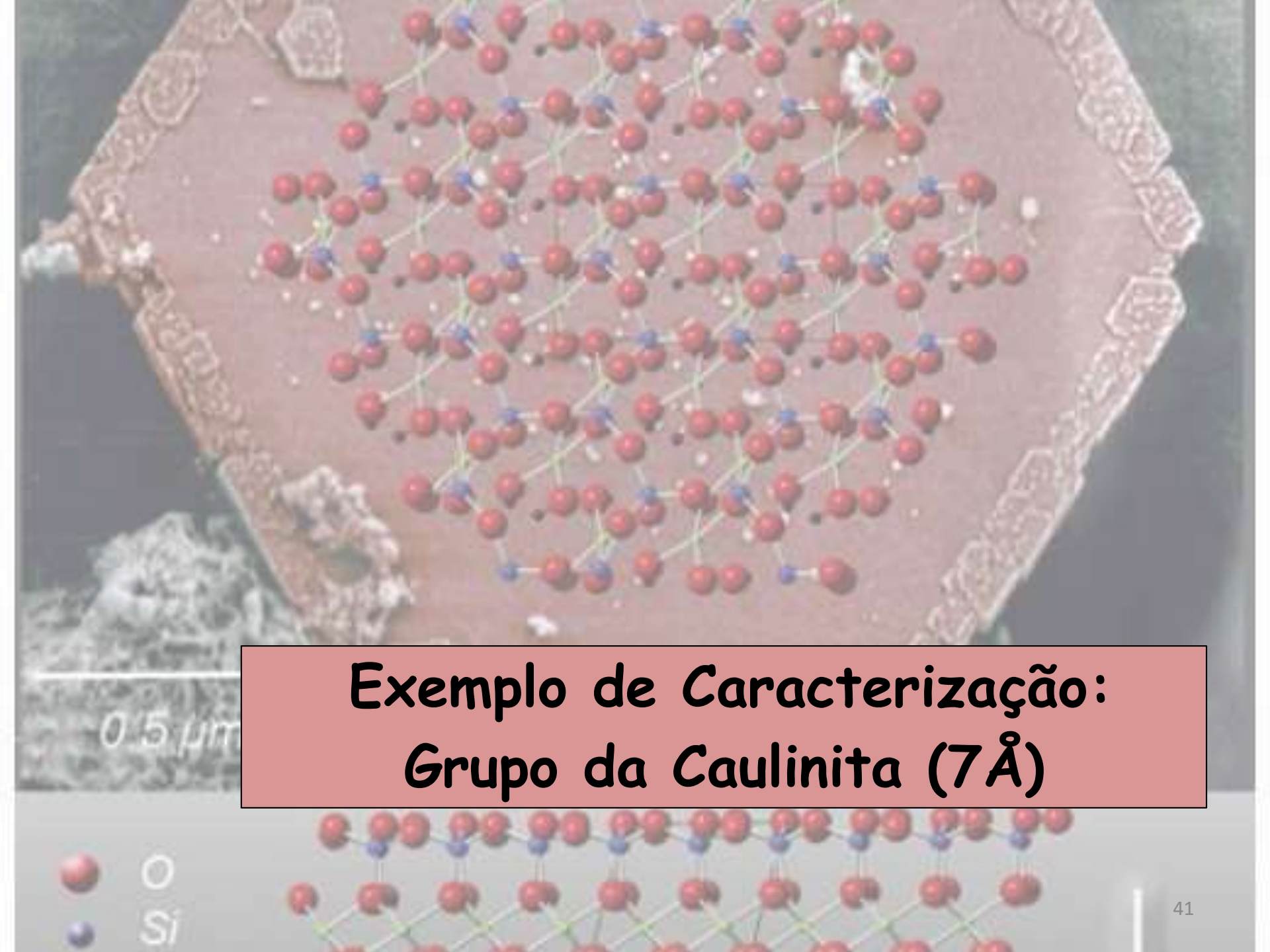

Exemplo de Caracterização: Grupo da Caulinita (7Å)

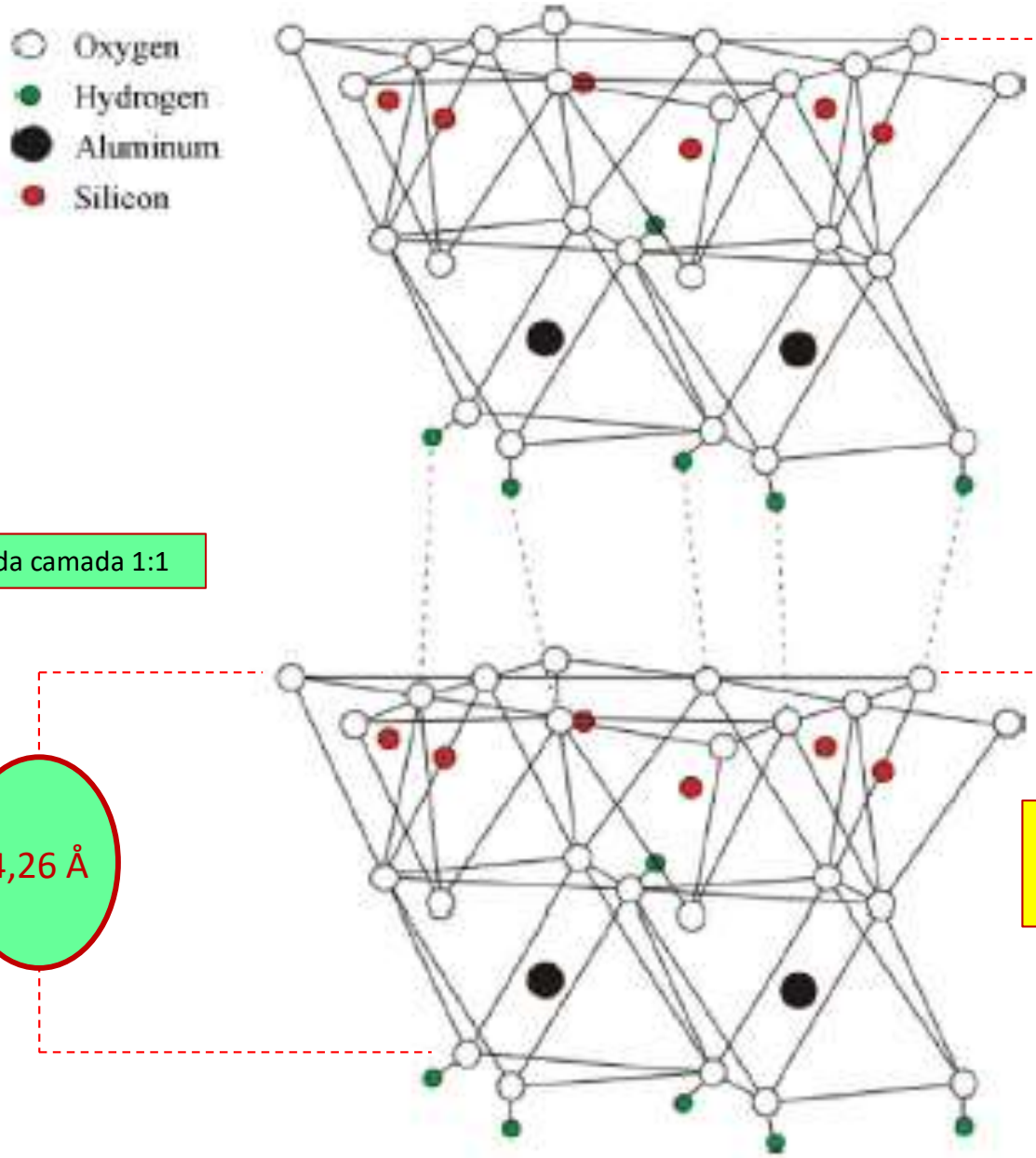

Schematic view of the structure of kaolinite.

7Å

7,1 Å

camada 1:1 +
ligação hidrogênio entre camadas
(camada + espaço interlamelar)

Espessura da camada 1:1

4,26 Å

FIGURE 1 (**Top**) Kaolinite crystal in pseudohexagonal form (false-color image from a scanning electron microscope). Edges are adorned with spiral growth forms, which emphasize the multigenerational nature of kaolin-group minerals. The scale bar is 180 times smaller than the diameter of a human hair. Overlain on top of the crystal (not to scale) is the atomic structure of kaolinite, showing atom locations parallel and perpendicular (**Bottom**) to the sheet structure. The bottom image also shows the repeat distance of the 1:1 layer structure. The scale in lower right is about 125,000 times smaller than the diameter of a human hair.

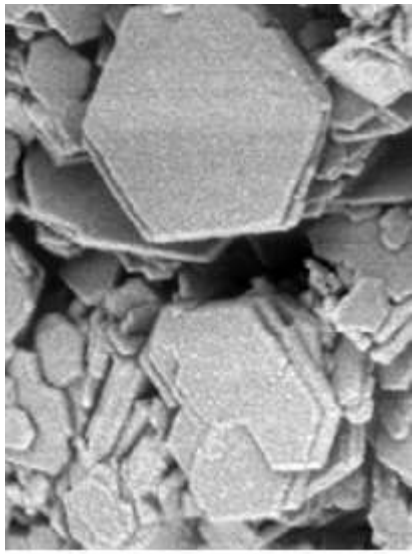

Kaolinite crystals from Twiggs County, Georgia, USA. The largest crystal is 50 µm.

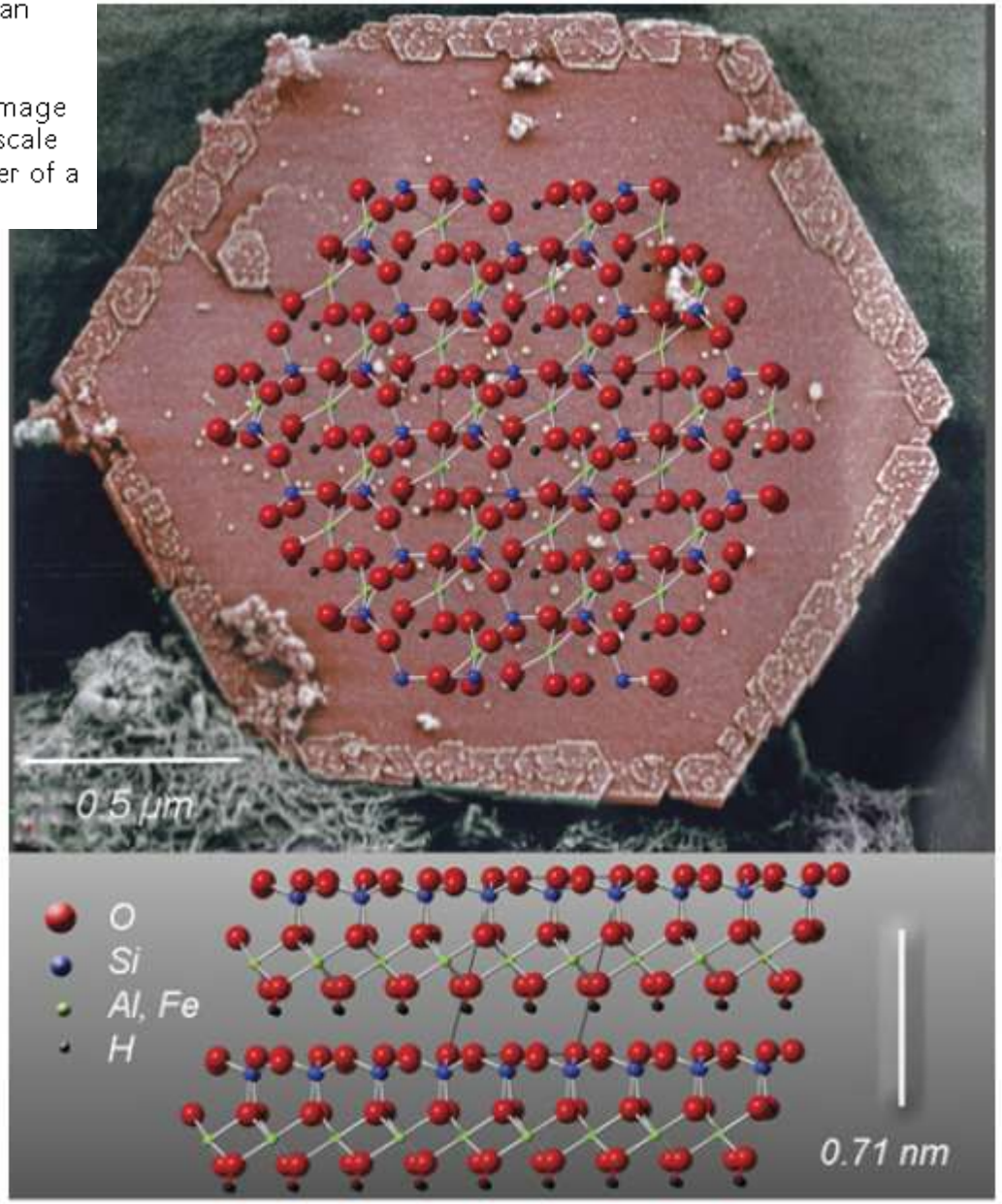

*Schoeder, P.A.; Erickson, G. Elements **10** (3), 177-182 (2014).*

Curvas de DRX
Amostra ORIENTADA

Caulinita
$Al_2Si_2O_5(OH)_4$

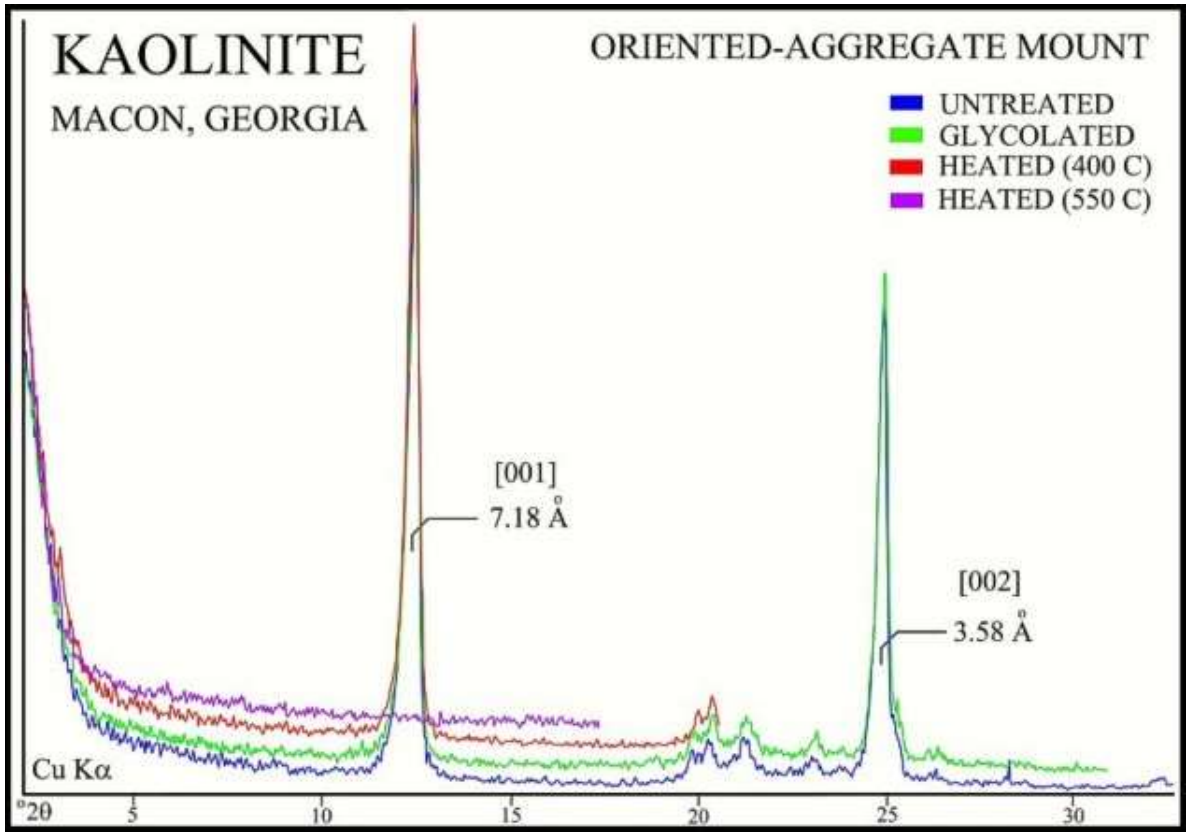

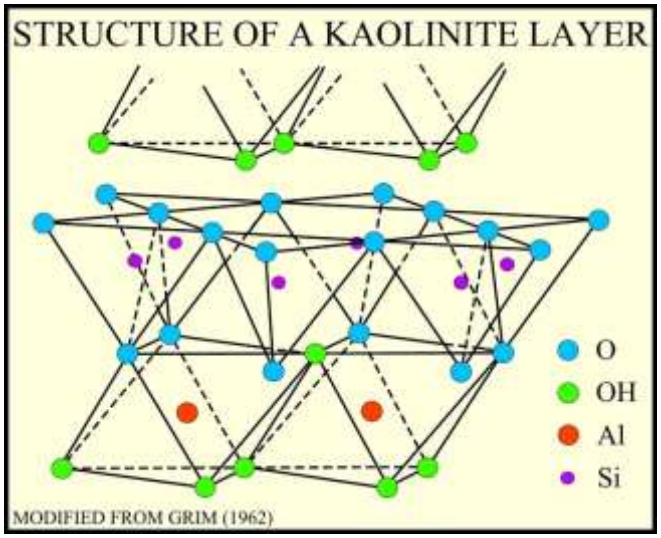

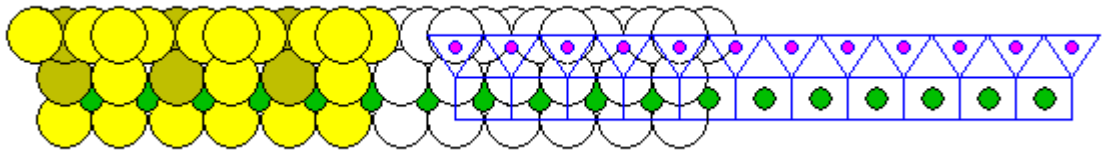

Curvas de DRX
Amostra ORIENTADA

Caulinita
$Al_2Si_2O_5(OH)_4$

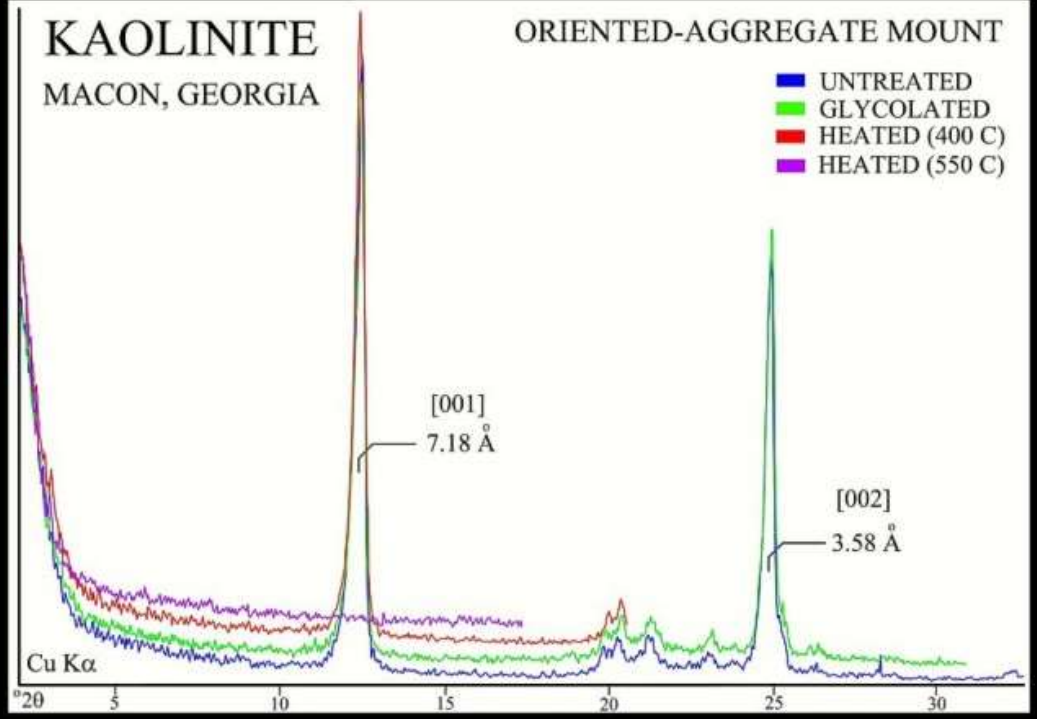

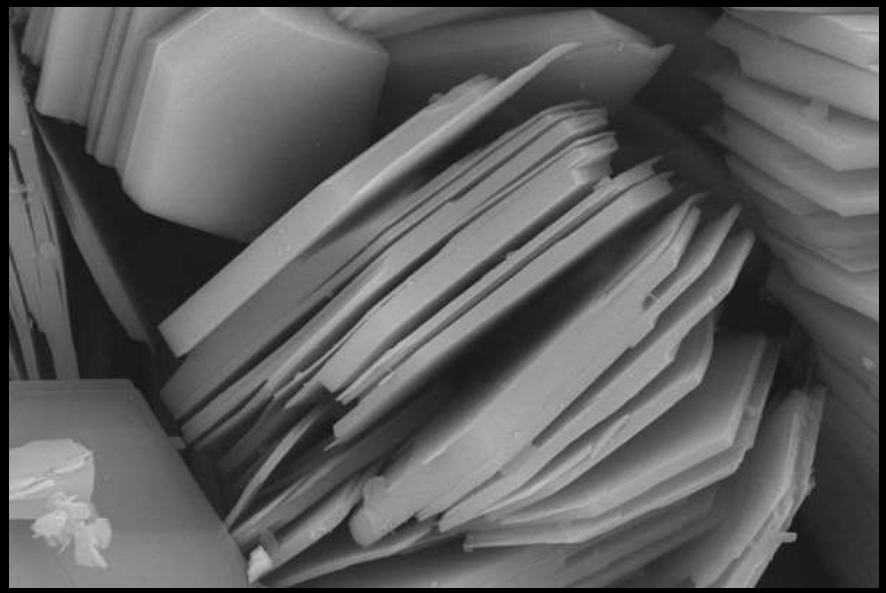

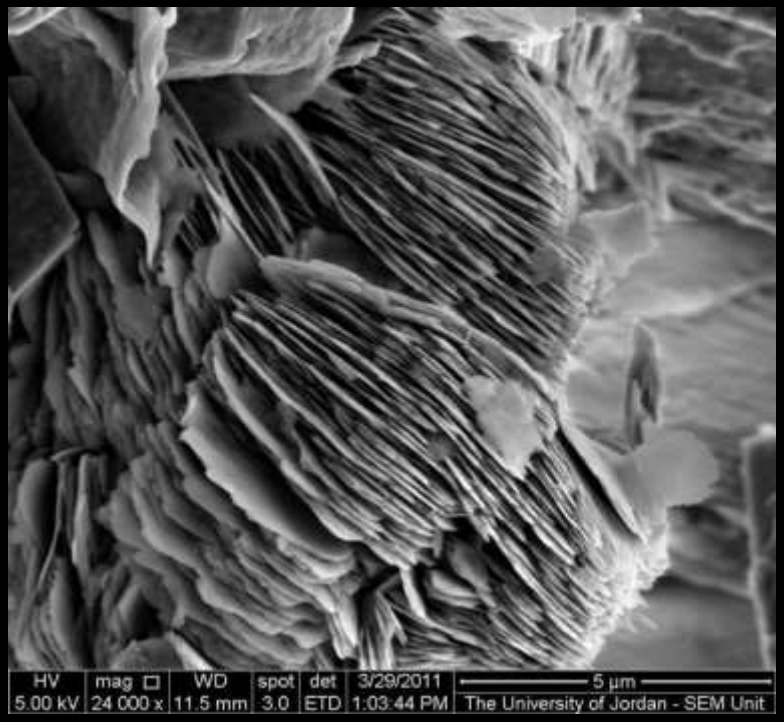

Caulinita – Ordem e Desordem

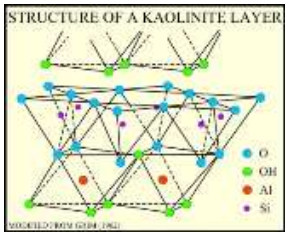

- Kaolin minerals has well-known tendency to form a wide variety of ordered and disordered polytypes.
- The diffraction patterns of ordered kaolinite are significantly different from those of disordered kaolinite.
- **Ordered kaolinite** shows sharp and narrow peaks, while its **disordered** counterpart gives less defined, broad, and asymmetrical peaks.

- **Stacking faults** are mainly produced by disorder of alternating +a/3 and –a/3+b/3 layer displacements. Furthermore, stacking faults can be isolated or form interstratifications of two kinds of multilayer blocks, showing regular a/3 and –a/3+b/3 layer displacements.

Bergaya, F.; Lagaly, G. (Eds.) – Handbook of Clay Science. 2ª Ed. Elsevier. Amsterdam. 2013. cap. 2.

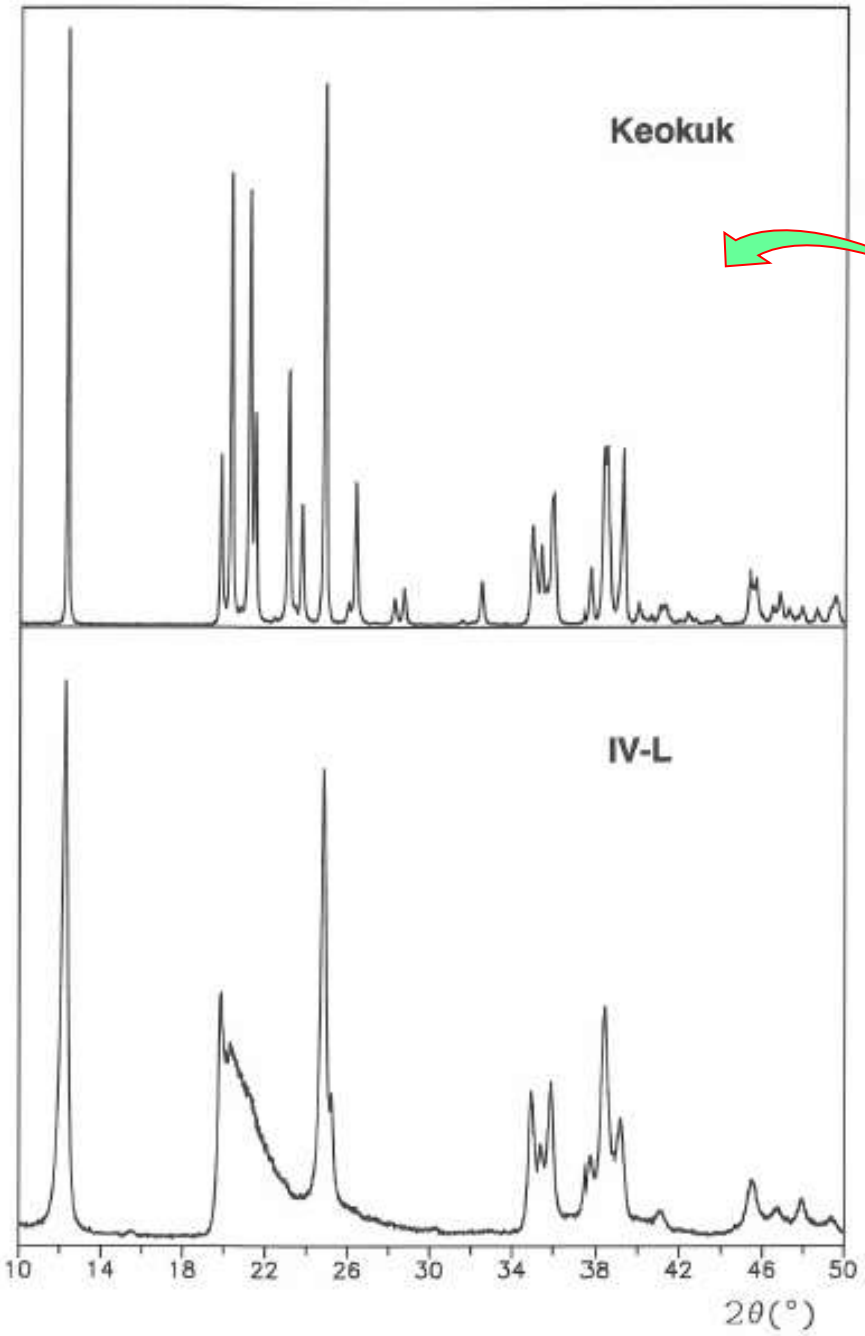

Figure 6. Observed XRD profiles for Keokuk kaolinite (upper) and a kaolinite from Warren County, Georgia. The latter has considerably more defects as shown by the loss of definition in the 02,11 band (19 to 24° 2θ). The differences between the two profiles are less marked for the 20,13 band (34 to 40° 2θ).

Caulim Bem Ordenado
(Keokuk)

Caulim Desordenado
(Georgia, KGa-2)

Caulinita – Ordem e Desordem

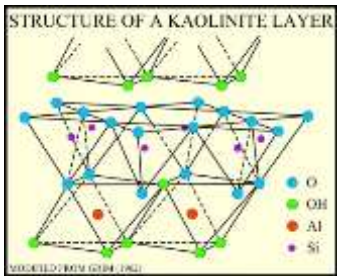

Curvas de DRX de caulinita
com diferentes "cristalinidades"

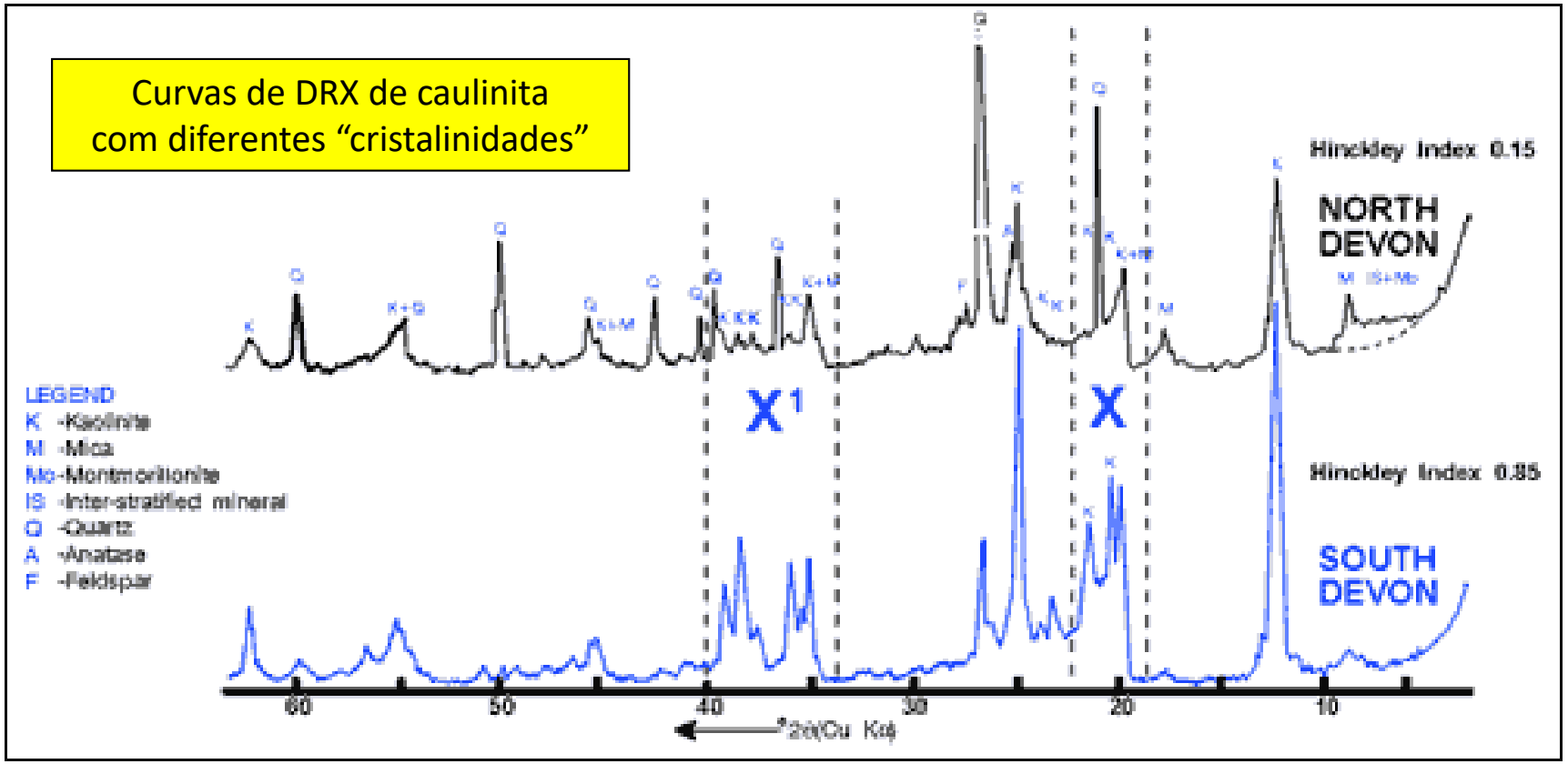

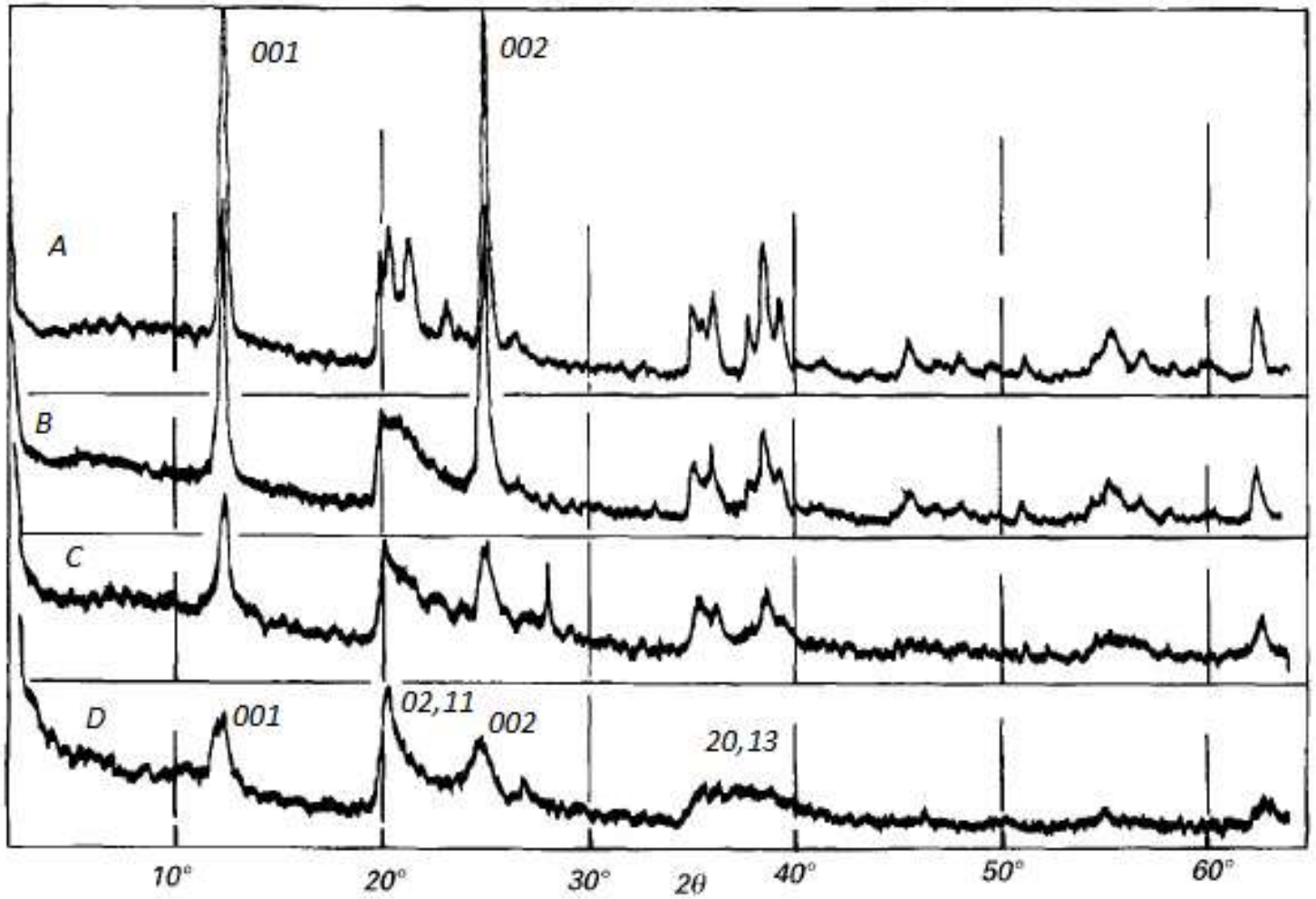

FIG. 1. X-ray powder diffraction patterns of four types of monomineralic kaolin minerals. (a) Well-ordered, well-formed (euhedral) crystals, enhanced basal reflections. (b) Platey crystals with *b*-axis disordered sequence, enhanced basal reflections (disordered kaolinite). (c) Crystals with layer sequence partially disordered with respect to both *a* and *b*-axes, little enhancement of basal reflections, rolled forms (7 Å-halloysite). (d) Crystals with highly disordered layer sequence, no enhancement of basal reflections, tubular forms (7 Å-halloysite). Back-filled rotating sample holder. Cu-$K\alpha$ radiation; 1° 2θ/min.

Souza Santos, P. Clay Minerals 28, 539-553 (1993)

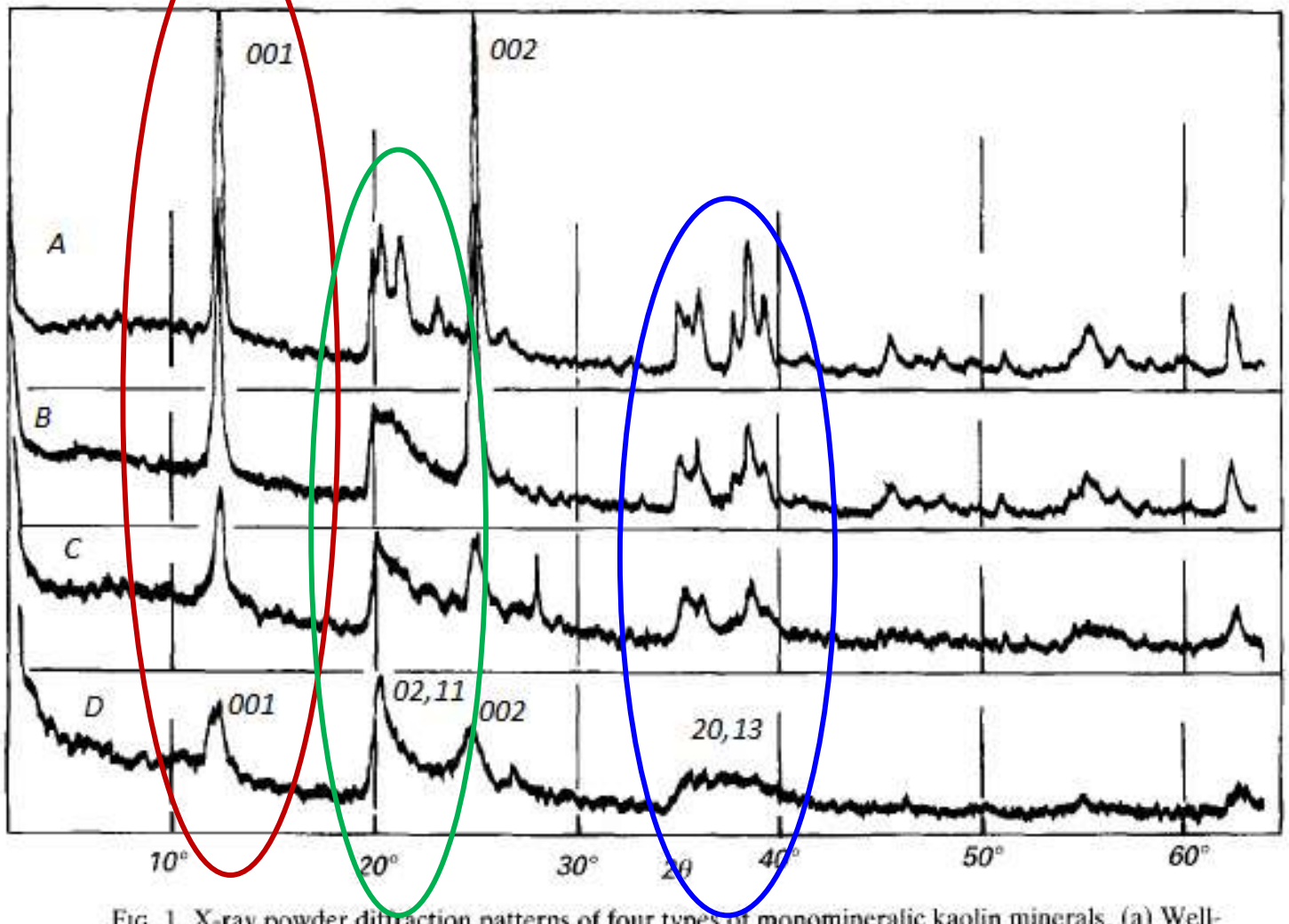

FIG. 1. X-ray powder diffraction patterns of four types of monomineralic kaolin minerals. (a) Well-ordered, well-formed (euhedral) crystals, enhanced basal reflections. (b) Platey crystals with *b*-axis disordered sequence, enhanced basal reflections (disordered kaolinite). (c) Crystals with layer sequence partially disordered with respect to both *a* and *b*-axes, little enhancement of basal reflections, rolled forms (7 Å-halloysite). (d) Crystals with highly disordered layer sequence, no enhancement of basal reflections, tubular forms (7 Å-halloysite). Back-filled rotating sample holder. Cu-$K\alpha$ radiation; 1° 2θ/min.

Caulinita
Ordem e Desordem

Stacking faults are mainly produced by disorder of alternating +a/3 and –a/3+b/3 layer displacements. Furthermore, stacking faults can be isolated or form interstratifications of two kinds of multilayer blocks, showing regular a/3 and –a/3+b/3 layer displacements.

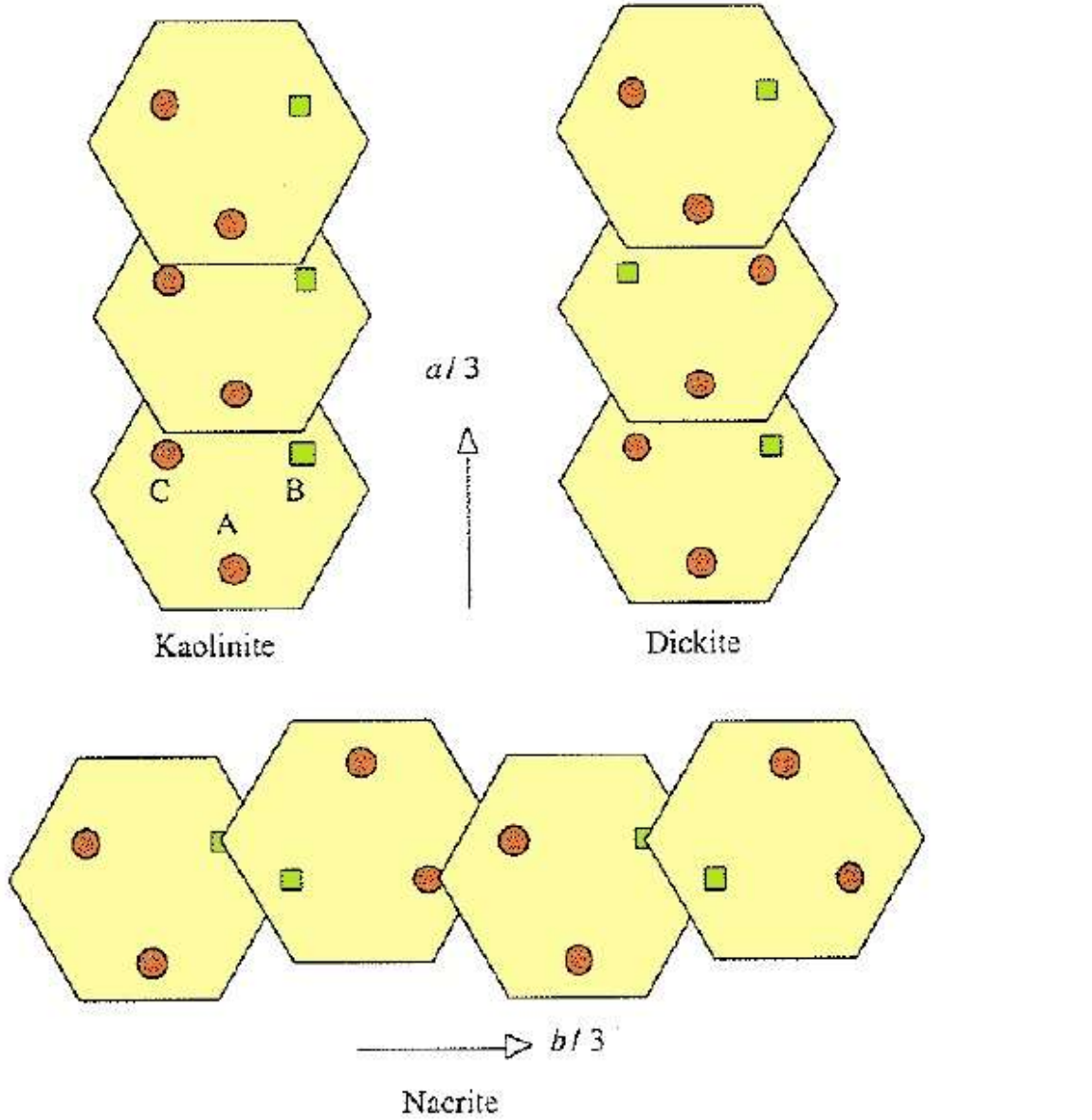

Stacking sequences in kaolinite, dickite, and nacrite viewed normal to the (001) plane. Filled circles represent occupied octahedral sites. Squares depict the vacant site. Translation magnitudes have been exaggerated for clarity.

Moore, D.M..; Reynolds, R.C.– X-Ray Diffrction and the Identification and Analysis of Clay Minerals 2ª Ed. Oxford University Press. 1997.

Caulinita – "Índices de Cristalinidade"

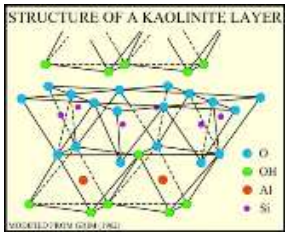

- Structural order/disorder in kaolinite can be assessed by means of different methods.
- The most widely used are those based on changes in two groups of XRD reflections, that is, the 02ℓ and 11ℓ sequences that are sensitive to arbitrary and special interlayer displacements (such as b/3) and the 13ℓ and 20ℓ sequences that are affected by arbitrary displacements (Cases et al., 1982).
- Several indices have been developed to quantify the degree of structural order in kaolinite:
  - the **Hinckley** index (HI) (1963) ;
  - the **Range–Weiss** index (QF) (1969);
  - the **Stoch** index (IK) (1974) which is measured in the same zone as the previous two indices but is less sensitive to the presence of quartz;
  - the **Liétard** index (R2) (1977) which is sensitive to the presence of arbitrary defects only.

Bergaya, F.; Lagaly, G. (Eds.)– Handbook of Clay Science. 2ª Ed. Elsevier. Amsterdam. 2013

Caulinita – "Índices de Cristalinidade"

Índice de Hinckley

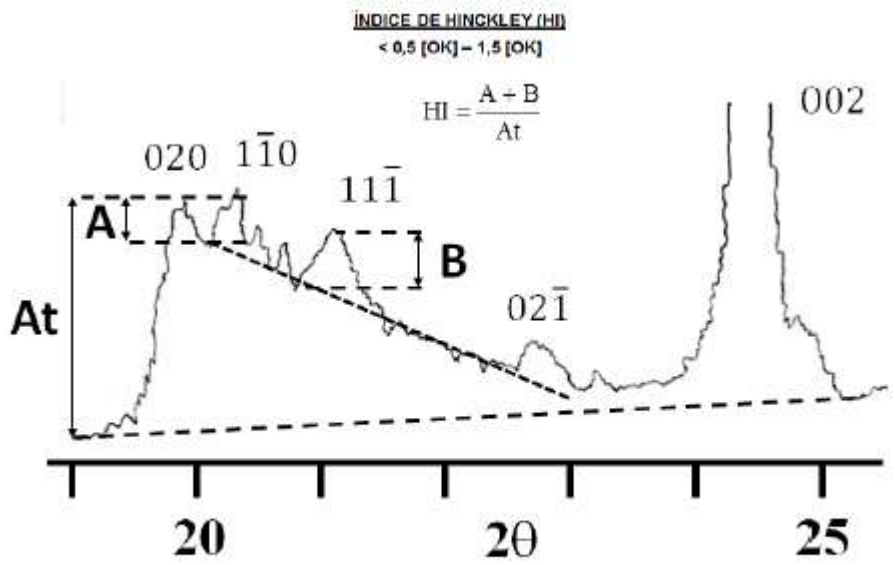

Cálculo do índice de Hinckley no DRX da caulinita
FONTE: KOGURE et al. (2010); PTÁČEK et al. (2013).

Índice de Range e Weiss

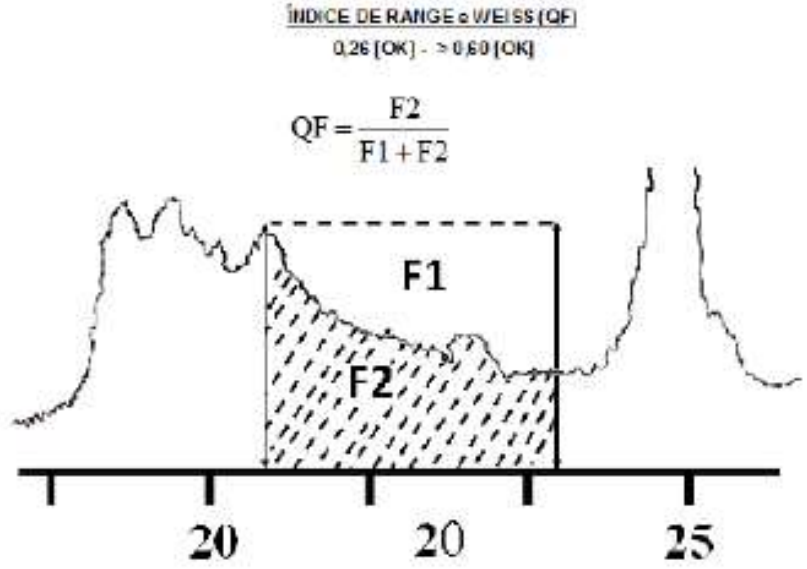

Cálculo dos índices de Range e Weiss no DRX da caulinita. FONTE: BRIGATTI et al. (2006).

Caulinita – "Índices de Cristalinidade"

Índice R2 de Lièтard

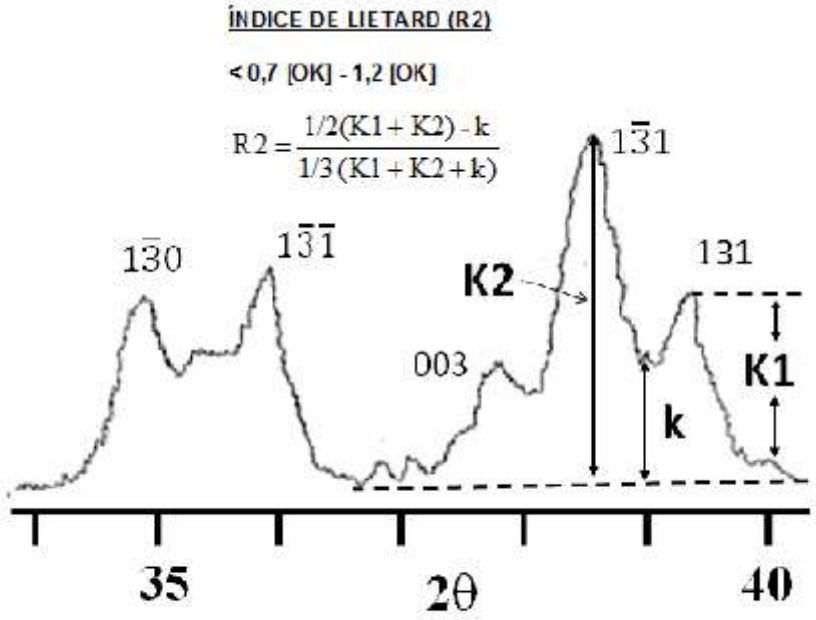

Cálculo do índice de Lietárd do DRX da caulinita.
FONTE: APARÍCIO et al. (2006).

Índice de Stoch

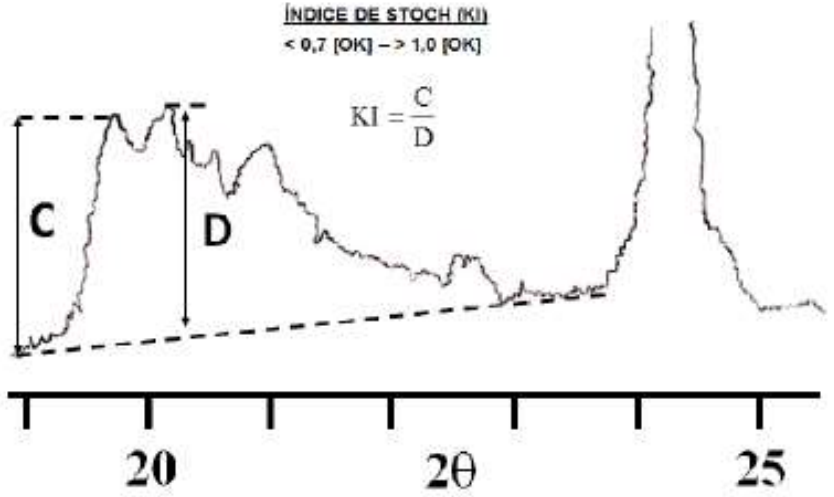

Cálculo do índice de Stoch no DRX da caulinita.
FONTE: APARÍCIO et al. (2006).

Caulinita – "Índices de Cristalinidade"

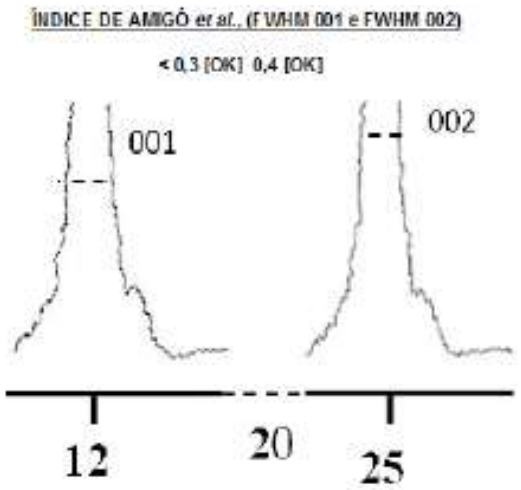

Índice de Amigó

Cálculo do índice de Amigó no DRX da caulinita. FONTE: APARÍCIO et al. (2006).

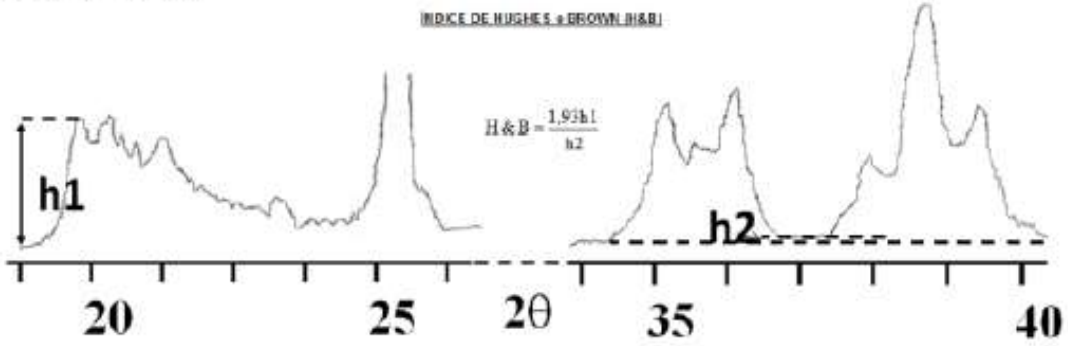

Índice de Hughes e Brown

Cálculo do índice de Hughes e Brown no DRX da caulinita. FONTE: GIAROLA et al., (2009); WISAWAPIPAT et al., (2010).

Caulinita – "Índices de Cristalinidade"

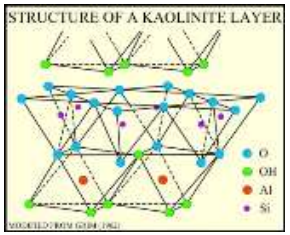

- **Aparicio and Galán** (1999) investigated the influence of mineral and amorphous phases, associated with kaolin and kaolinitic rock, on kaolinite order–disorder measurements by XRD.
- Both the **Hinckley** and **Range–Weiss** indices appear to be influenced by quartz, feldspar, iron gels, illite, smectite, and halloysite.
- On the other hand, the **Stoch** index can be used in the presence of quartz, feldspar, iron, and silica gels, while the **Liétard** index is not affected by phases other than halloysite.
- As a result, Aparicio et al. (2006) proposed the **Aparicio–Galán–Ferrell** index, which is derived from the intensity of reflections in the 02l and 11l sequence and obtained by pattern fitting, as being less influenced by peak overlap.
- **Plançon and Zacharie** (1990) proposed an 'expert system' based on direct measurements of the diffraction pattern. The results of this system are acceptably consistent with the theoretical and experimental diffraction patterns for kaolinite.

Caulinita – “Índices de Cristalinidade”

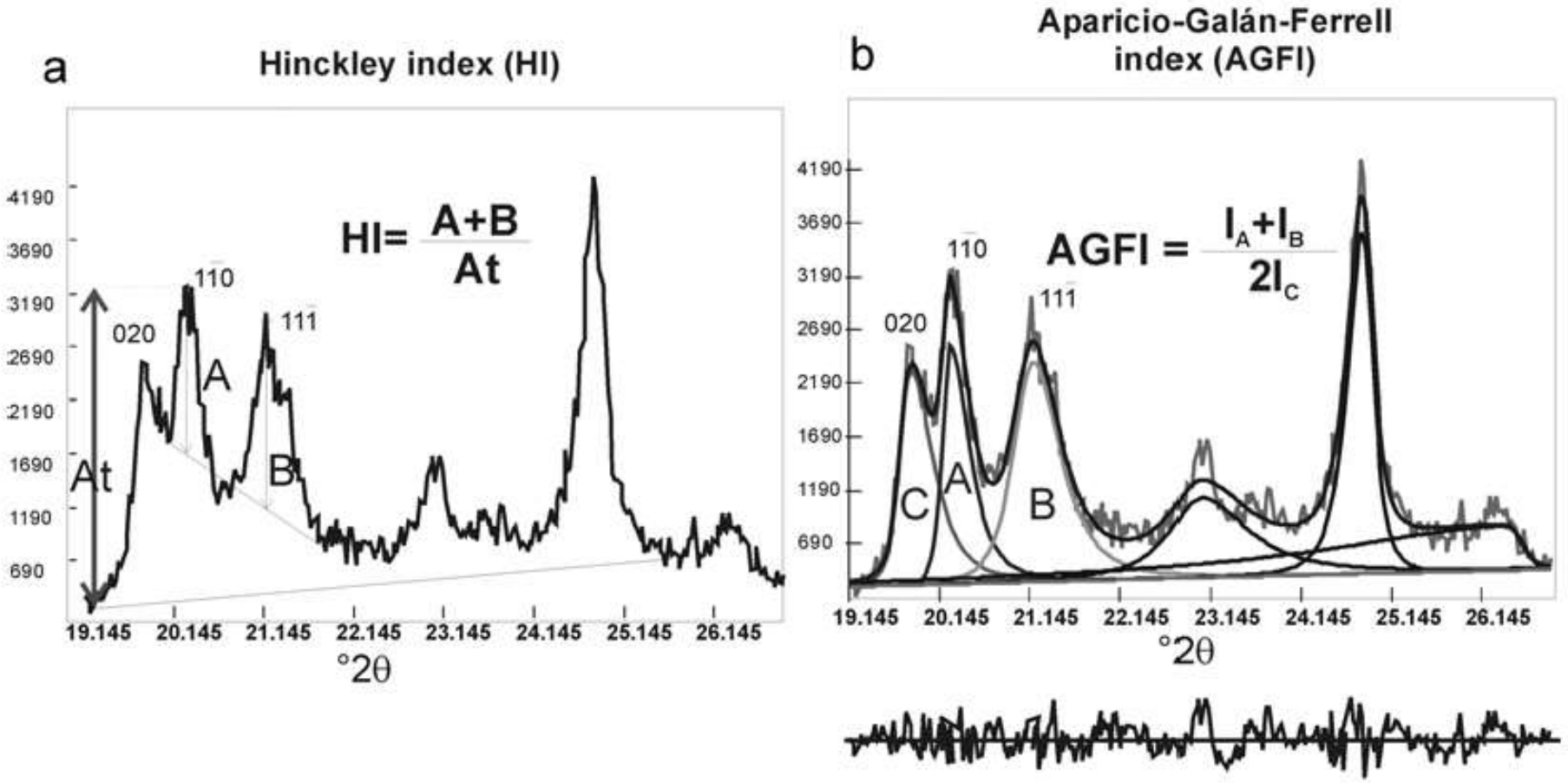

FIG. 1. KCI determinations: (a) Hinckley index; (b) Aparicio-Galán-Ferrell index (AGFI).

Caulinita – "Índices de Cristalinidade"

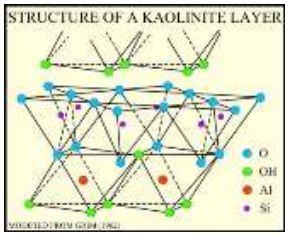

- The **expert system** provides a quantitative assessment of translational defects of kaolinite but does not distinguish between the t_0 translation (roughly t_1– b/3) and the t_2 translation (roughly t_1+b/3).
- This method identifies the number of different phases in the sample (one or two phases) and, for bi-phase samples, it establishes the percentage of low-defect or well-crystallized phases (% wp).
- In the case of single-phase samples, it fixes the amount of C layers (W_C), the variation of interlayer translations about the mean values (d), the proportion of translation defects (p), and the mean number of layers (M).
- **Aparicio and Galán** (1999) suggested that the 'expert system' I s the best method for determining the degree of order–disorder in kaolinite, although it is highly affected by the presence of other phases, particularly when more than 25% of well-crystallized kaolinite is present. However, the system can be used with single-phase kaolinite (disor dered kaolinite).

Bergaya, F.; Lagaly, G. (Eds.)– Handbook of Clay Science. 2ª Ed. Elsevier. Amsterdam. 2013

Caulinita – "Índices de Cristalinidade"

Índice de Plançon e Zacharie

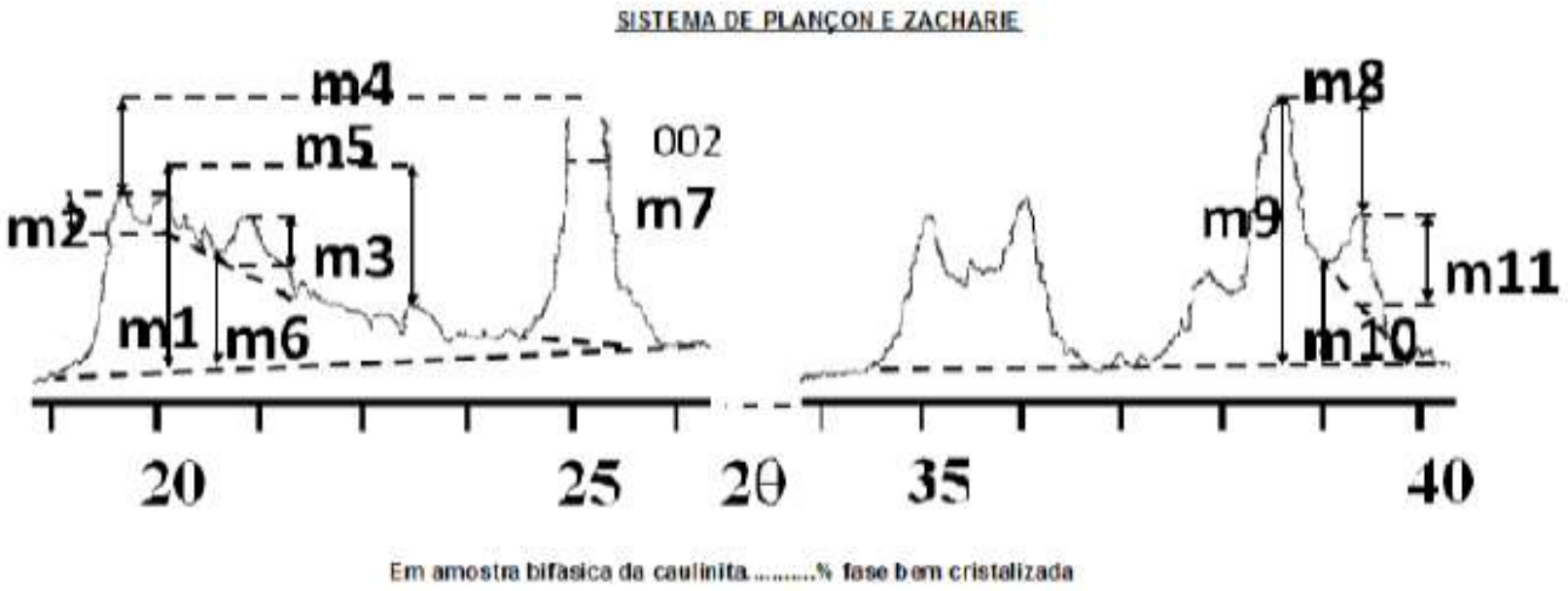

Cálculo do índice de Plançon e Zacharie no DRX da caulinita. FONTE: APARÍCIO et al. (2006).

Curvas de DRX
Amostra ORIENTADA

Diquita (Dickite)
$Al_2Si_2O_5(OH)_4$

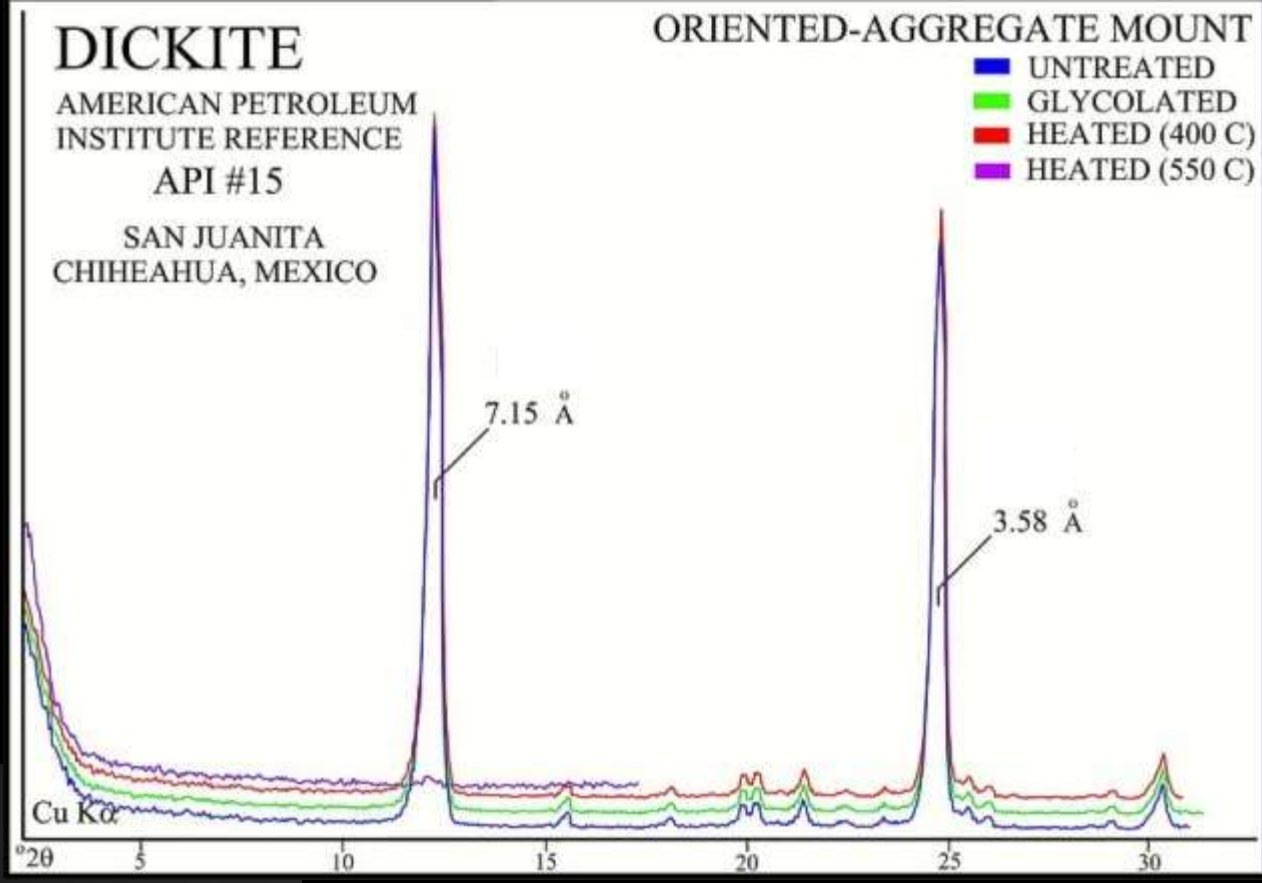

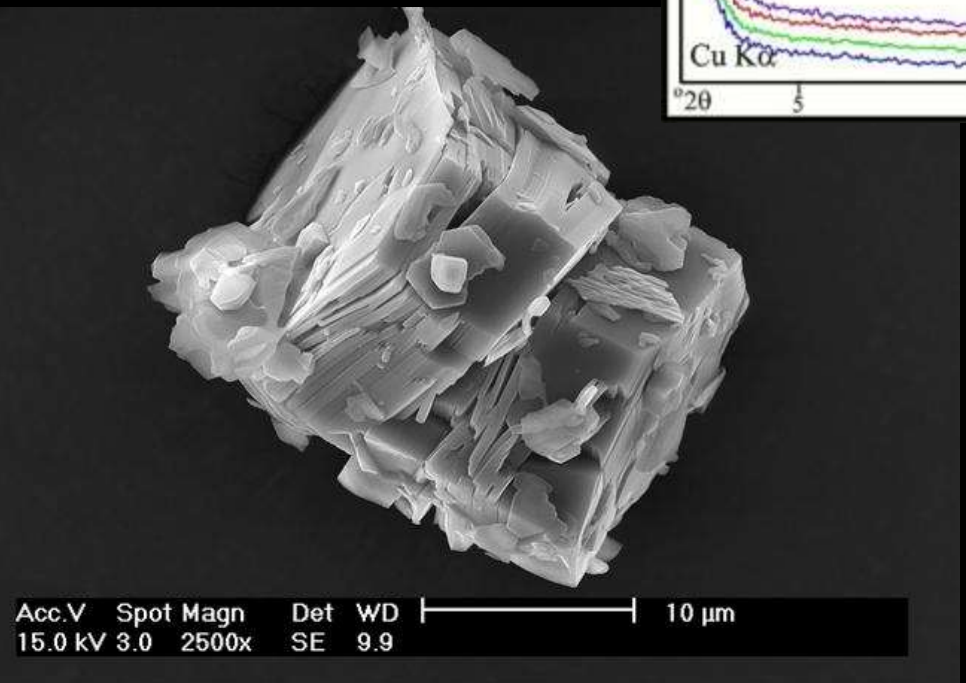

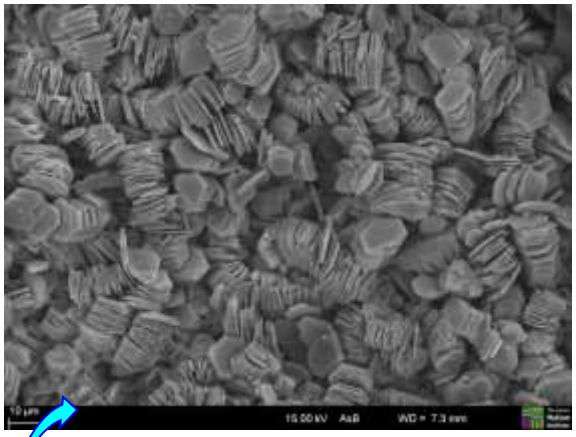

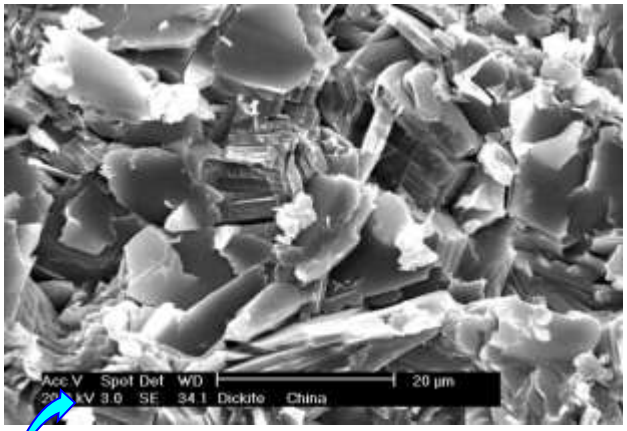

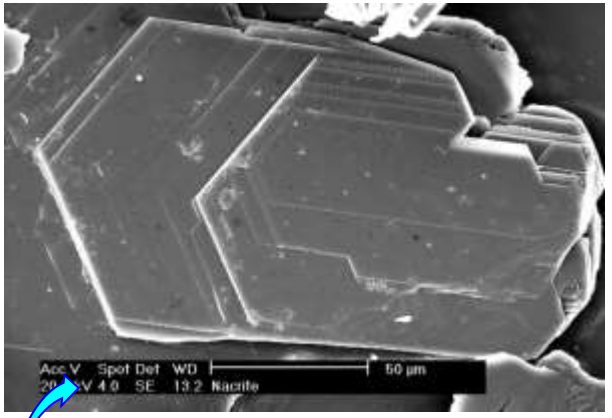

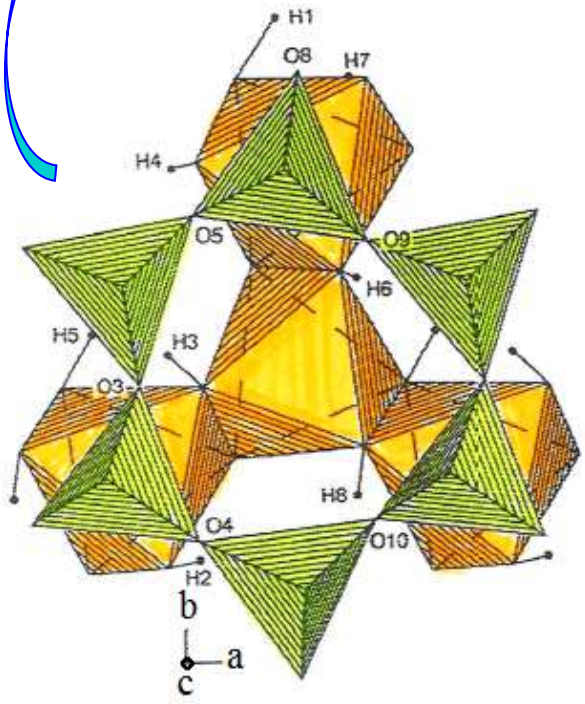

Kaolinite

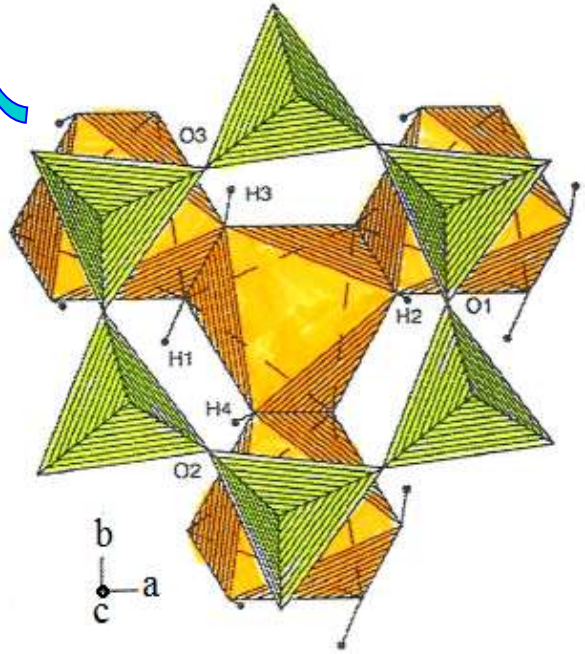

Dickite

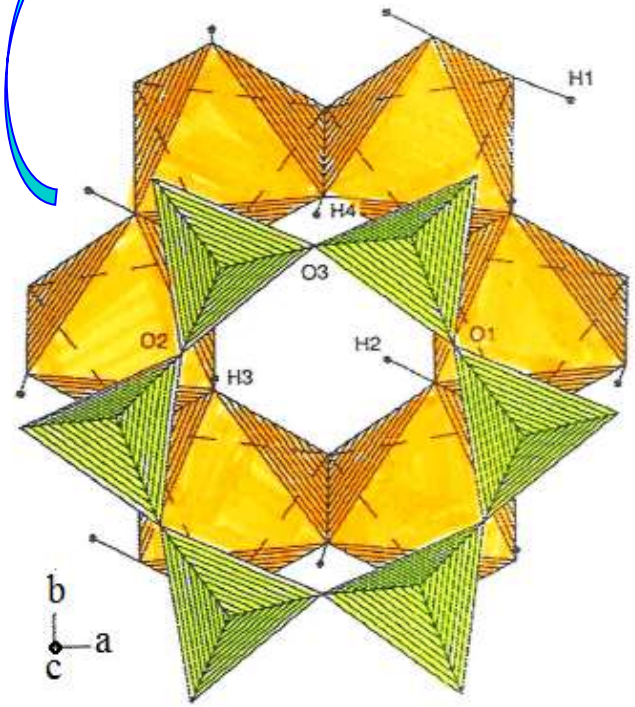

Nacrite

Figure 5. Projections of the structure of kaolinite (a), dickite (b), and nacrite (c) onto (001) showing the octahedral sheet of one layer and the tetrahedral sheet of the layer lying above. The hydroxyl hydrogen positions for kaolinite are from Young and Hewat (1988), for dickite are from Joswig and Drits (1986), while for nacrite the positions are those calculated by Giese and Datta (1973) from electrostatic energy calculations.

*Giese, R.F. Reviews in Mineralogy **19**, chap. 3*

Haloisita

Named after the Belgian geologist
Jean-Baptiste d'Omalius d'Halloy,
(February 16th 1783 - January 15th 1875),
who discovered the mineral.
He was a nobleman, a statesman,
and pioneer of modern geology in Belgium.

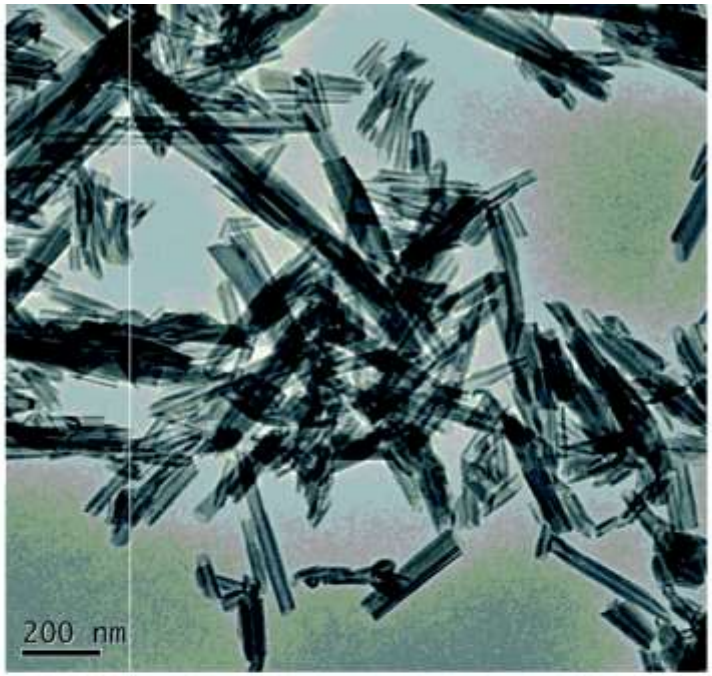

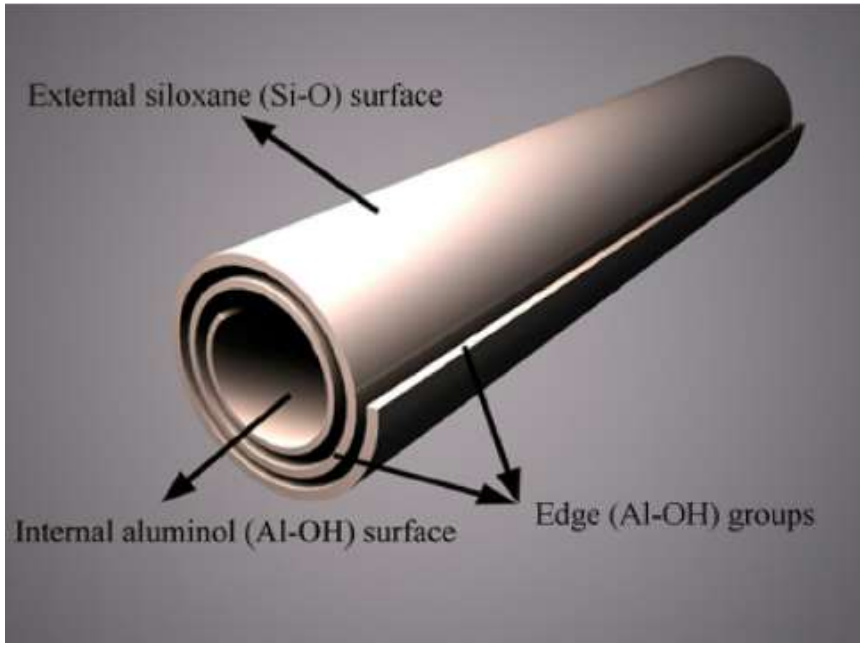

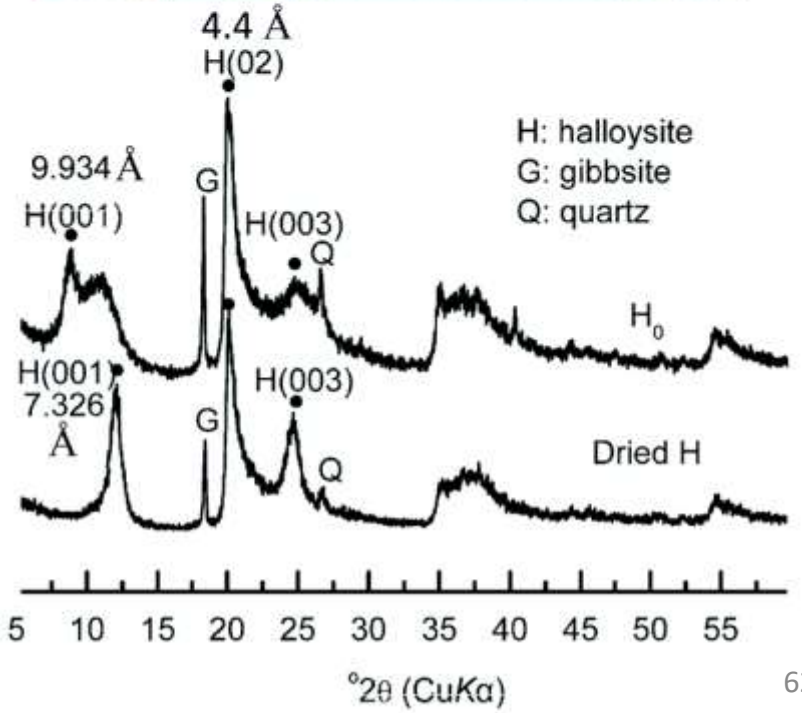

Haloisita

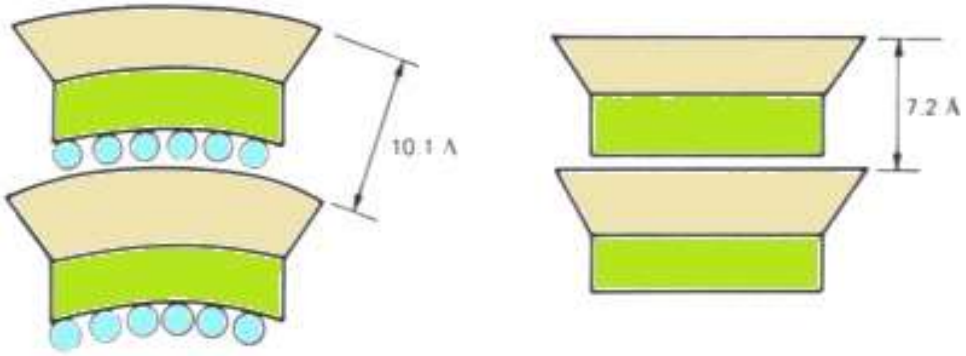

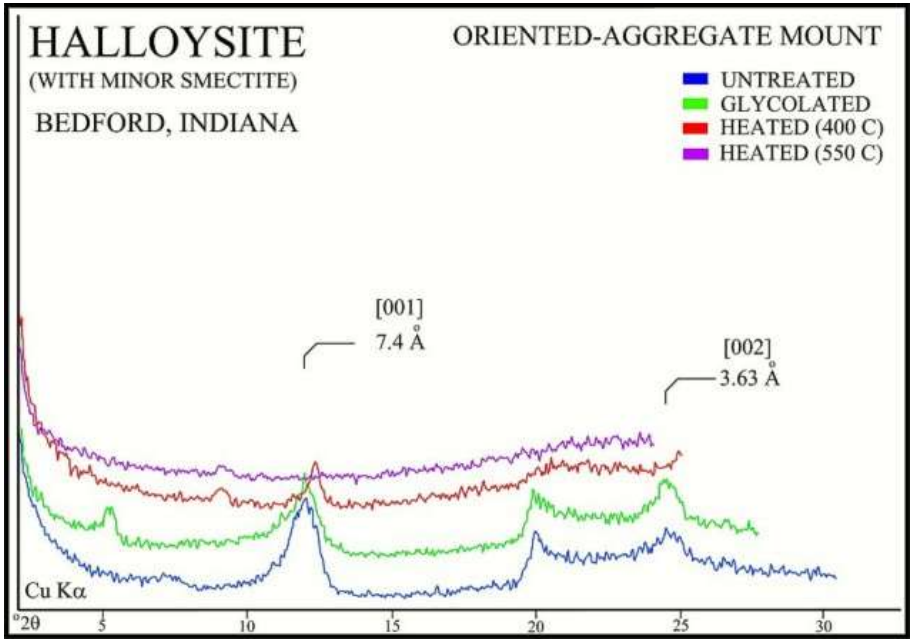

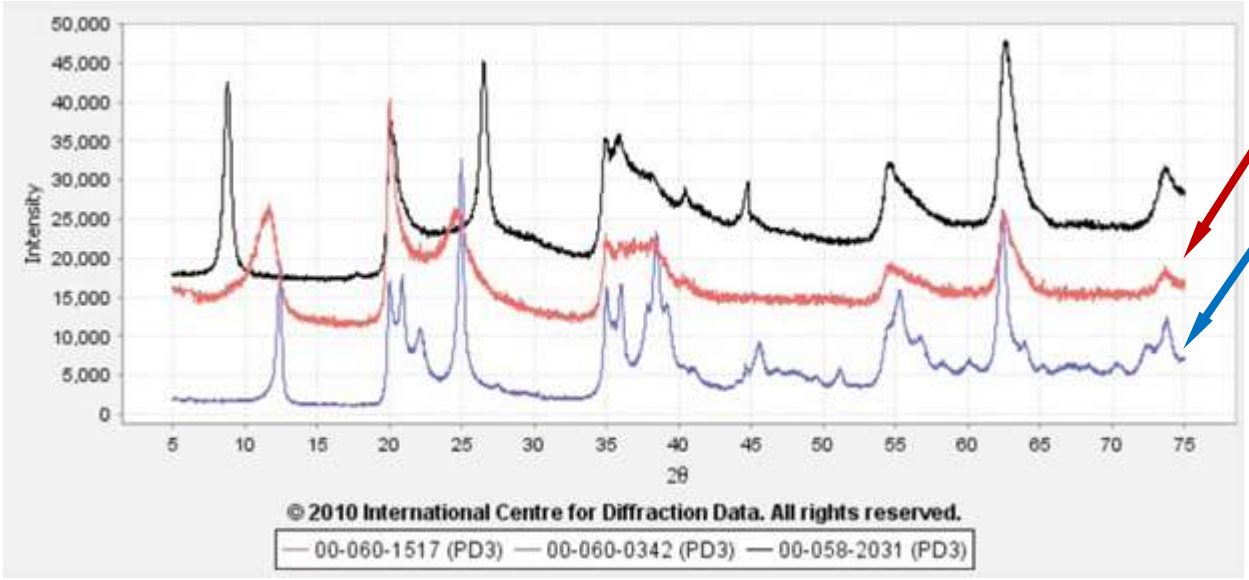

Haloisita 10Å
$Al_2Si_2O_5(OH)_4.2(H_2O)$
Haloisita 7Å
$Al_2Si_2O_5(OH)_4$

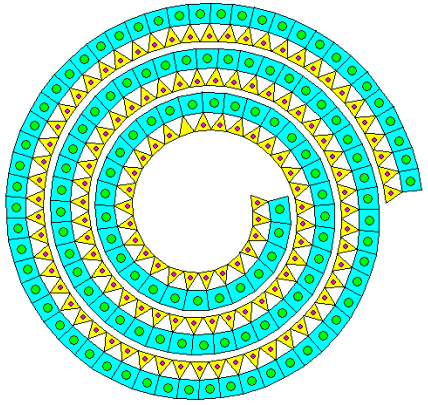

Table SUMMARY OF NOMENCLATURE AND CLASSIFICATION OF KAOLIN-GROUP MINERALS

	Kaolinite	Halloysite	Nacrite	Dickite
Crystal shape (SEM image)	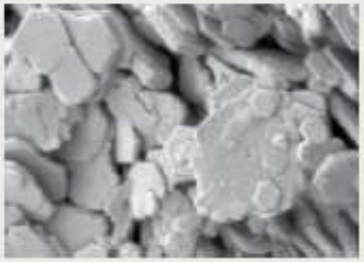		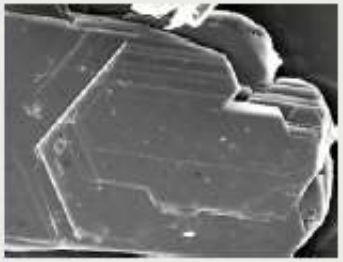	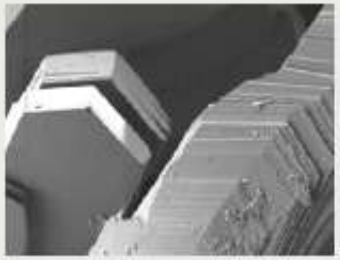
Space group Unit-cell parameters	$C\bar{1}$ $a = 0.5154$ nm $b = 0.8942$ nm $c = 0.7402$ nm $\alpha = 91.69°$ $\beta = 104.61°$ $\gamma = 89.92°$	Cc $a = 0.51$ nm $b = 0.89$ nm $c = 2.07$ nm $\alpha = 99.7°$	Cc $a = 0.8906$ nm $b = 0.5146$ nm $c = 1.5664$ nm $\beta = 113.58°$	Cc $a = 0.5137$ nm $b = 0.8918$ nm $c = 1.4389$ nm $\beta = 96.74°$
(reference)	Bish (1993)	Joussein et al. (2005)	Zheng and Bailey (1994)	Joswig and Drits (1986)
Structural views of hydroxyl orientations in octahedral sheet H = black, O = red Al = green	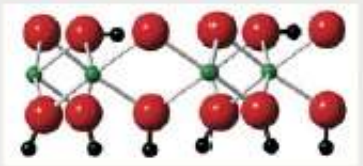	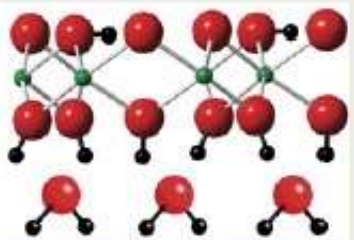	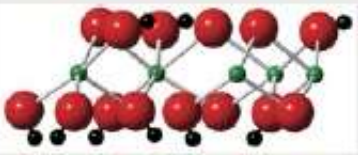	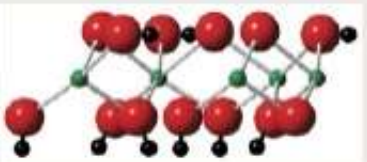
Environmental occurrences	Weathered volcanic ash, pumice, granite, laterites, shales, sandstones	Weathered volcanic ash, pumice, granite, hot springs, hydrothermal systems	Hydrothermal systems (rare)	Diagenesis, hydrothermal systems

The differences among the kaolin-group minerals result from the distribution of vacancies in the octahedral sheet and nature of stacking shifts (Kogure et al. 2005). In kaolinite and halloysite, the directions of the 1:1 interlayer shift are easily disordered, which results in a wide range of stacking order (informally referred to as high to low crystallinity). Disorder is commonly distinguished in X-ray diffraction by peak broadening of the $k \neq 3n$ region of the pattern, but it is also seen in infrared spectra, electron diffraction patterns, and dehydroxylation temperatures. Halloysite is influenced by the substitution of larger Fe^{3+} for Al^{3+}, creating a misfit of the 1:1 layers and causing them to curl into tube- and sphere-like forms (Joussein et al. 2005). Halloysite expands and accommodates interlayer H_2O molecules (schematically shown above). Most importantly, the kaolin-group minerals display a wide range of crystal shapes and surfaces, all affecting their hydroxyl-group orientations and hence their physical-chemical properties.

Detellier, C.; Schoonheydt, R.A. *Elements* **10** (3), 201-206 (2014).

Grupo da Caulinita - IR

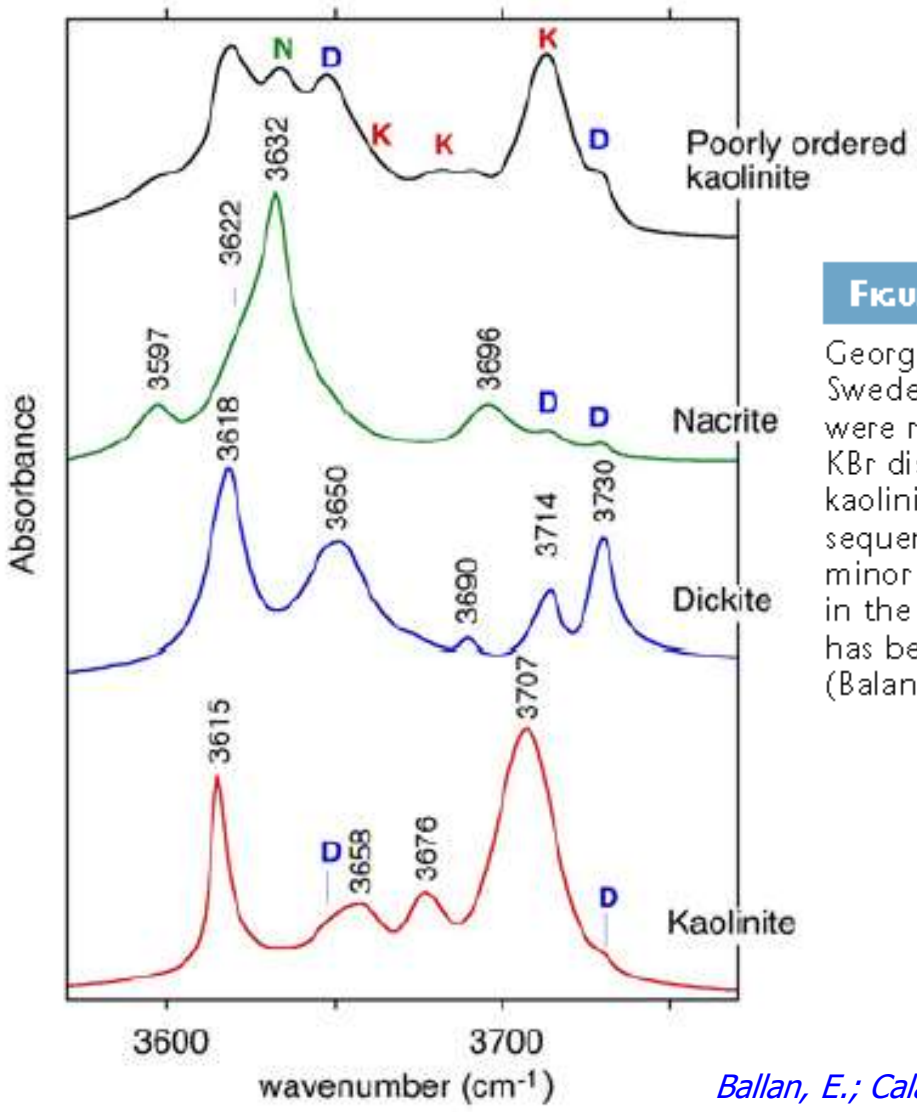

FIGURE 3 Low-temperature infrared absorption spectra of kaolin-group mineral samples: kaolinite (KGa-1) from Georgia, USA; dickite from Nowa Ruda, Poland; nacrite from Sweden; poorly ordered kaolinite from Manaus, Brazil. The spectra were recorded at 10 K in transmission geometry using dilution in KBr disks. The poorly ordered sample reveals contributions from kaolinite-like (K), dickite-like (D), and nacrite-like (N) stacking sequences. The ordered nacrite and kaolinite samples also reveal minor contributions from dickite. The band at 3690 cm^{-1} observed in the dickite sample displays a distinct anharmonic character that has been tentatively ascribed to a kaolinite-like configuration (Balan et al. 2010).

*Ballan, E.; Calas, G.; Bish, D.L. Elements **10** (3), 183-188 (2014).*

...somente para diferenciar...

Exemplos de 7Å Trioctaédricos

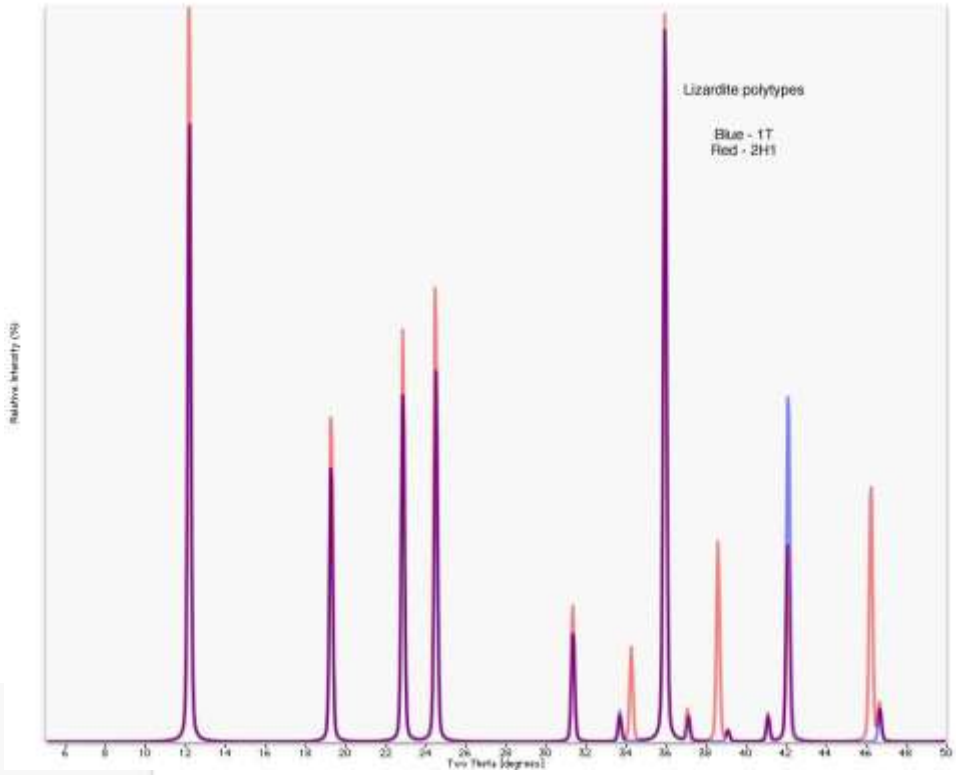

Antigorita
$Mg_3Si_2O_5(OH)_4$
Trioctaédrica

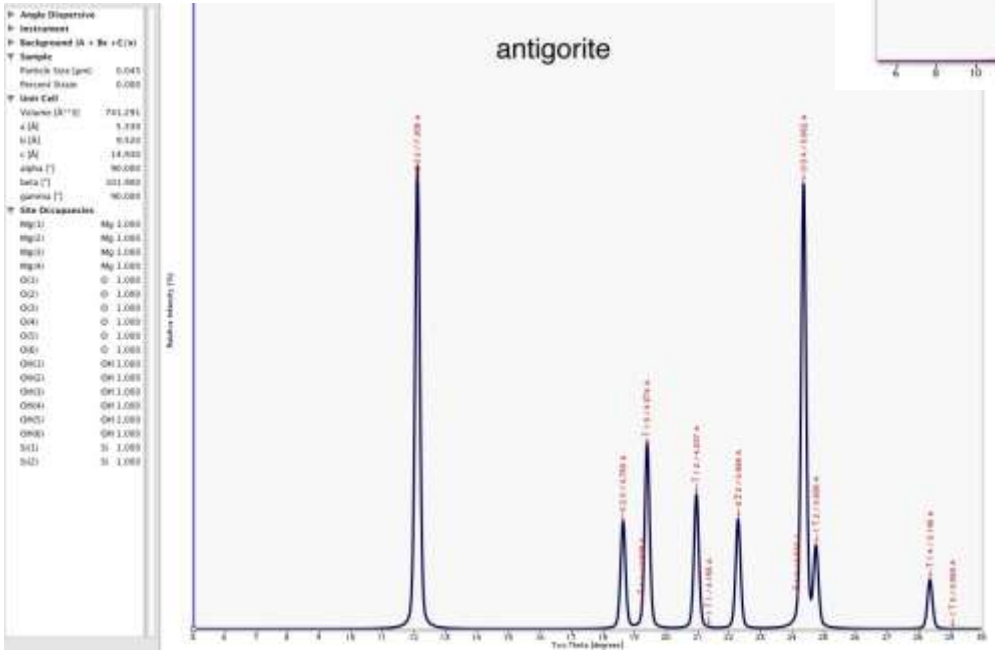

Lizardita
$Mg_3Si_2O_5(OH)_4$
Trioctaédrica

7 Å – Argilominerais 1:1

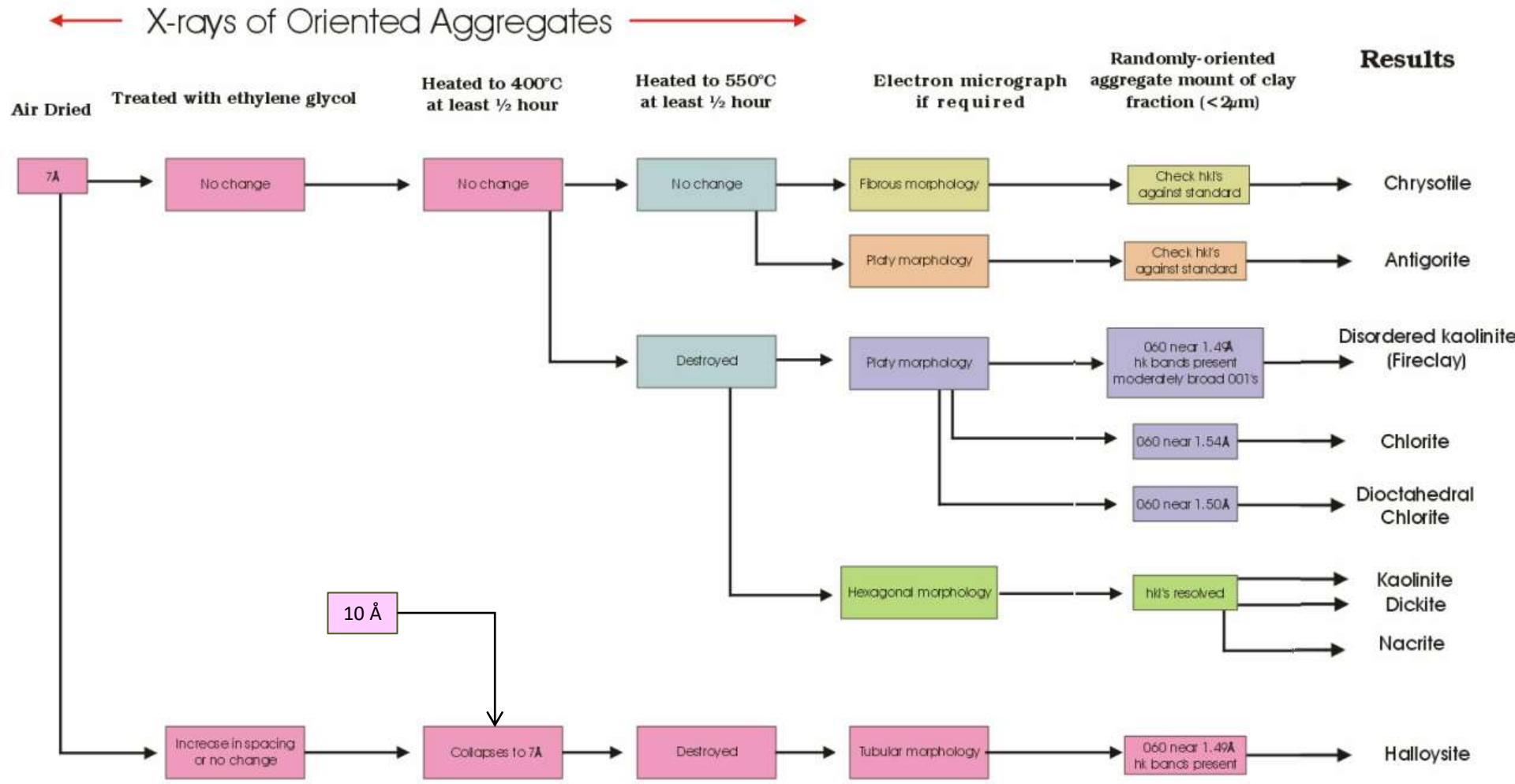

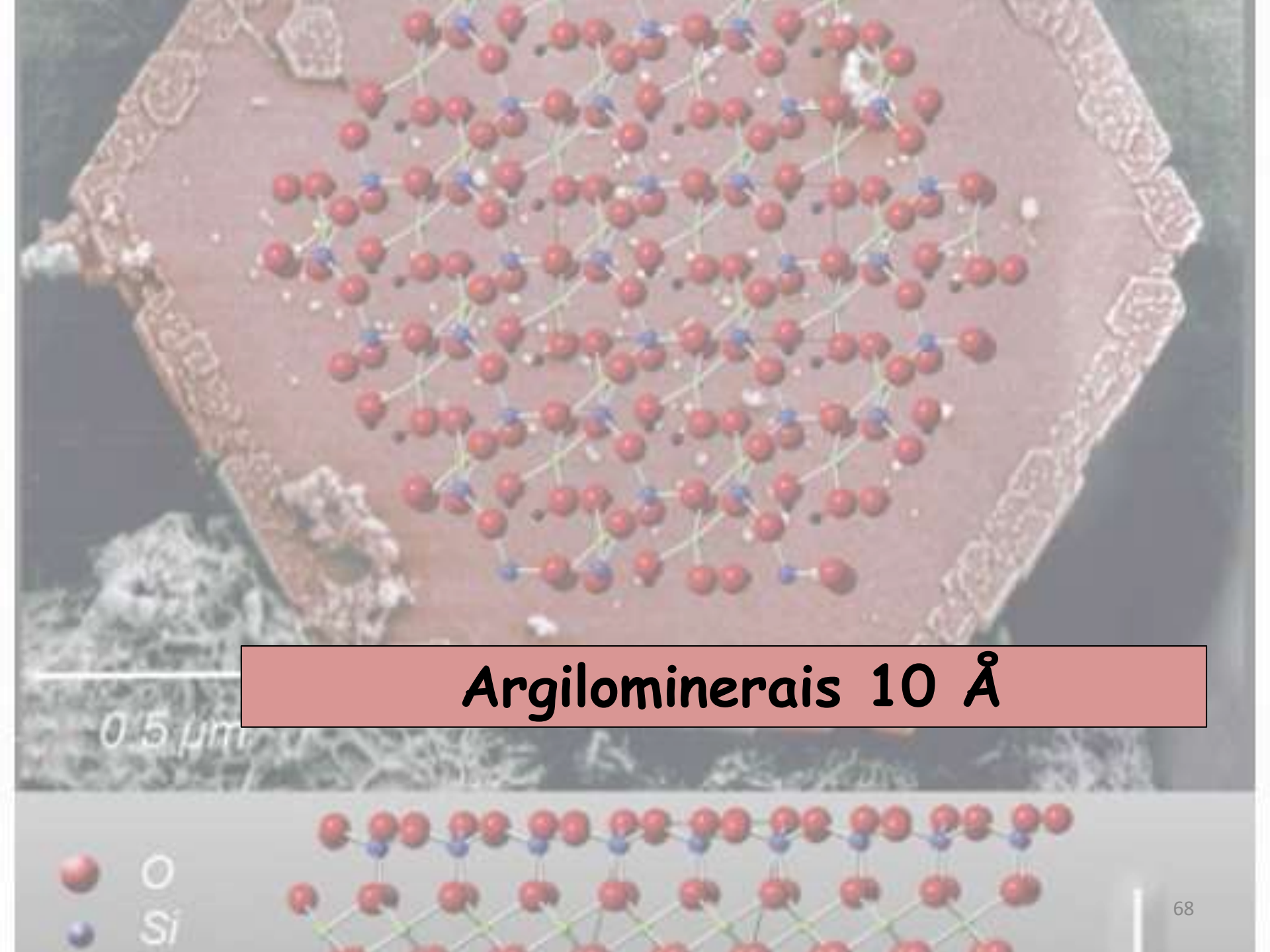

Argilominerais 10 Å

9 Å – Talco e Pirofilita

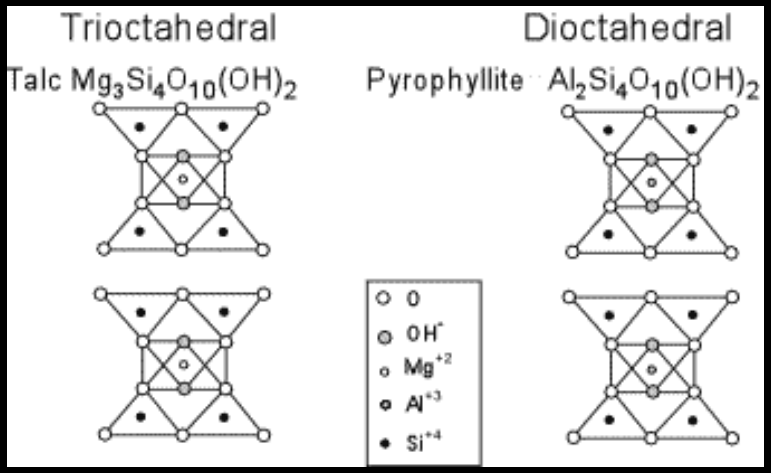

Pirofilita

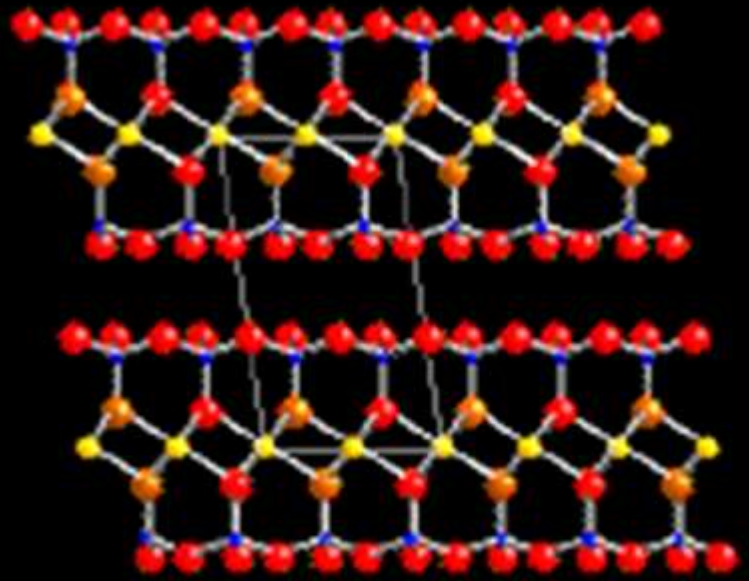

Talco

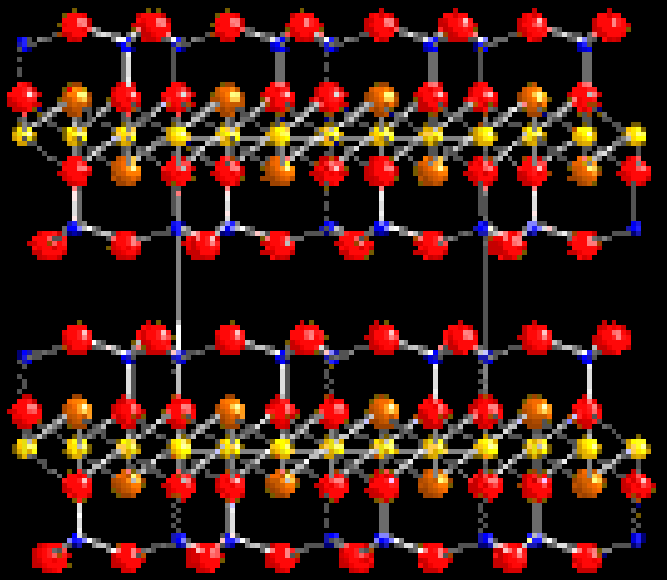

9 Å – Talco e Pirofilita

Talco de Mariana, MG

Cristal de Luzenac, França

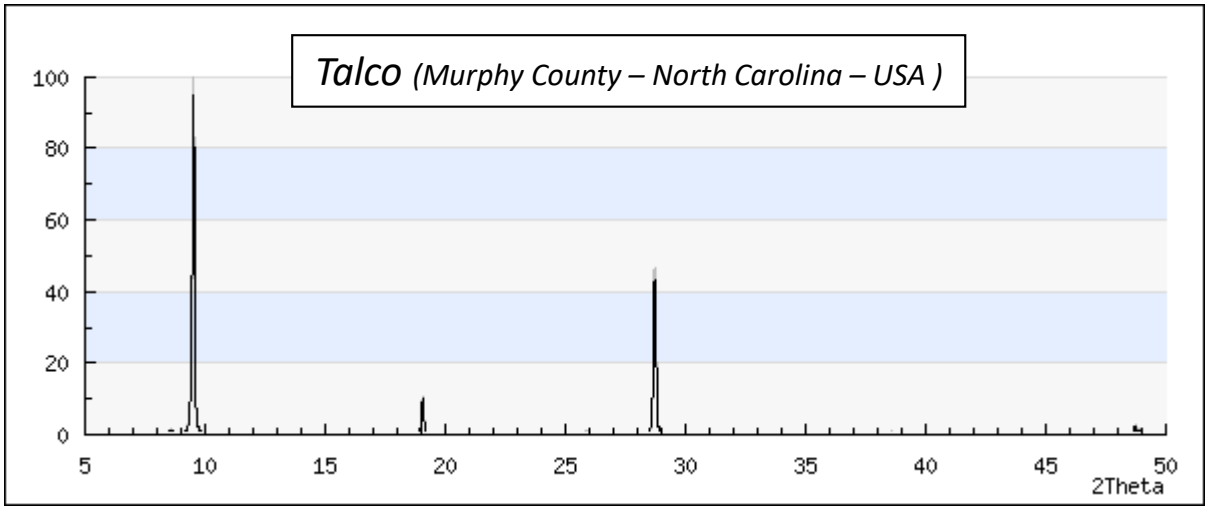

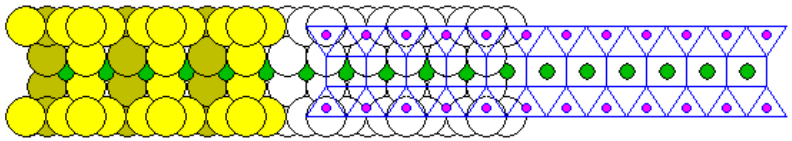

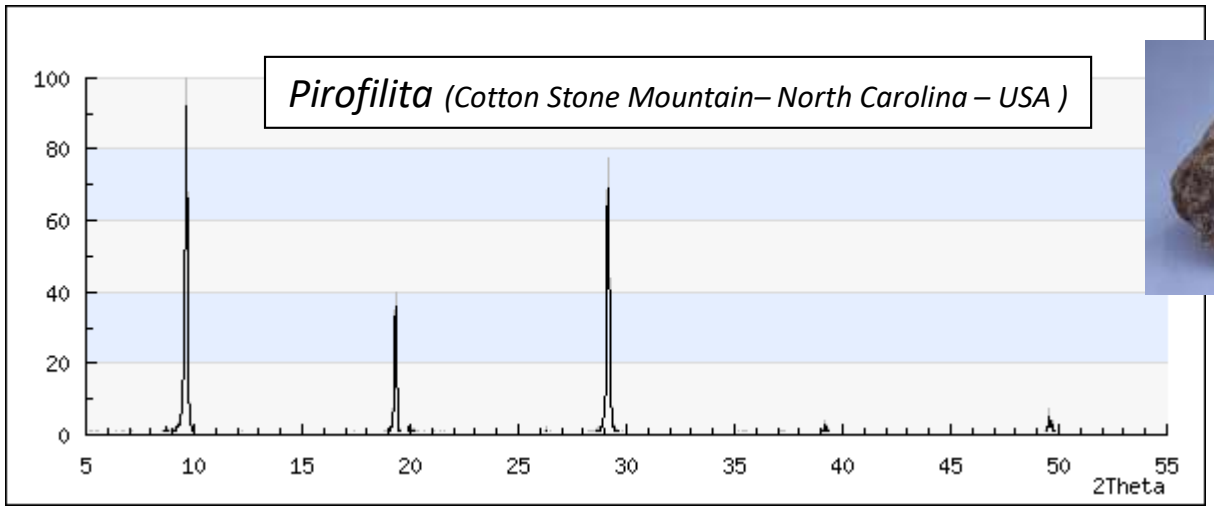

Pirofilita de Cova da Onça, MG

~10 Å – Argilominerais 2:1

Mica e Ilita

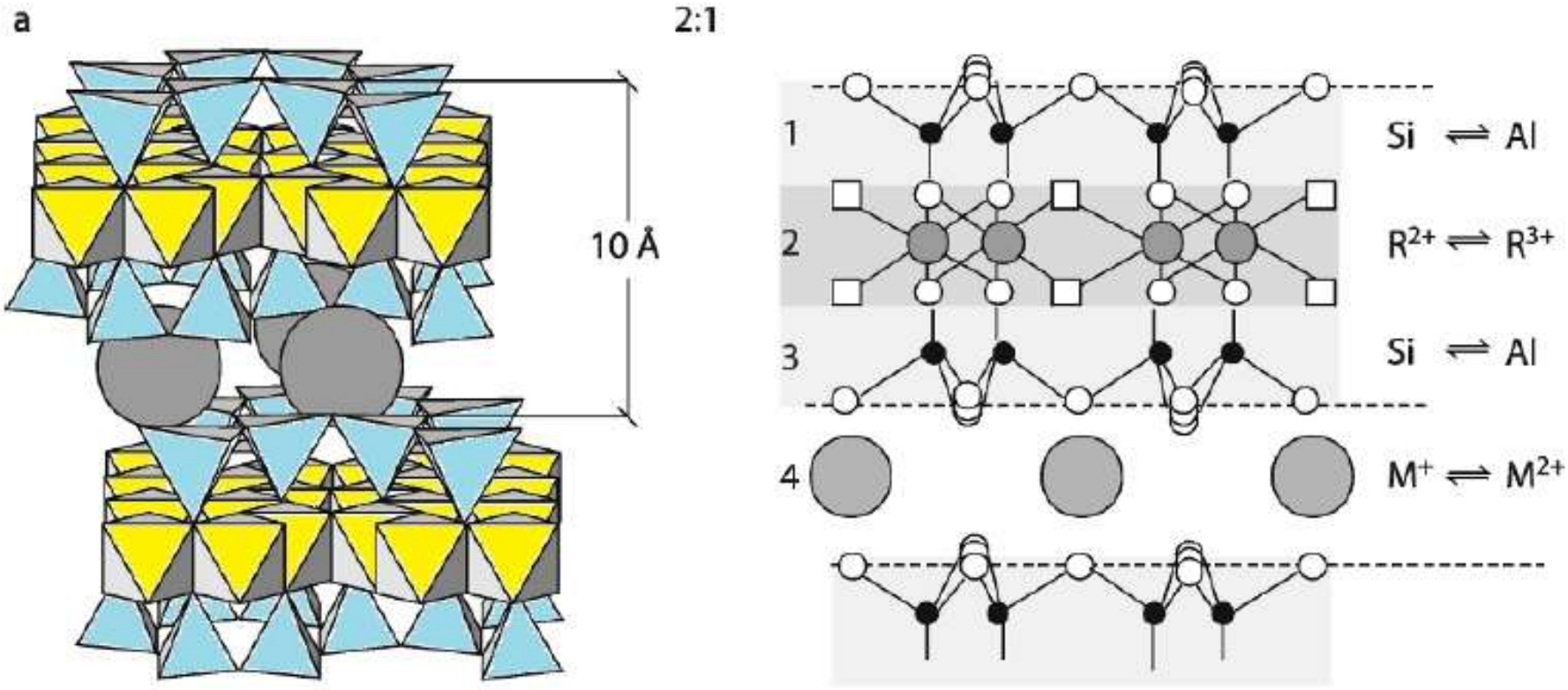

Ilitas

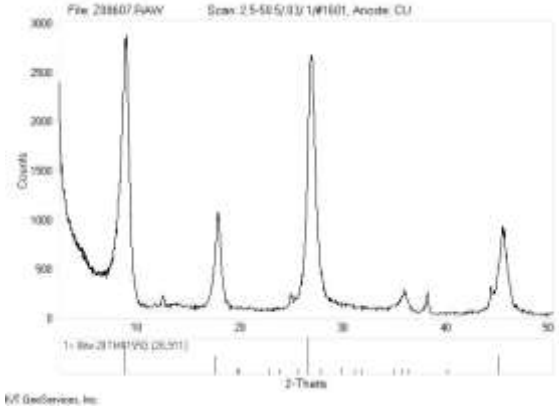

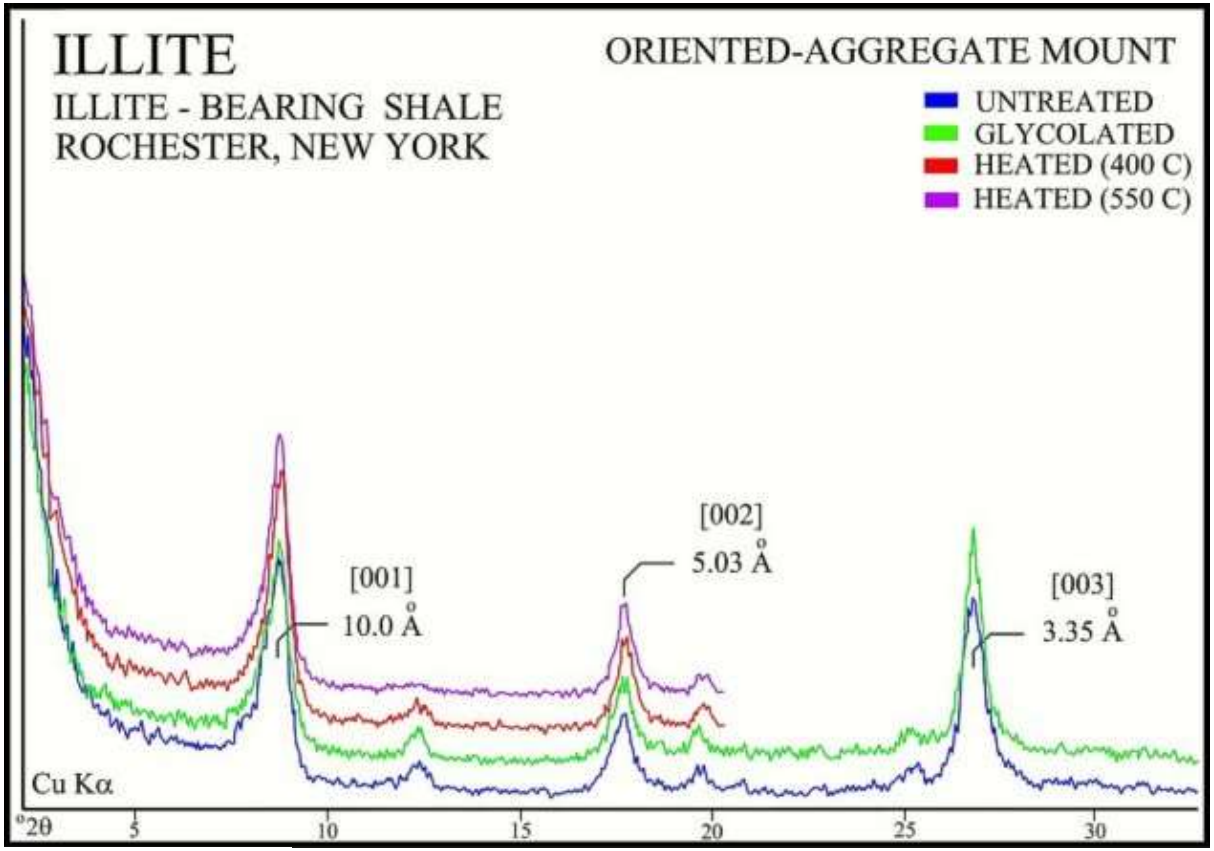

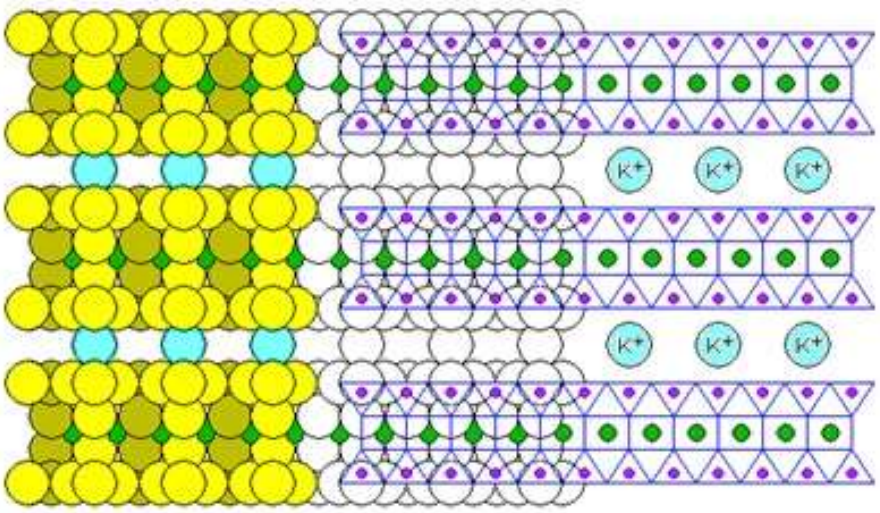

Ilita

$(K,H_3O)(Al,Mg,Fe)_2(Si,Al)_4O_{10}[(OH)_2,(H_2O)]$

Dioctaédrica

Micas

Muscovita : $KAl_2(AlSi_3)O_{10}(OH)_2$
Biotita : $K(MgFe)_3(AlSi_3)O_{10}(OH,F)_2$

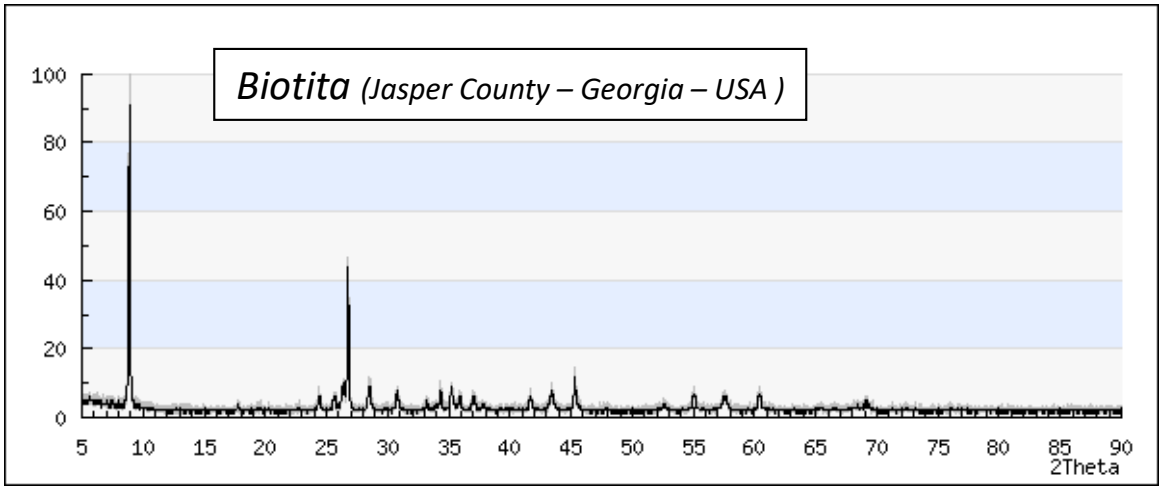

Biotita de Mabubas, Província de Bengo, Angola

Muscovitas de Minas Gerais

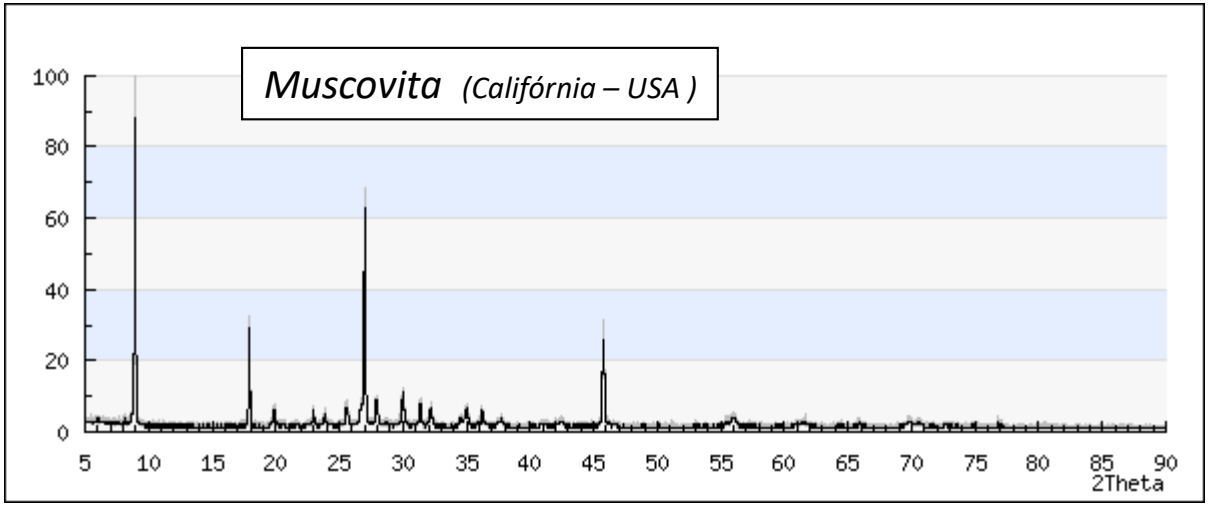

Micas

Lepidolita: $K(LiAl)_2(Si,Al)_4O_{10}(OH,F)_2$
Flogopita: $KMg_3(AlSi_3)O_{10}(OH,F)_2$

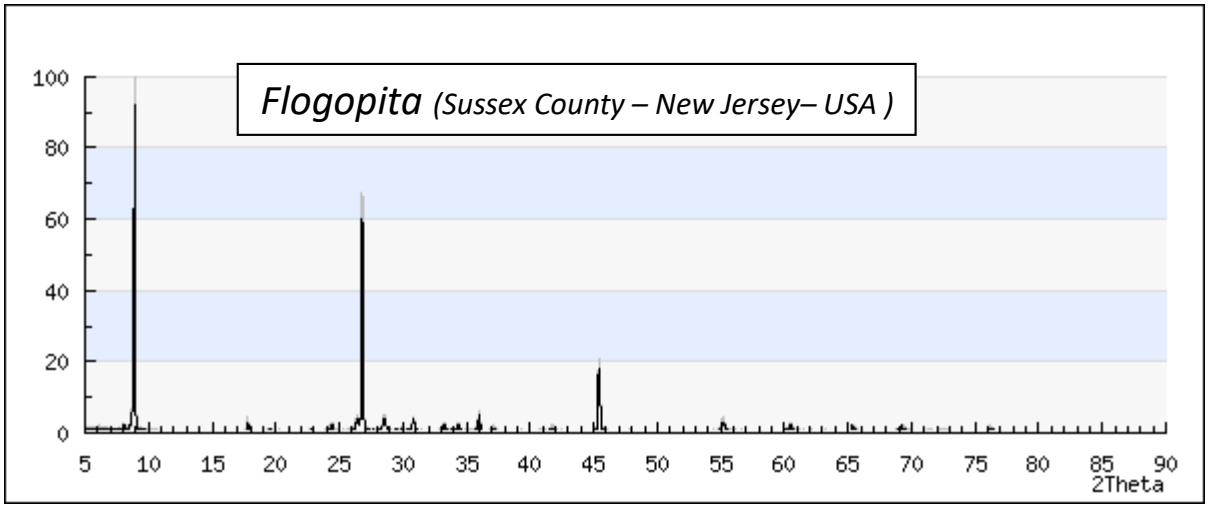

Flogopita de Minas Gerais

(1)

(2)

Lepidolitas de Minas Gerais (1) e do Afganistão (2)

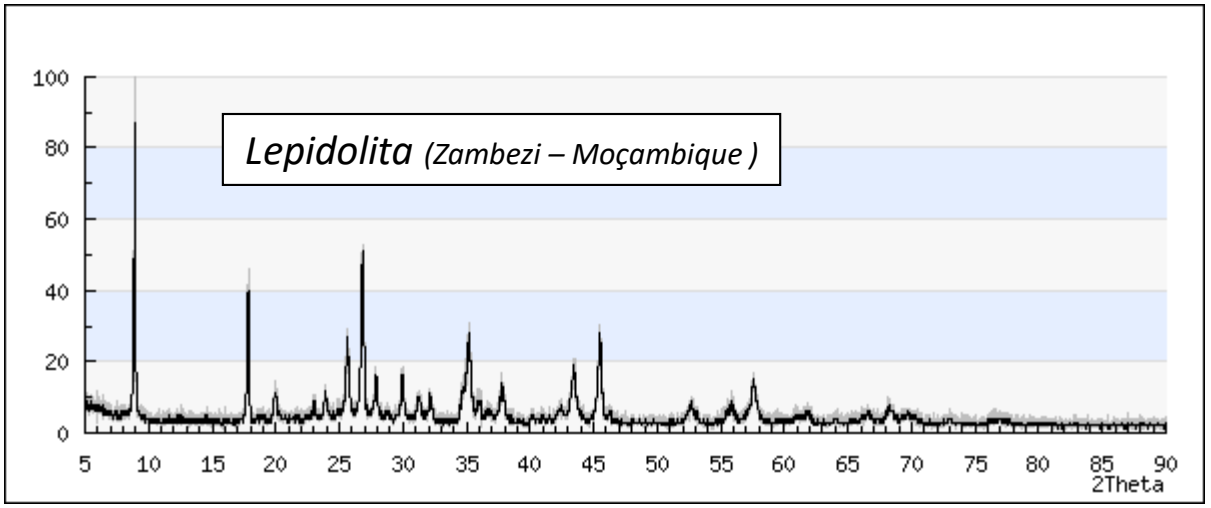

~10 Å – Argilominerais 2:1

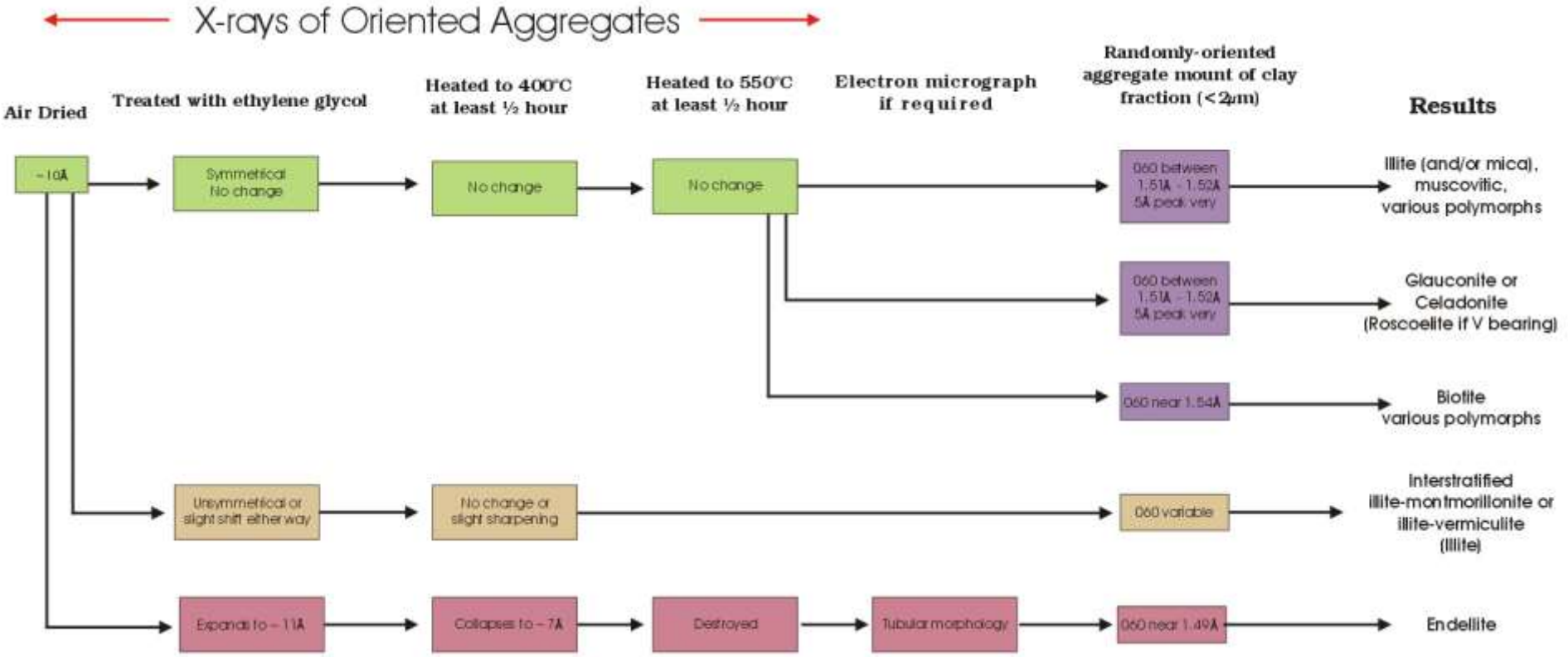

Argilominerais 14 Å
Esmectitas e Vermiculitas

~14 Å – Argilominerais 2:1

TABLE 1 CLASSIFICATION OF NATURAL AND SYNTHETIC (MARKED*) SMECTITES

	DIOCTAHEDRAL SMECTITES (TYPE I)		TRIOCTAHEDRAL SMECTITES (TYPE II)	
Charge distribution over octahedral and tetrahedral sites	Principal octahedral cations: M^{+3} and (M^{2+} substitutions)	Mineral name	Principal octahedral cations: M^{2+} and (M^{+3} M^{1+}, ☐ substitutions)	Mineral name
Octahedral charges predominant	$Al^{3+}(Mg^{2+},Fe^{2+})$	montmorillonite	$Mg^{2+}(☐)$ $Mg^{2+}(Li^{1+})$ $Mg^{2+}(☐,Li^{1+})$ $Mg^{2+}(☐,Li^{1+})$ $Mg^{2+}Li^{1+}Al^{3+}$ single or mixed 3d transition metals	stevensite hectorite laponite* fluorohectorite* (F for OH) swinefordite transition metal "defect" trioctahedral smectites*
Tetrahedral charges predominant	Al^{3+} Fe^{3+} Cr^{3+} V^{3+}	beidellite nontronite volkonskoite V-smectite	Mg^{2+} Fe^{2+} Zn^{2+} Co^{2+} Mn^{2+} Ni^{2+} single or mixed 3d transition metals	saponite Fe-saponite sauconite Co-smectite Mn-smectite Ni-smectite transition metal trioctahedral smectites*

☐ indicates a vacancy

Güven, N. Elements ***5*** *(2), 89-92 (2009).*

Esmectitas

TABLE 2 HISTORICAL SUMMARY OF THE NOMENCLATURE OF BENTONITE AND NATURAL SMECTITES (BERGAYA ET AL. 2006a)

Bentonite	Name given by Knight in 1898 for a soapy clay from the Fort Benton Formation of Cretaceous age in Wyoming, USA
Montmorillonite	A clay found near Montmorillon, France; named by Cronsted in 1788 and later referred to by Damour and Salvetat in 1847
Beidellite	Name given by Larson and Wherry in 1925 for a clay from a mine at Beidell, Colorado, USA. The mine was later flooded and is no longer accessible.
Nontronite	Name used by Berthier in 1827 for clay in a manganese ore from Nontron County near the village of Saint Paradox, France
Saponite	A soap-like clay named by Svanberg in 1840 after sapo, (Latin for soap)
Sauconite	Named after the location of the Ueberroth Mine, Saucon Valley, near Friedensville, Leigh County, Pennsylvania, USA
Hectorite	Clay from Hector, California, USA, named by Strese and Hoffman in 1941
Stevensite	Clay found in the Watchung Basalt near Springfield, New Jersey, USA; named by Faust and Murata in 1953 after E. A. Stevens, founder of the Stevens Institute of Technology, New Jersey, USA
Volkonskoite	Name honoring Prince Volkonskoi, given to a clay found in his province of Perm, Ural Mountains, Russia
Swinefordite	(pronounced "Swainfedait") – A clay from the Carolina Pegmatite; named by Tien et al. in 1975 after Ada Swineford

Güven, N. Elements ***5*** *(2), 89-92 (2009).*

~14 Å – Argilominerais 2:1

Montmorilonita
14 Å expansível

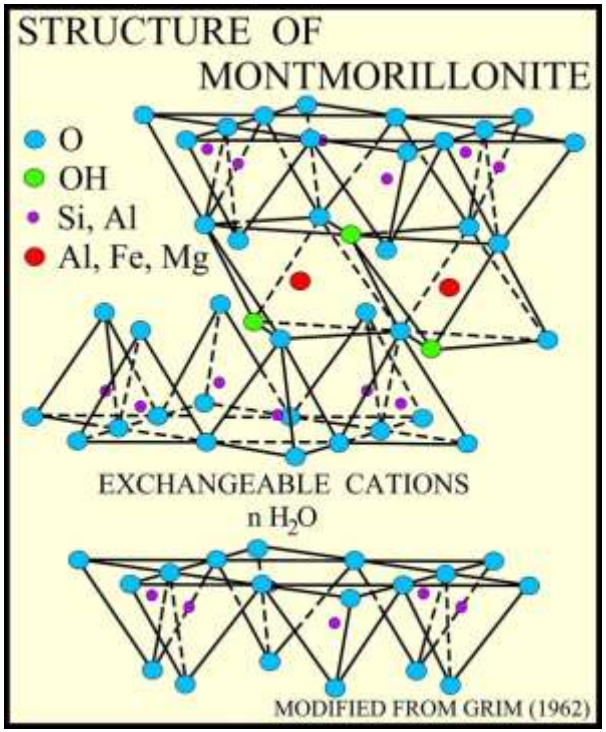

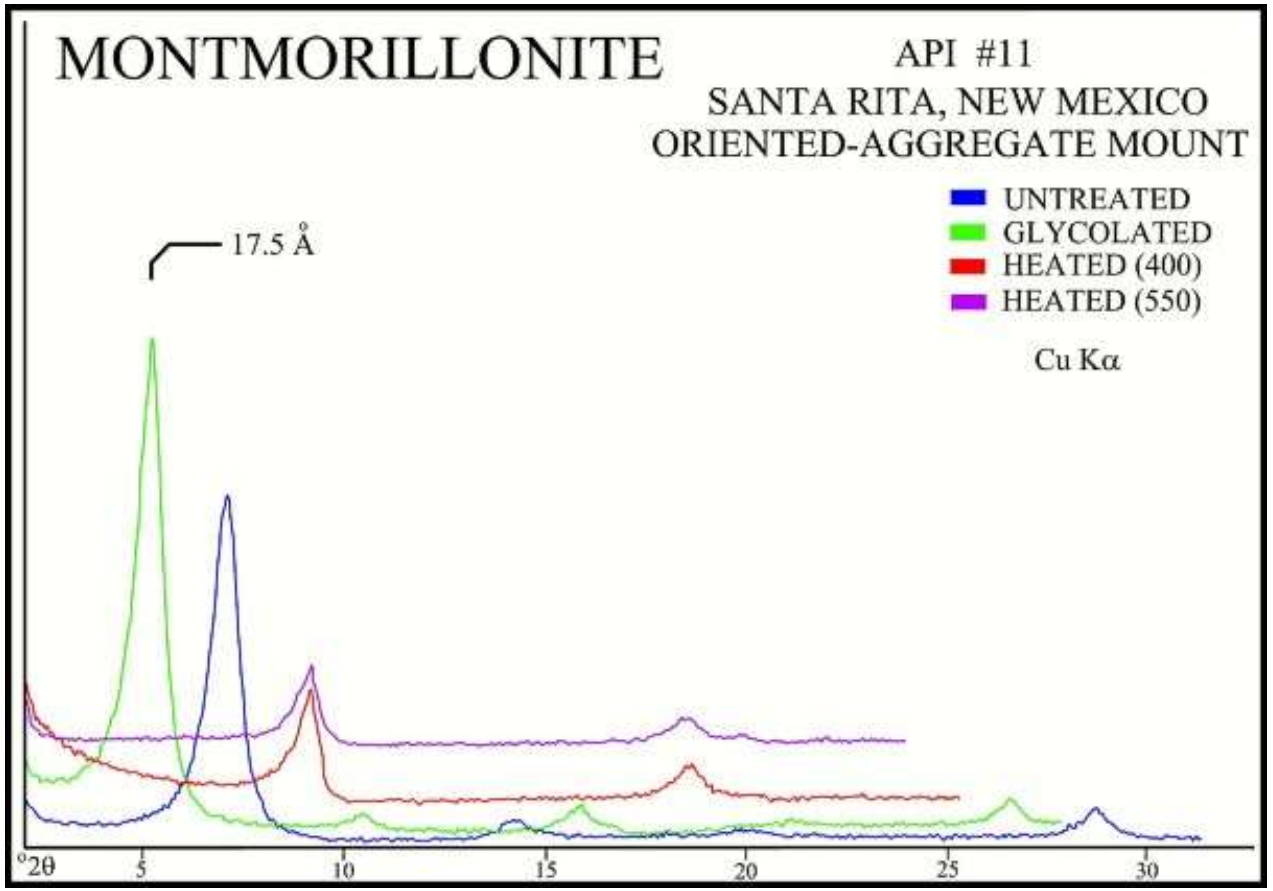

Montmorilonita
$yM^{+}(Al_{2-y}Mg_y)\ Si_4O_{10}(OH)_2.nH_2O$

Montmorilonita

$yM^{+}(Al_{2-y}Mg_{y})\ Si_4O_{10}(OH)_2.nH_2O$

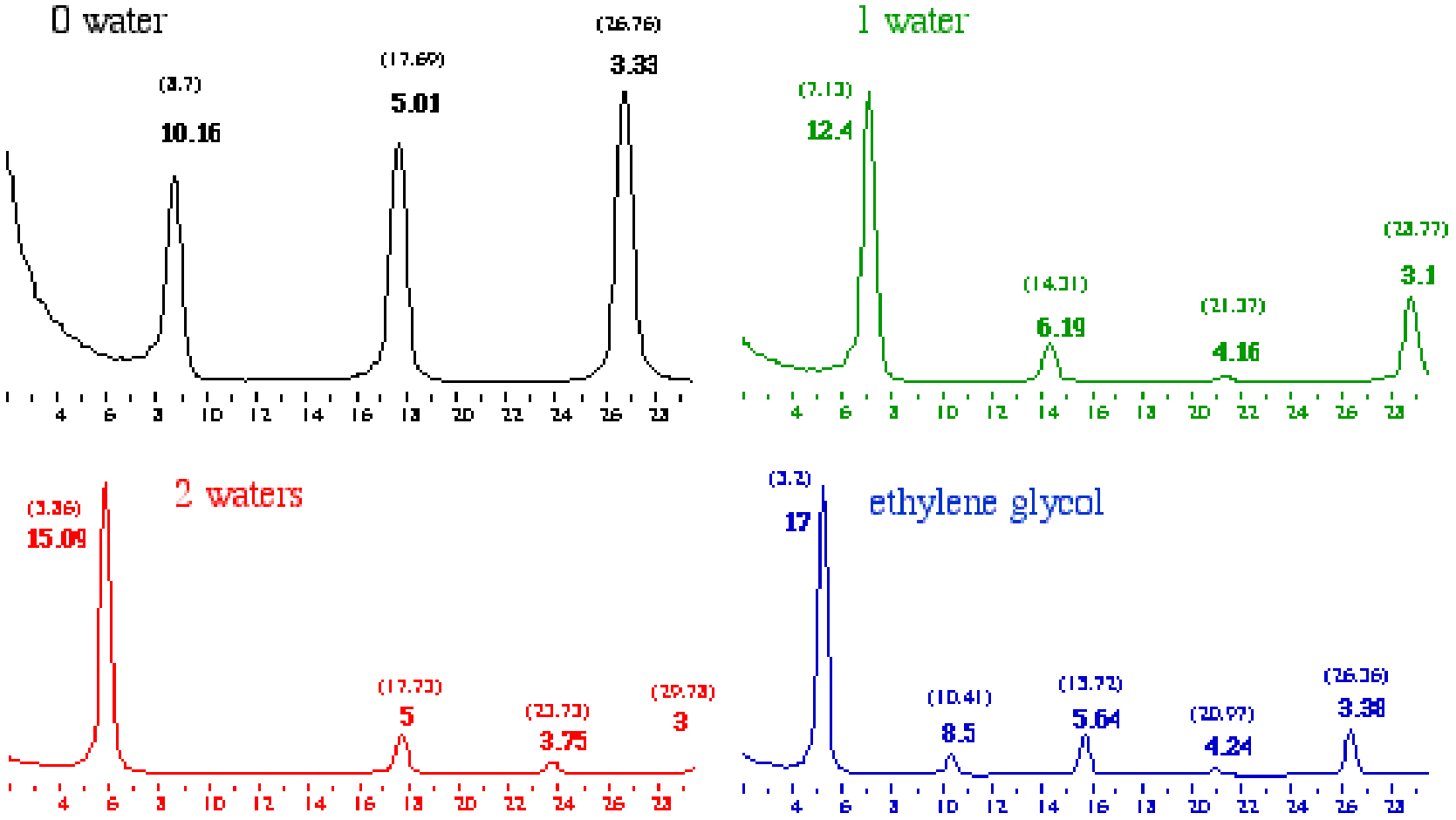

Montmorilonita

$yM^{+}(Al_{2-y}Mg_{y})\ Si_4O_{10}(OH)_2.nH_2O$

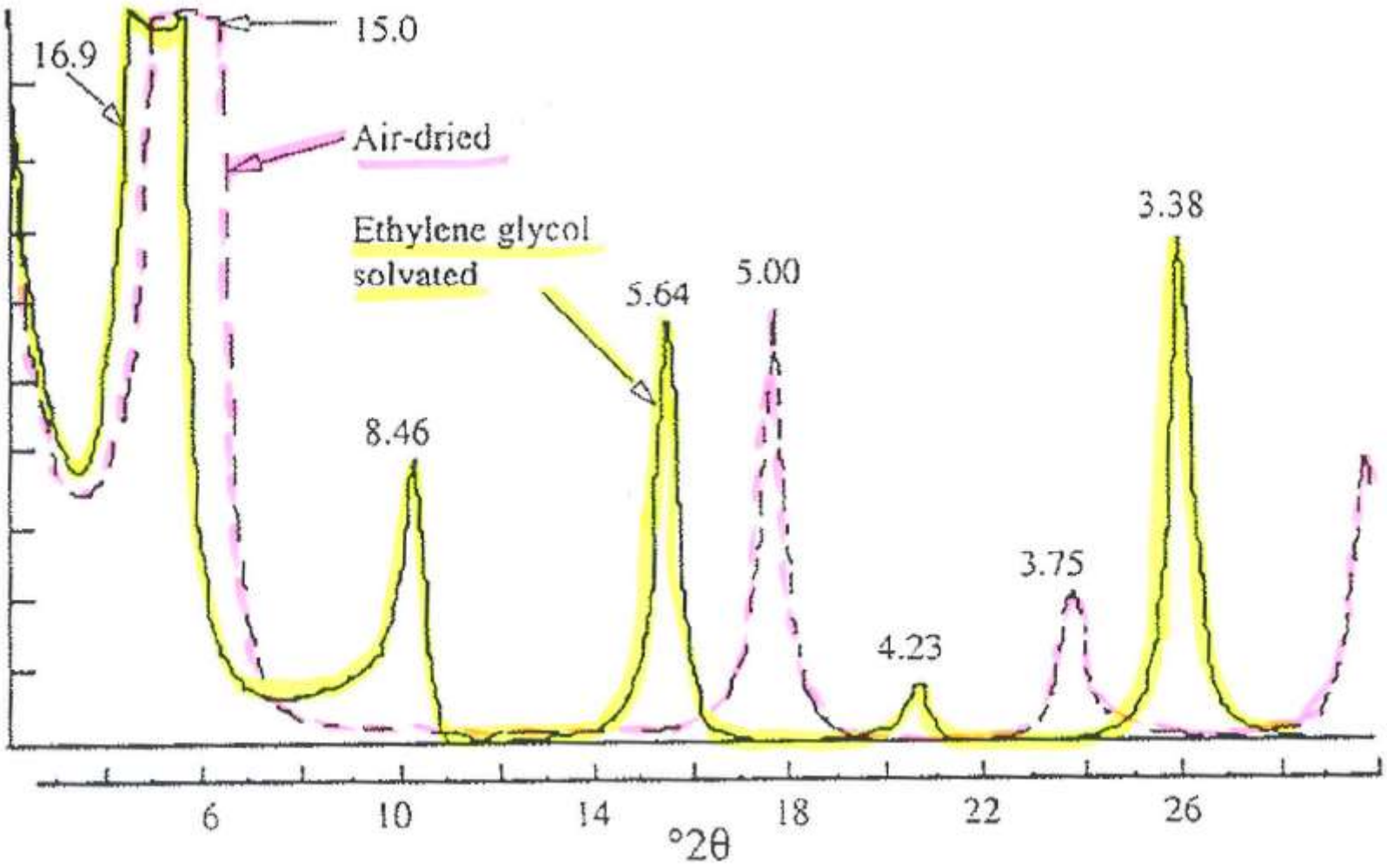

Fig. 7.8. Montmorillonite in the air-dried and ethylene glycol-solvated states.

Moore, D.M.; Reynolds, Jr., R.C. – X-ray Diffraction and the Identification and Analysis of Clay Minerals

~14 Å – Argilominerais 2:1

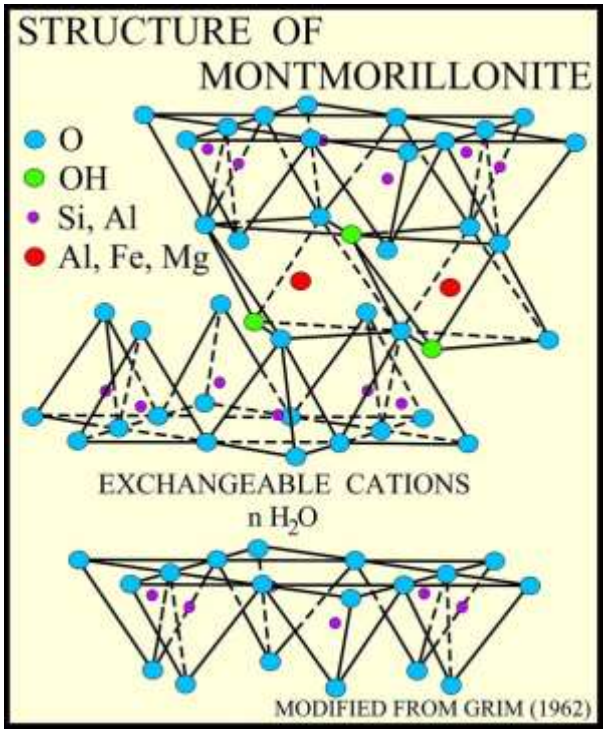

- Individual smectites can sometimes be differentiated by their higher-order peaks or by cation saturation.
  - For example, **dioctahedral** smectites have **060** reflections at 1.50-1.52 Å, whereas **trioctahedral** smectites have **060** reflections at 1.53-1.54 Å.
  - Li saturation can be used to differentiate some montmorillonites from beidellite.

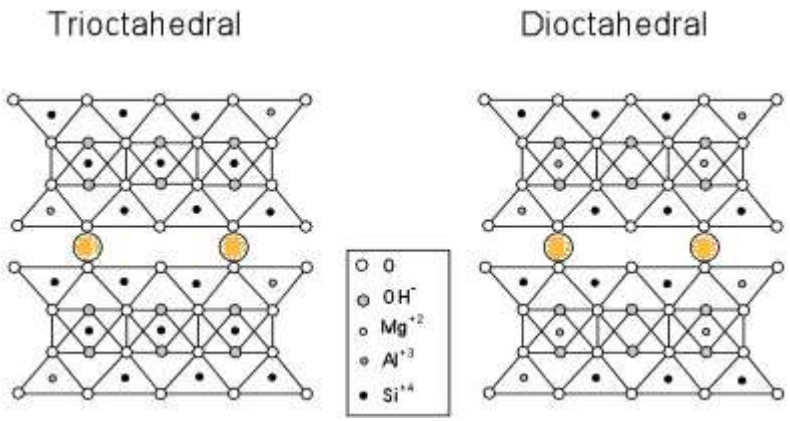

~ 14 Å

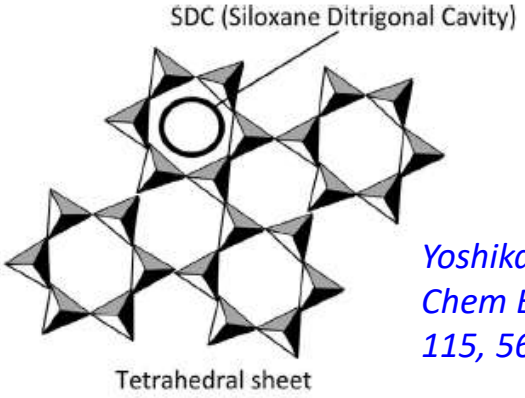

Yoshikawa et al., Chem Eng Process 115, 56-62 (2017)

Cátions Intercalados

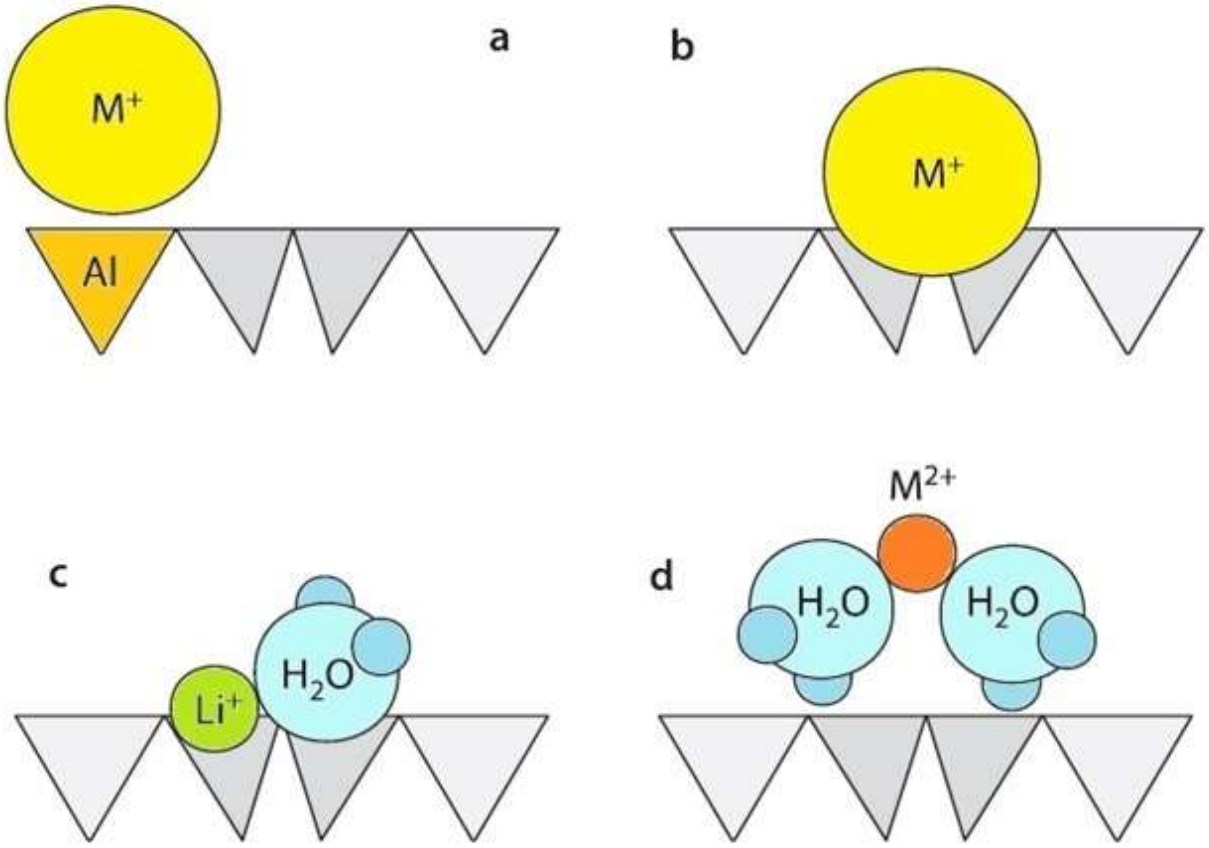

Fig. 1.17. The possible positions of interlayer cations according to their hydration energy; **a** dehydrated cation close to the Al^{3+} cation replacing a Si^{4+} in a tetrahedral sheet; **b** dehydrated cation inside the ditrigonal cavity; **c** partially hydrated cation inside the ditrigonal cavity; **d** hydrated cation above the ditrigonal cavity

Nontronita

$yM^{+}Fe_2(Si_{4-x}Al_x)O_{10}(OH)_2.nH_2O$

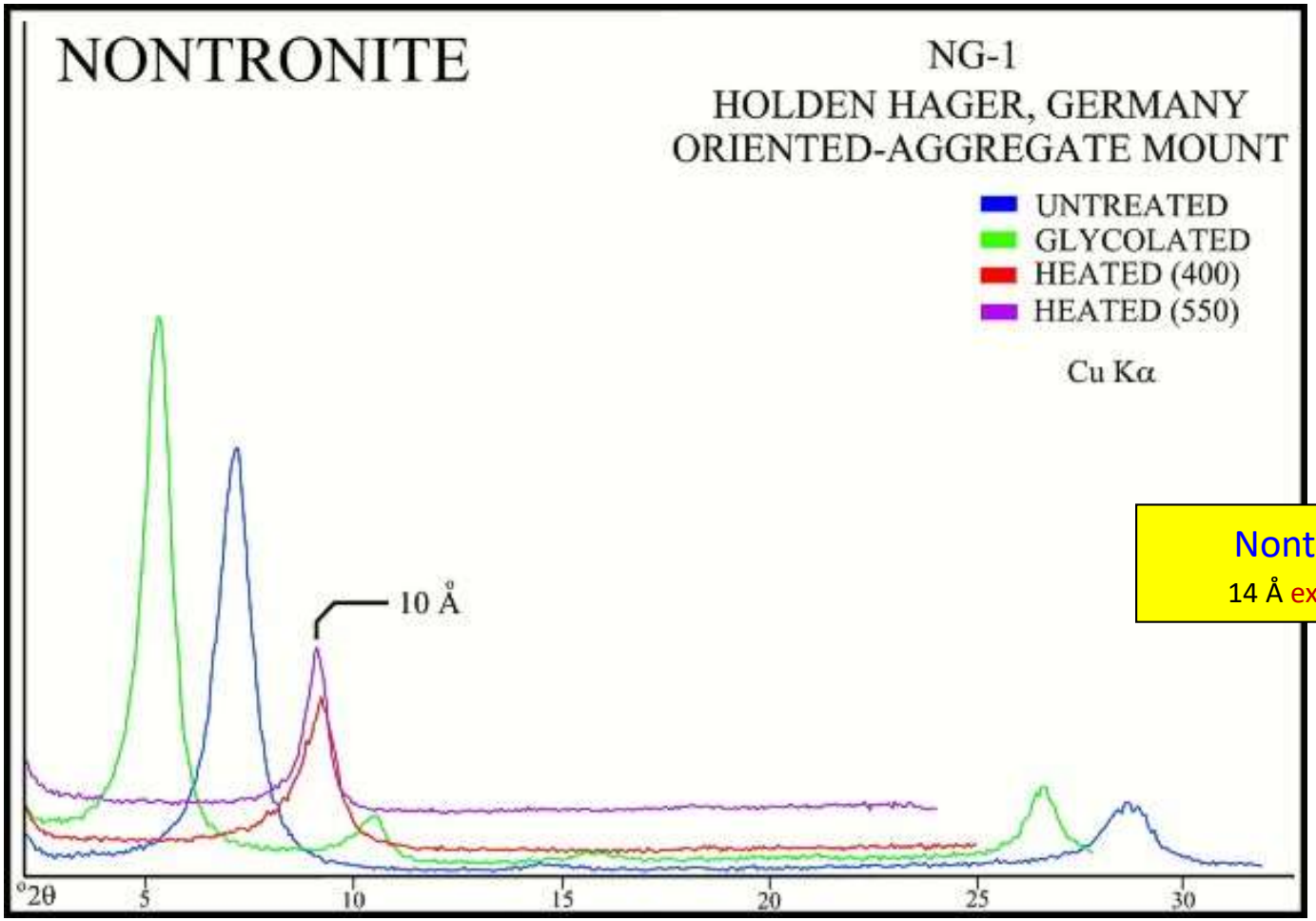

Nontronita

14 Å expansível

Saponita

$yM^{+}Mg_3(Si_{4-x}Al_x)O_{10}(OH)_2.nH_2O$

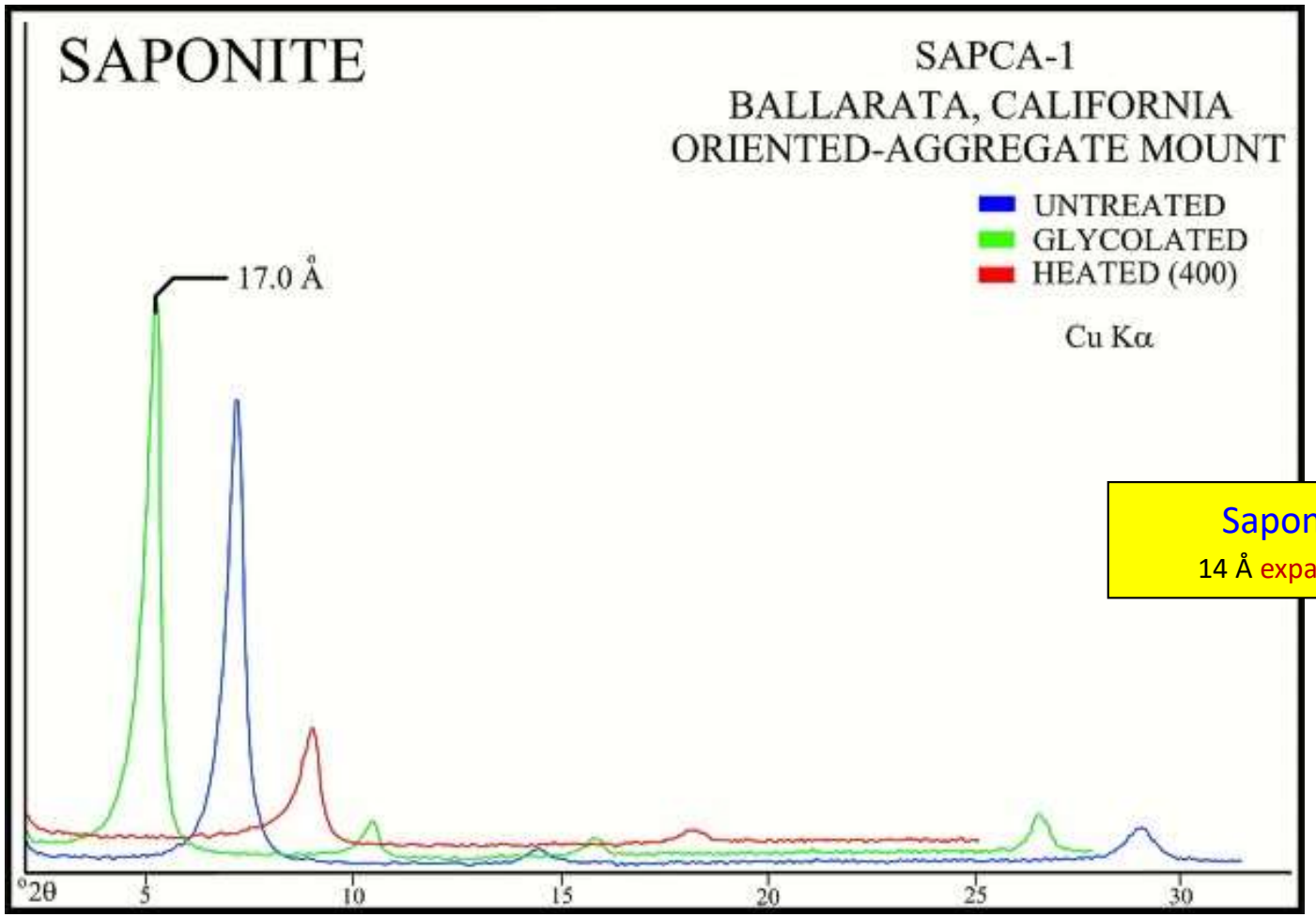

Saponita

14 Å expansível

Inchamento em Água - Esmectitas

Vermiculita : expansão limitada

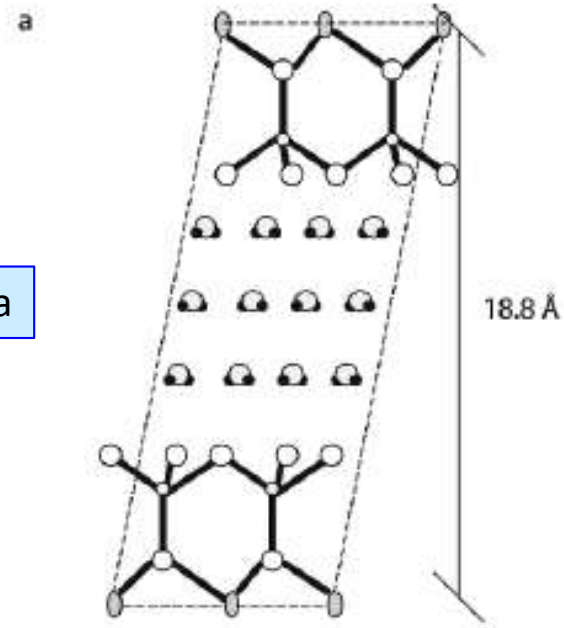

~ 14 Å

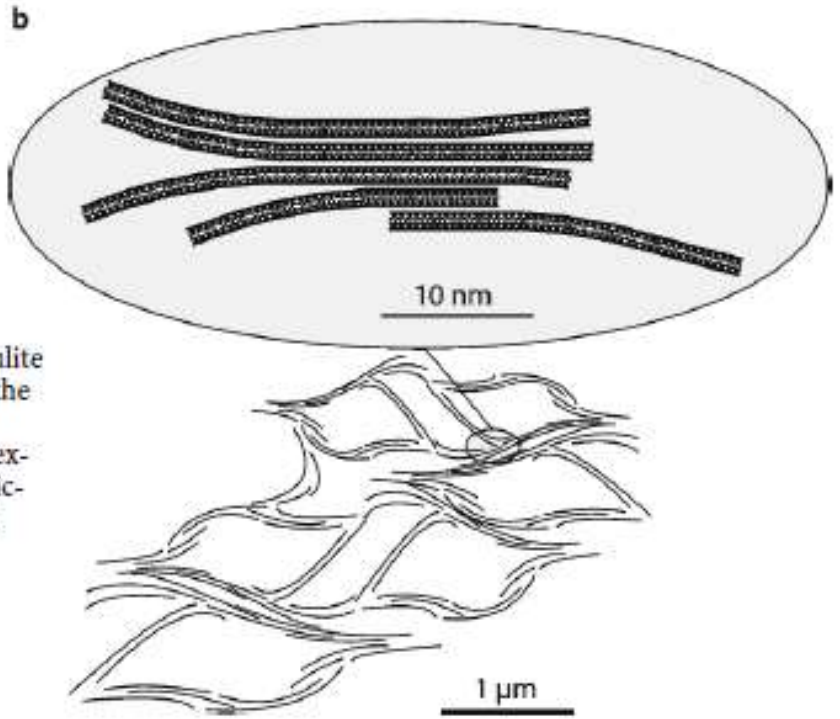

Crystallite and tactoïds; **a** expanded vermiculite (3 water sheets) conserving the periodicity along the c axis (crystallite); **b** honeycomb texture of smectite. The periodicity along the c axis is almost cancelled (tactoïd)

Esmectita : expansão "ilimitada" → "tactóide"

Organo-Esmectitas

(esmectitas organofílicas)

Applied Surface Science 320 (2014) 356–363

Contents lists available at ScienceDirect

Applied Surface Science

journal homepage: www.elsevier.com/locate/apsusc

Characterization of organo-modified bentonite sorbents: The effect of modification conditions on adsorption performance

María E. Parolo[a,*], Gisela R. Pettinari[a], Telma B. Musso[a,c], María P. Sánchez-Izquierdo[b], Laura G. Fernández[b]

[a] Instituto de Investigación y Desarrollo en Ingeniería de Procesos, Biotecnología y Energías Alternativas (PROBIEN), Facultad de Ingeniería, Universidad Nacional del Comahue, Neuquén 8300, Argentina
[b] Facultad de Ingeniería, Universidad Nacional del Comahue, Neuquén 8300, Argentina
[c] CONICET, Consejo Nacional de Investigaciones Científicas y Técnicas, Buenos Aires, Argentina

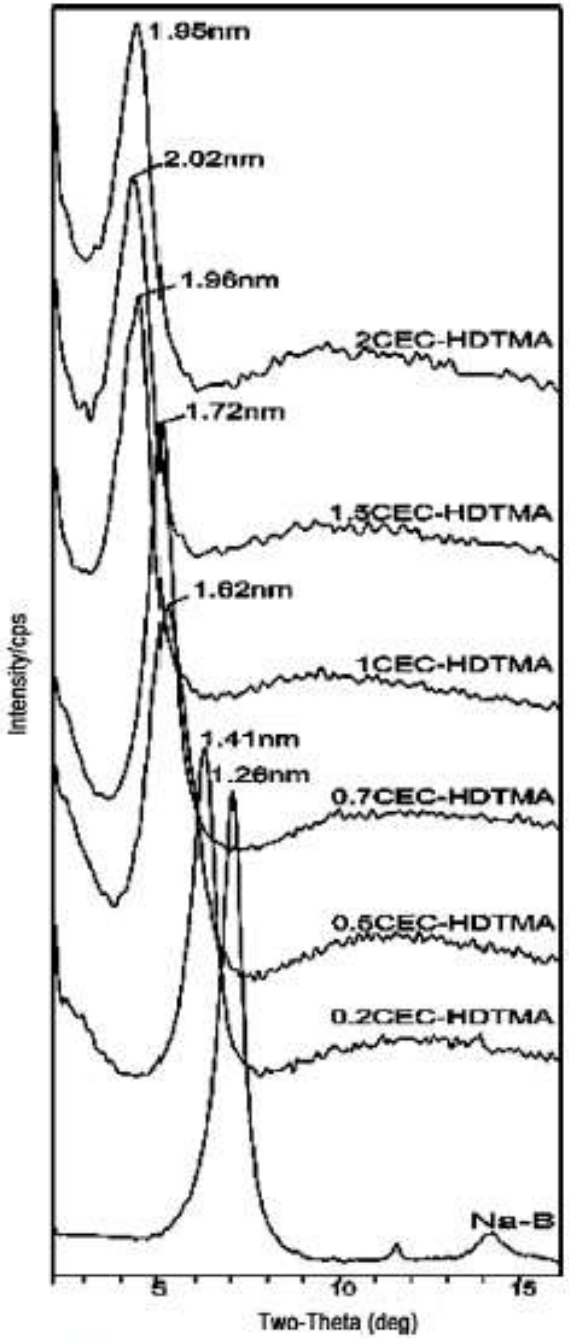

Fig. 2. XRD patterns of untreated bentonite and organobentonites.

Vermiculita

$(Mg,Ca)_{0,3}(Mg, Fe,Al)_3(Al,Si)_4O_{10}(OH)_2.4H_2O$

Vermiculita

14 Å **pouco** expansível

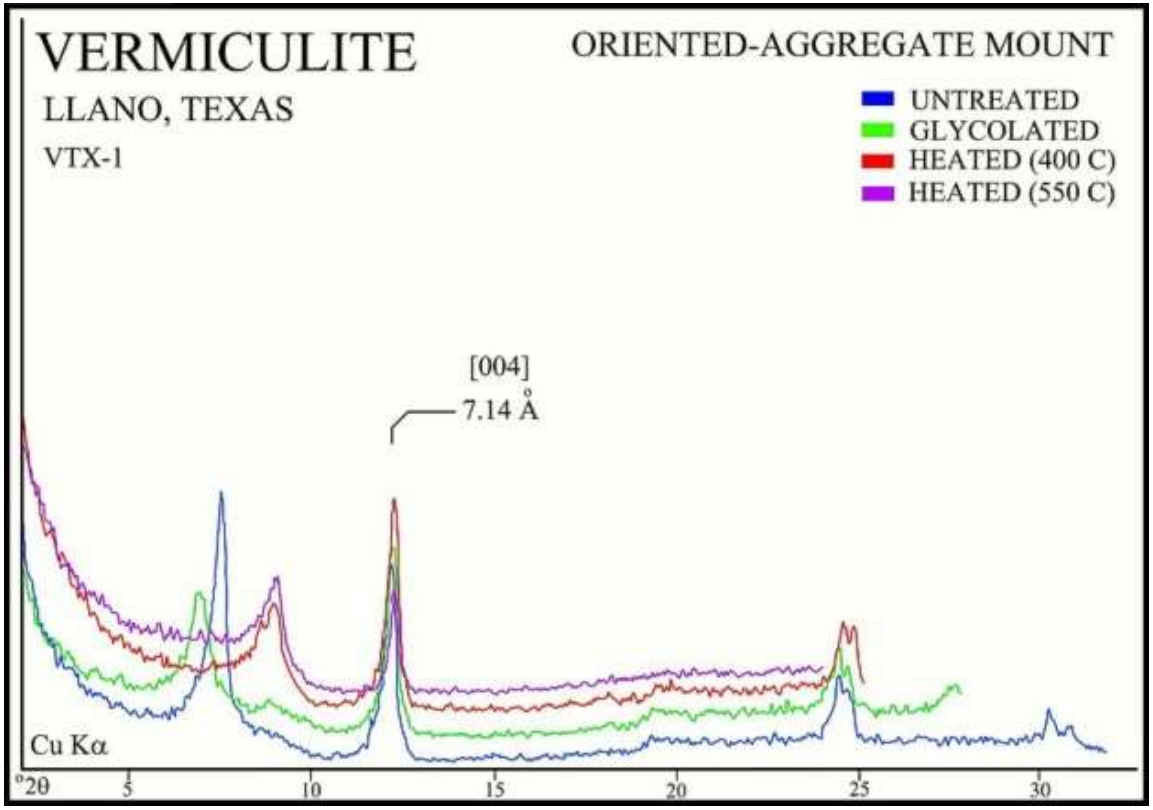

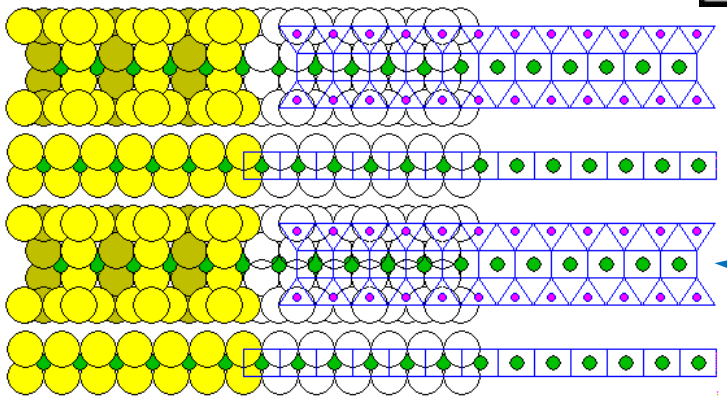

cátions trocáveis + água

camada 2:1

Vermiculita

Hillier et al. Clay Minerals 48, 563-582 (2013)

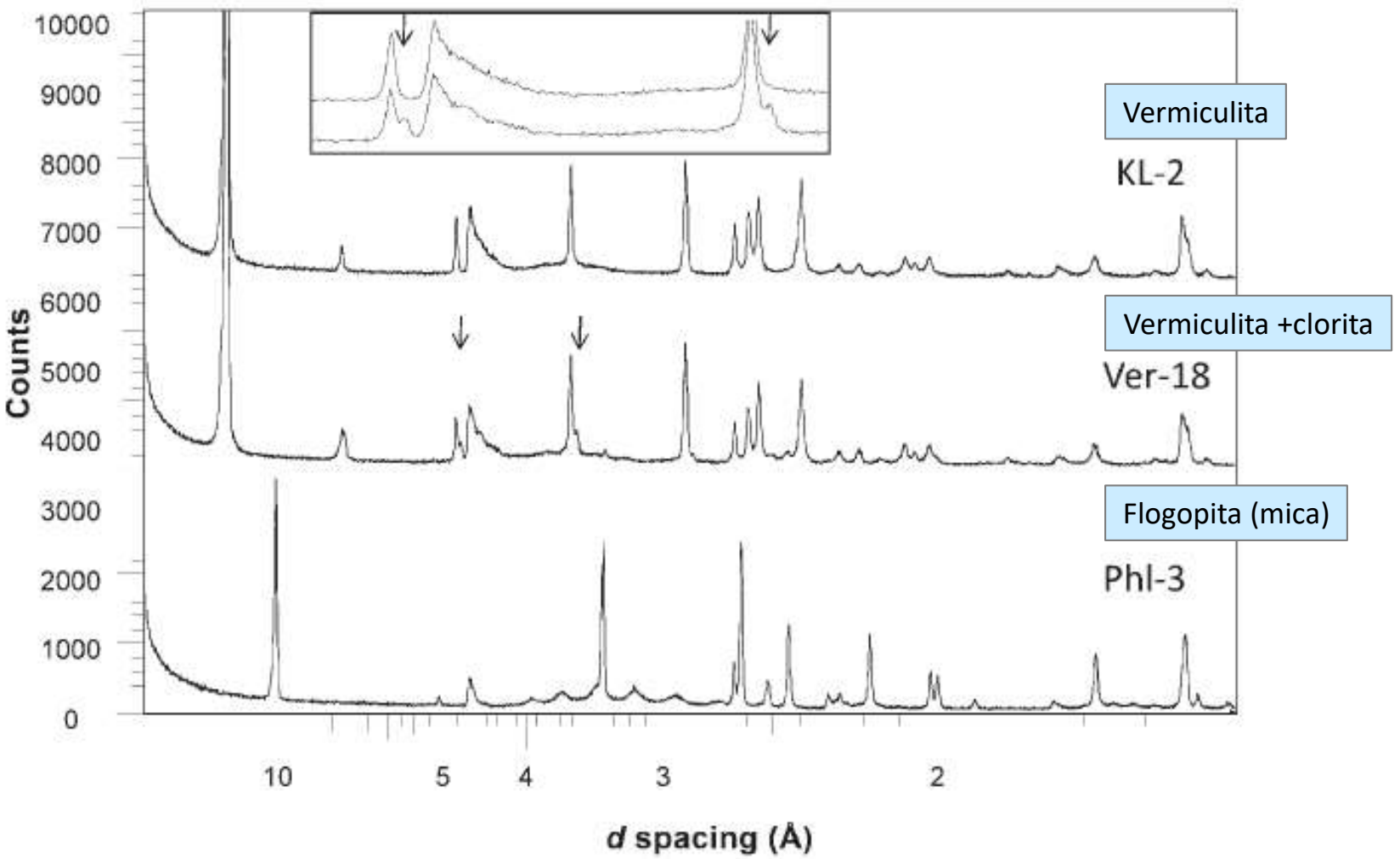

FIG. 1. (a) Random powder XRD patterns of samples KL-2 (pure vermiculite), Ver-18 (vermiculite, minor chlorite), and Phl-3 (pure phlogopite). Arrows show positions of chlorite 003 and 004 peaks in Ver-18, and insert expands this region for comparison of Ver-18 to KL-2.

Argilominerais 14 Å
Cloritas

Cloritas - 14 Å

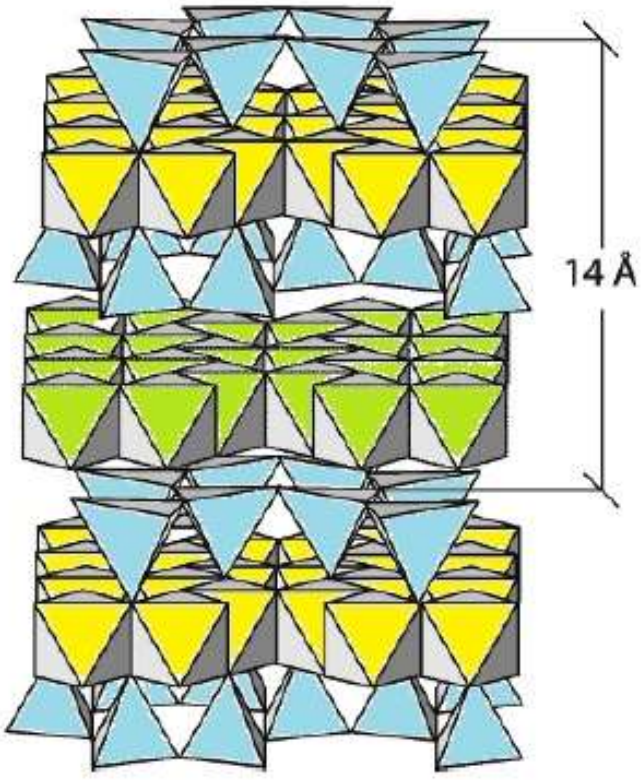

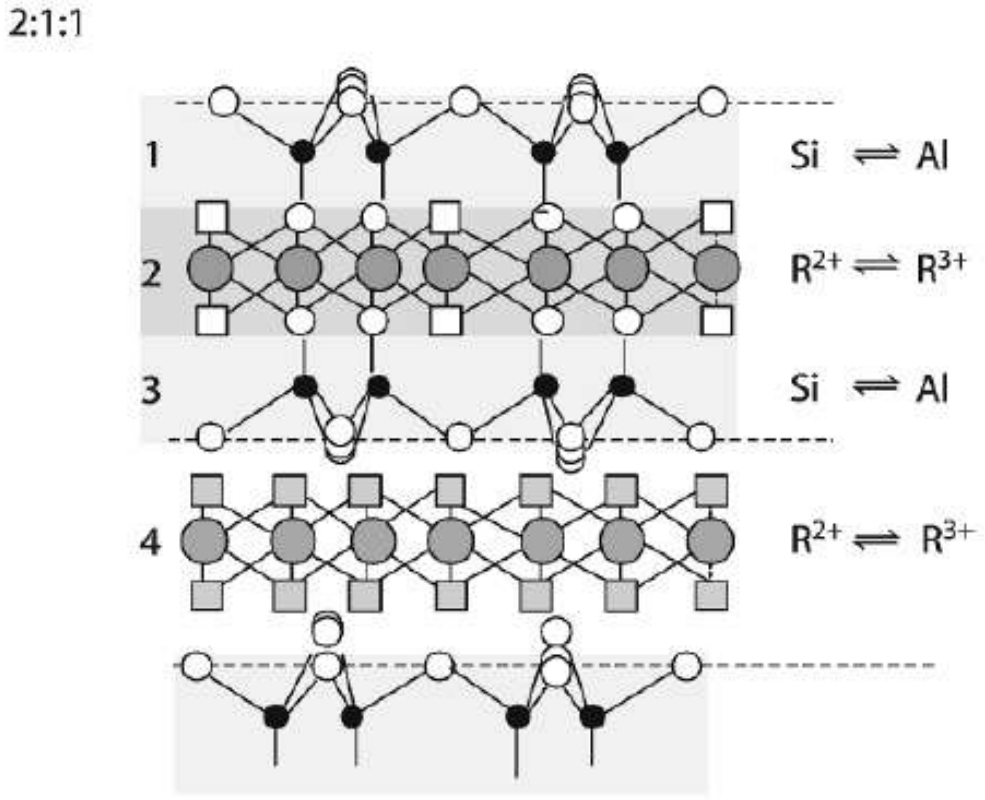

Cloritas : Estrutura cristalina

The negative charge of the 2:1 layer is compensated by interlayer cations or a "pseudo-brucitic" sheet respectively

Cloritas - 14 Å

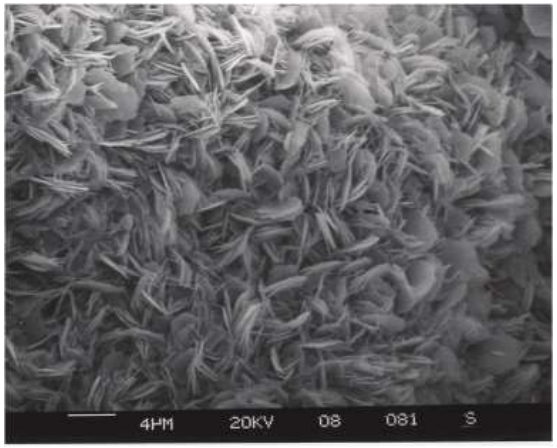

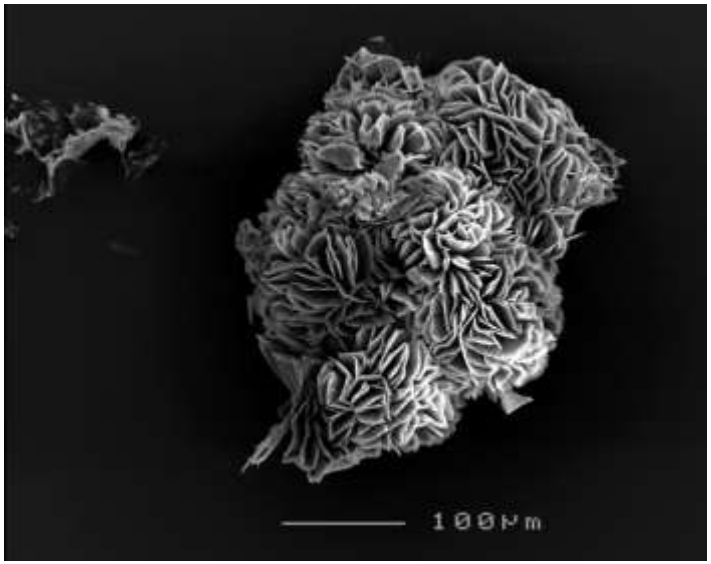

Baileychlore	$(Zn,Fe^{+2},Al,Mg)_6(Al,Si)_4O_{10}(O,OH)_8$
Chamosite	$(Fe,Mg)_5Al(Si_3Al)O_{10}(OH)_8$
Clinochlore	$(Mg,Fe^{2+})_5Al(Si_3Al)O_{10}(OH)_8$
Cookeite	$LiAl_4(Si_3Al)O_{10}(OH)_8$
Donbassite	$Al_2[Al_{2.33}][Si_3AlO_{10}](OH)_8$
Gonyerite	$(Mn,Mg)_5(Fe^{+3})_2Si_3O_{10}(OH)_8$
Nimite	$(Ni,Mg,Al)_6(Si,Al)_4O_{10}(OH)_8$
Odinite	$(Fe,Mg,Al,Fe,Ti,Mn)_{2.4}(Al,Si)_2O_5OH_4$
Orthochamosite	$(Fe^{+2},Mg,Fe^{+3})_5Al(Si_3Al)O_{10}(O,OH)_8$
Pennantite	$(Mn_5Al)(Si_3Al)O_{10}(OH)_8$
Ripidolite	$(Mg,Fe,Al)_6(Al,Si)_4O_{10}(OH)_8$
Sudoite	$Mg_2(Al,Fe)_3Si_3AlO_{10}(OH)_8$

Ripidolita

$(Mg, Fe,Al)_6(Al,Si)_4O_{10}(OH)_8$

Ripidolita

(variedade de clinocloro)

14 Å **NÃO** expansível

Ripidolita – agregados de cristais verdes escuros *(Ziller Valley, North Tyrol, Austria)*

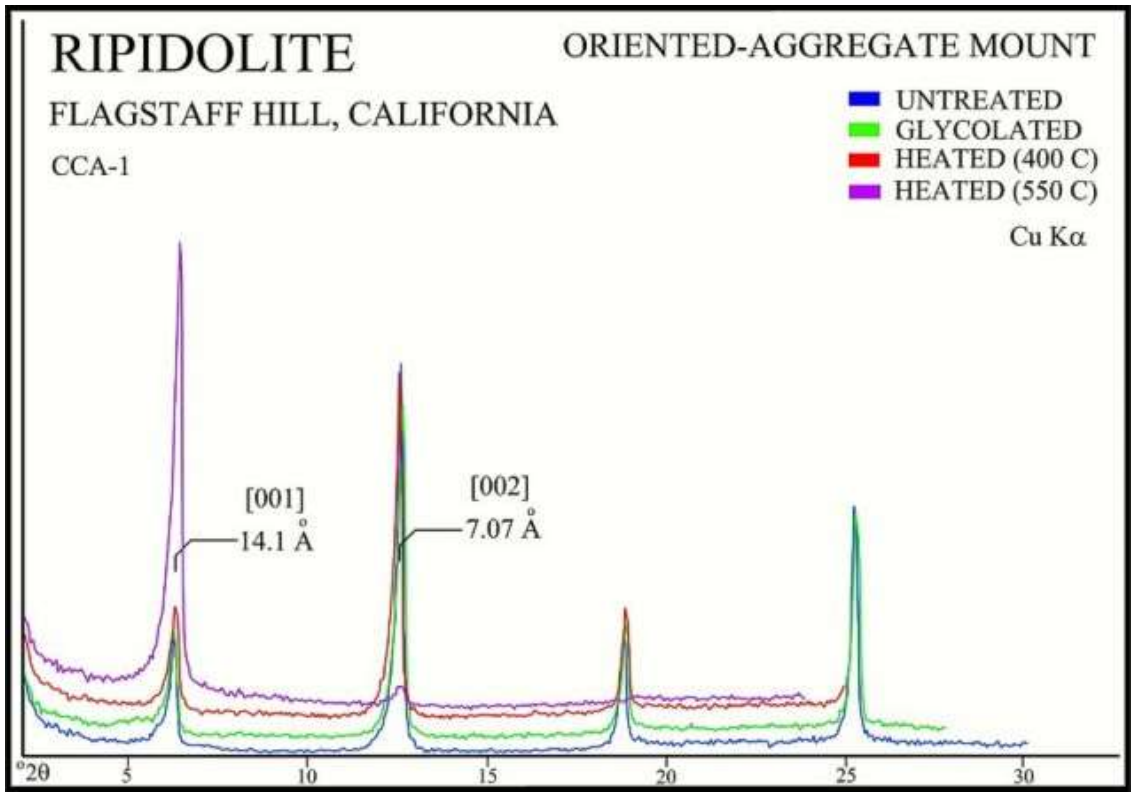

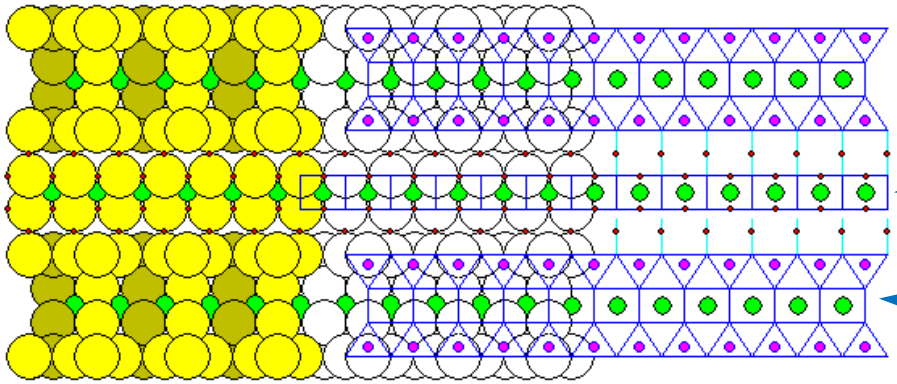

Camada de brucita

camada 2:1

~ 14 Å

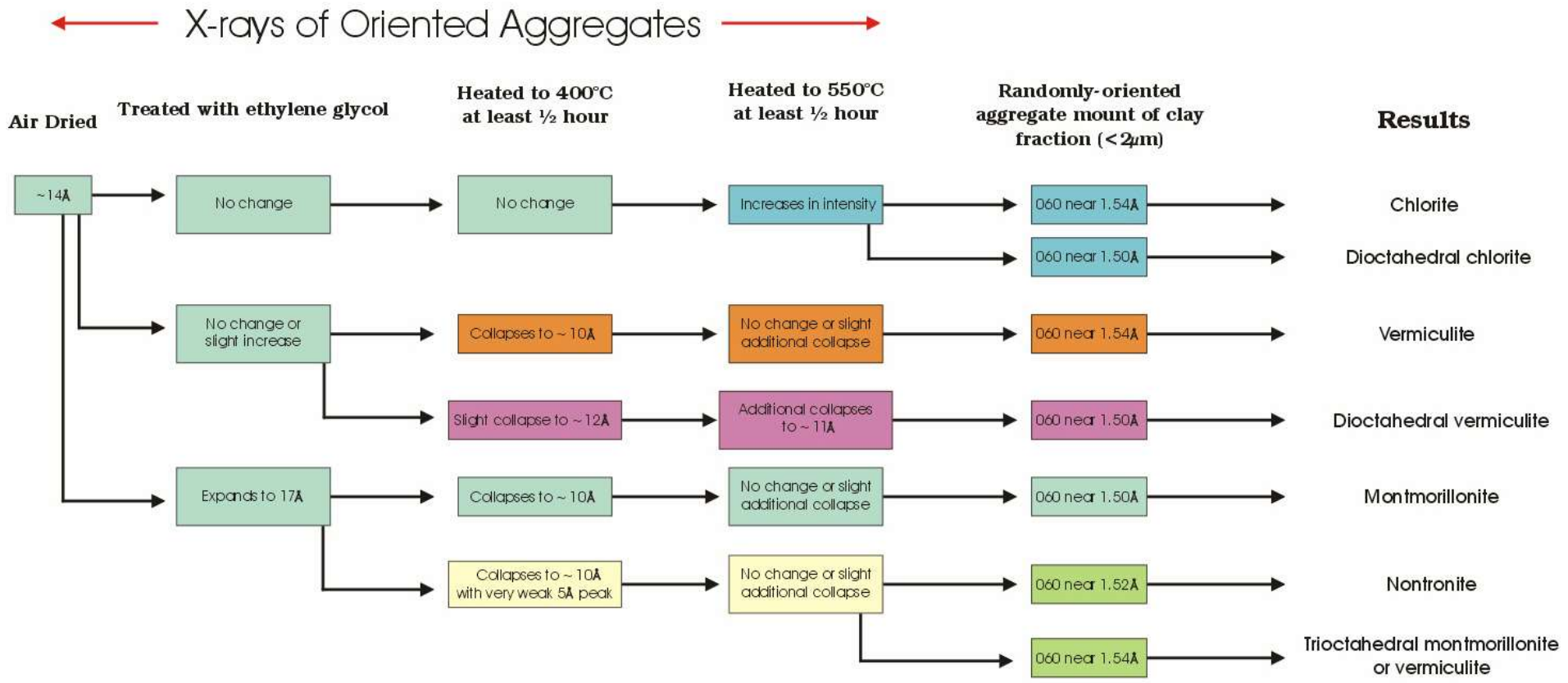
X-rays of Oriented Aggregates
Air Dried
Treated with ethylene glycol
Heated to 400°C at least ½ hour
Heated to 550°C at least ½ hour
Randomly-oriented aggregate mount of clay fraction (<2μm)
Results
~14Å
No change
No change
Increases in intensity
060 near 1.54Å
Chlorite
060 near 1.50Å
Dioctahedral chlorite
No change or slight increase
Collapses to ~10Å
No change or slight additional collapse
060 near 1.54Å
Vermiculite
Slight collapse to ~12Å
Additional collapses to ~11Å
060 near 1.50Å
Dioctahedral vermiculite
Expands to 17Å
Collapses to ~10Å
No change or slight additional collapse
060 near 1.50Å
Montmorillonite
Collapses to ~10Å with very weak 5Å peak
No change or slight additional collapse
060 near 1.52Å
Nontronite
060 near 1.54Å
Trioctahedral montmorillonite or vermiculite

Argilominerais > 14 Å
Interestratificados

>10-14 Å - Interestratificados

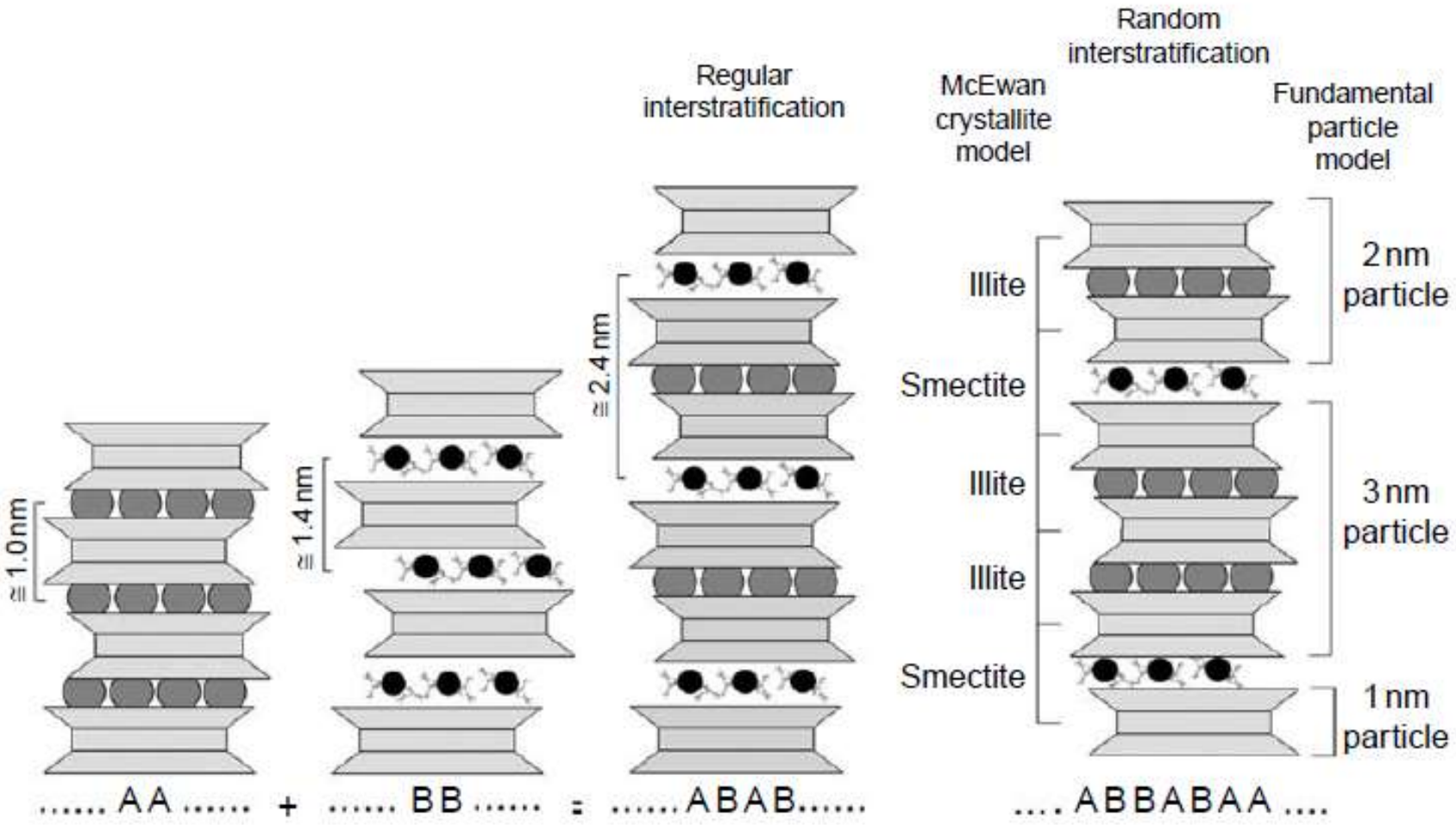

Regular and random interstratified clay minerals. A and B are layers with different periodicity along the *c* direction. The 'McEwan crystallite model' and the 'Fundamental particle model' are also indicated.

TABLE 2.1 Regularly Interstratified Phyllosilicates

Interstratified mineral name	Component layers	Octahedral character
Brinrobertsite	2:1 Pyrophyllite–2:1 smectite	Dioctahedral–dioctahedral
Aliettite	2:1 Talc–2:1 smectite	Trioctahedral–trioctahedral
Kulkeite	2:1 Talc–2:1 chlorite	Trioctahedral–trioctahedral
Rectorite	2:1 Mica–2:1 smectite	Dioctahedral–dioctahedral
Hydrobiotite	2:1 Mica–2:1 vermiculite	Trioctahedral–trioctahedral
Low-charge corrensite	2:1 Chlorite–2:1 smectite	Trioctahedral–trioctahedral
High-charge corrensite	2:1 Chlorite–2:1 vermiculite	Trioctahedral–trioctahedral
Tosudite	2:1 Chlorite–2:1 smectite	Dioctahedral on average
Dozyite	1:1 Serpentine–2:1 chlorite	Trioctahedral–trioctahedral

From Guggenheim et al. (2006)

Bergaya, F.; Lagaly, G. (Eds.) – Handbook of Clay Science. 2ª Ed. Elsevier. Amsterdam. 2013. cap. 2.

Camadas Mistas

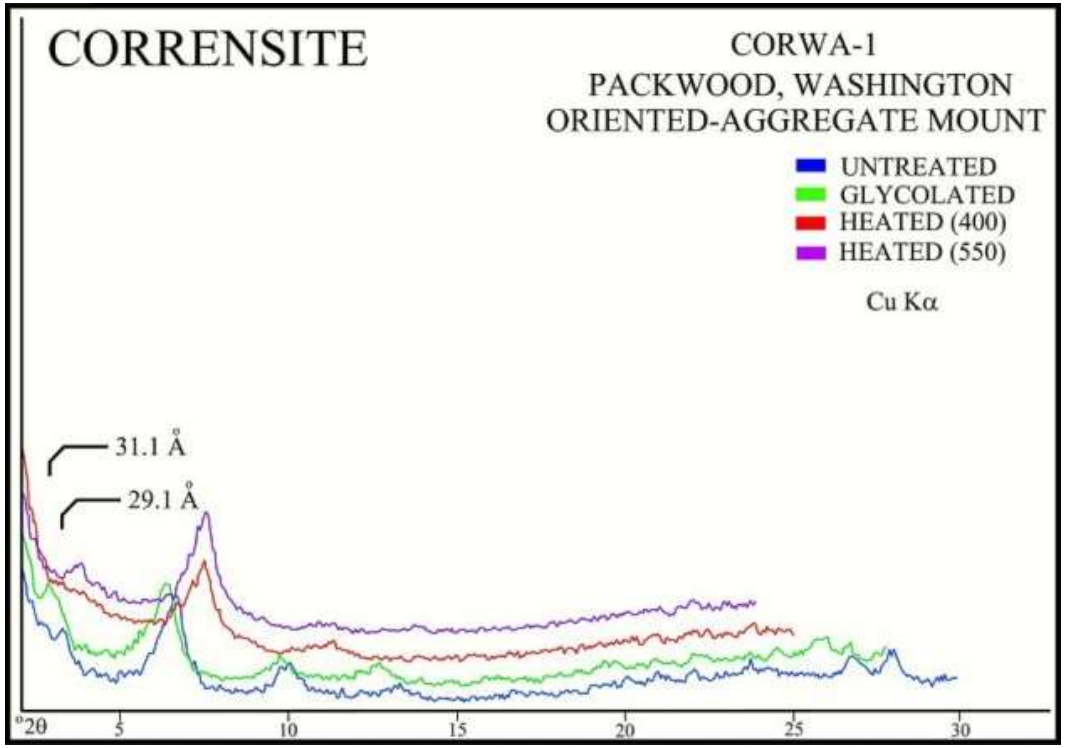

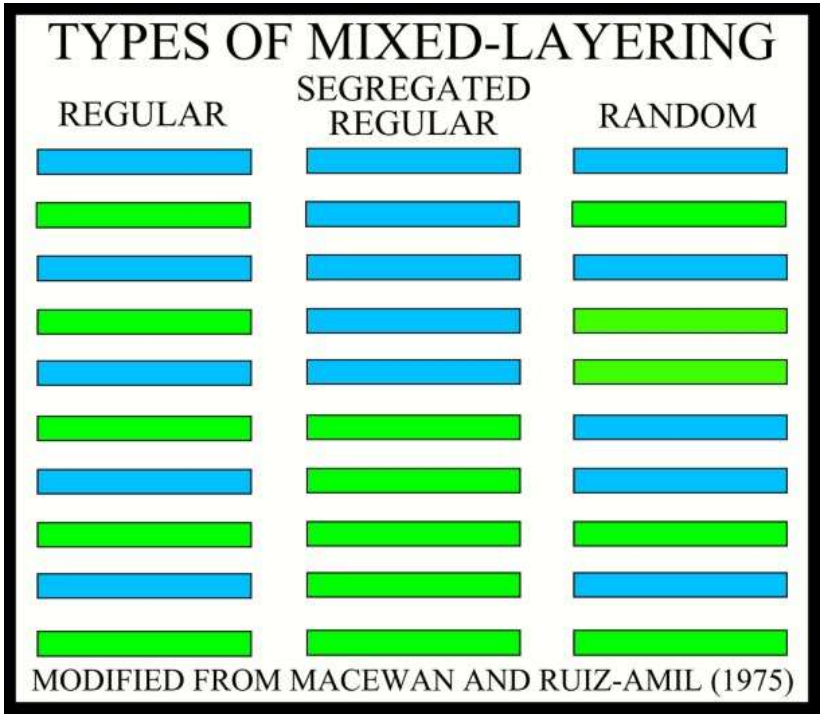

Fonte: http://pubs.usgs.gov/of/2001/of01-041/index.htm

X-rays of Oriented Aggregates

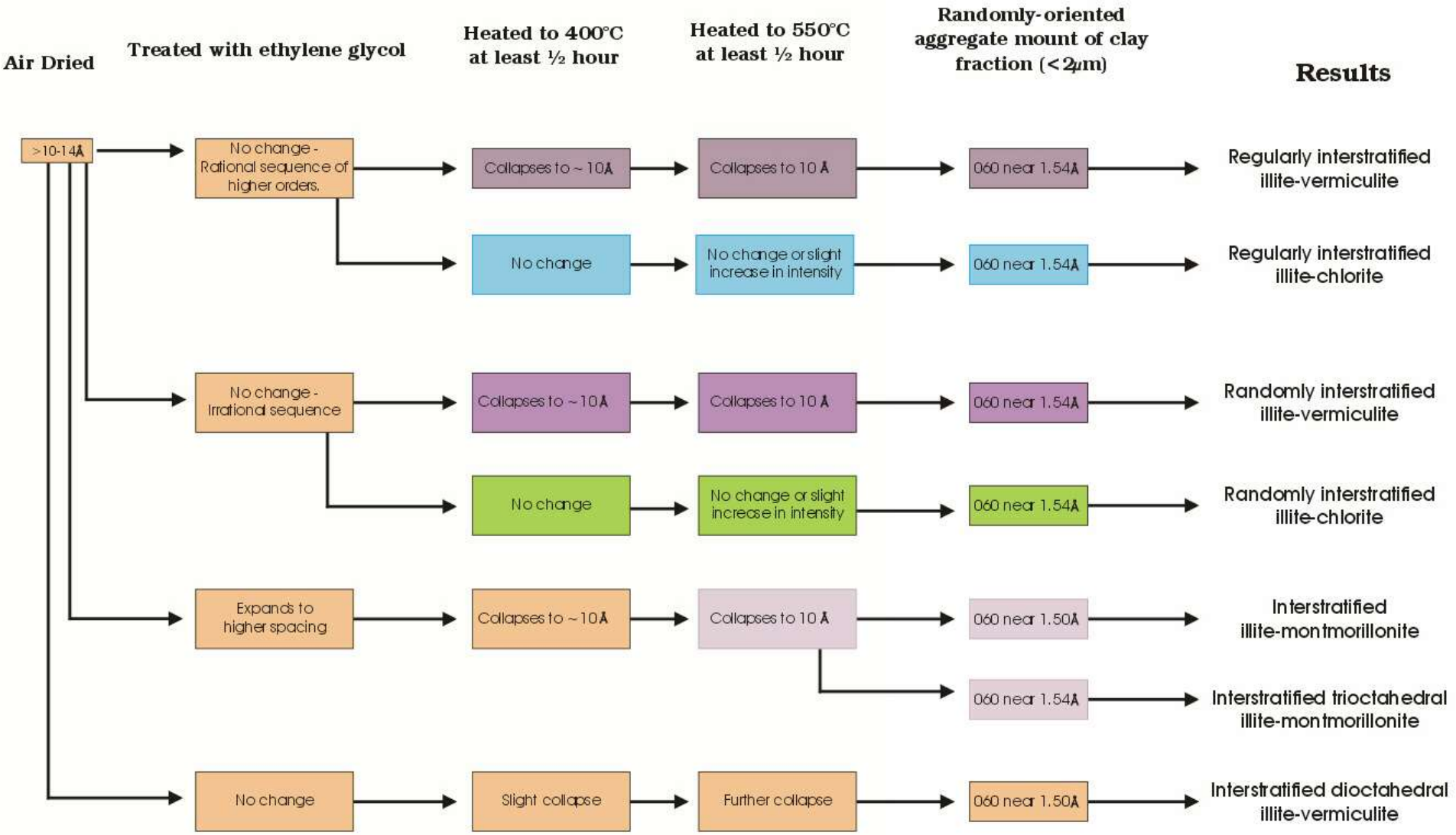

~29 Å com interestratificação

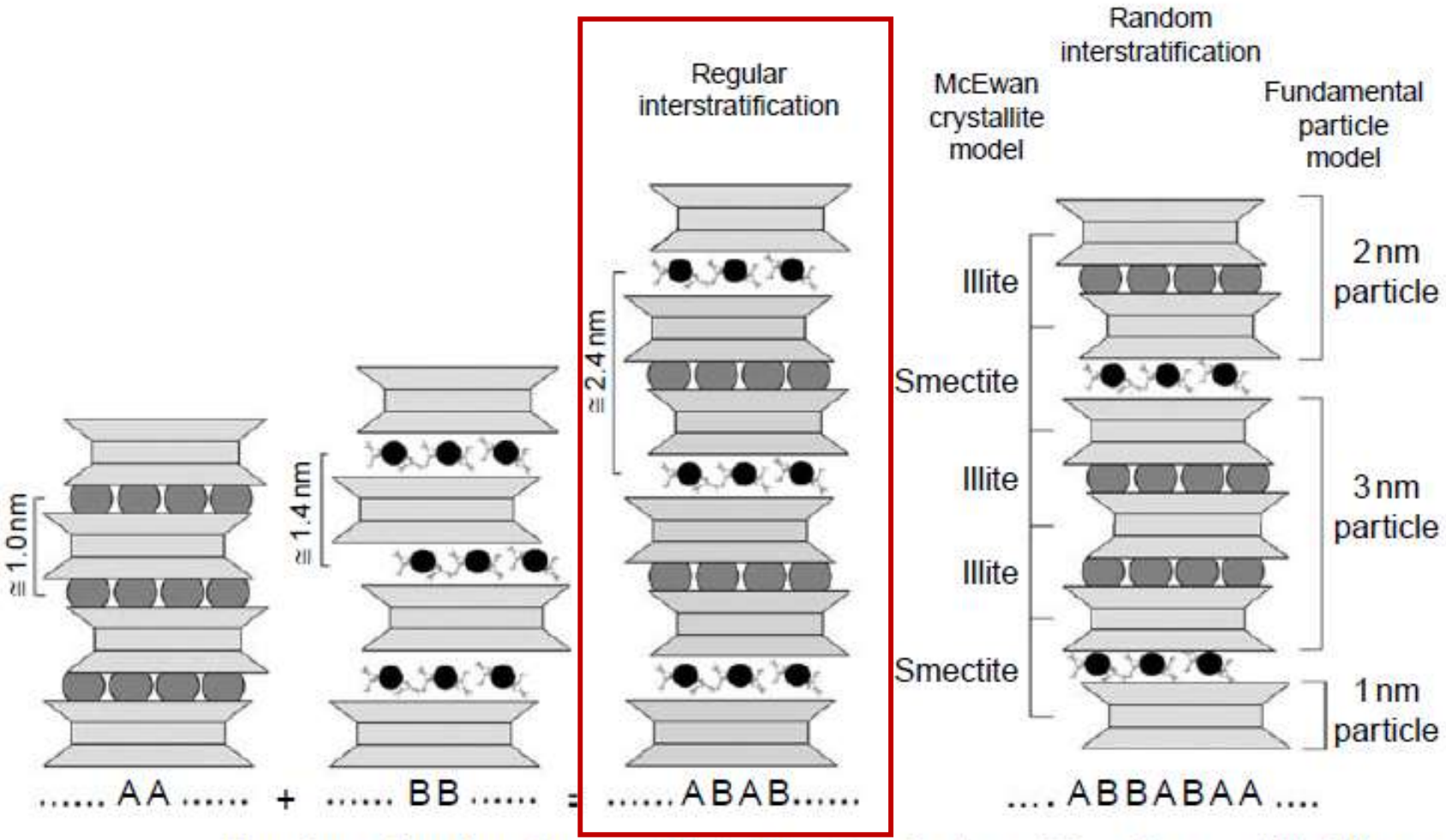

Regular and random interstratified clay minerals. A and B are layers with different periodicity along the *c* direction. The 'McEwan crystallite model' and the 'Fundamental particle model' are also indicated.

~29 Å com interestratificação

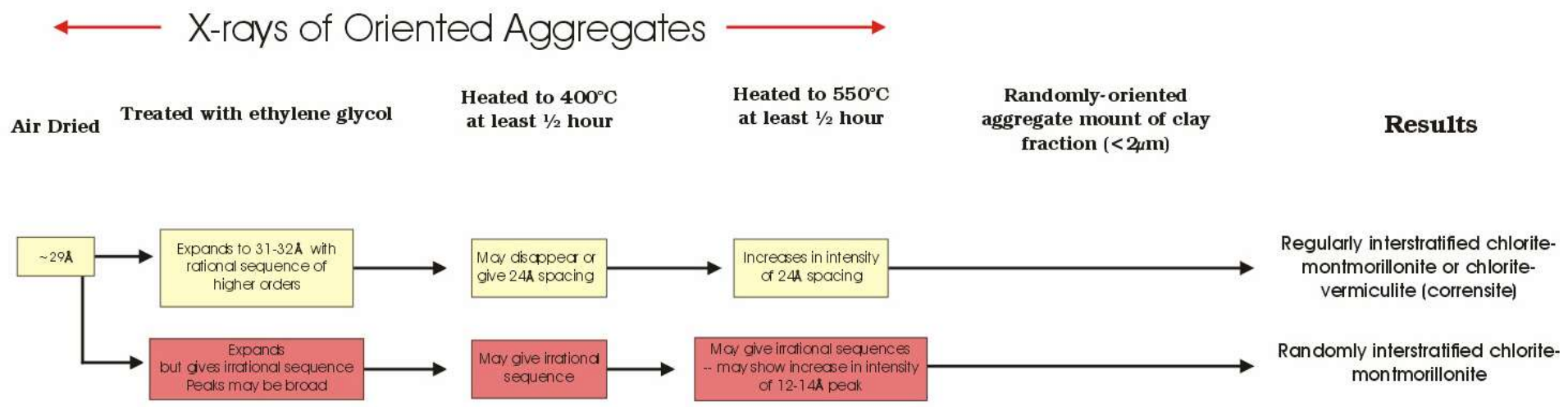

...é super comum aconteceram misturas, interestratificações...

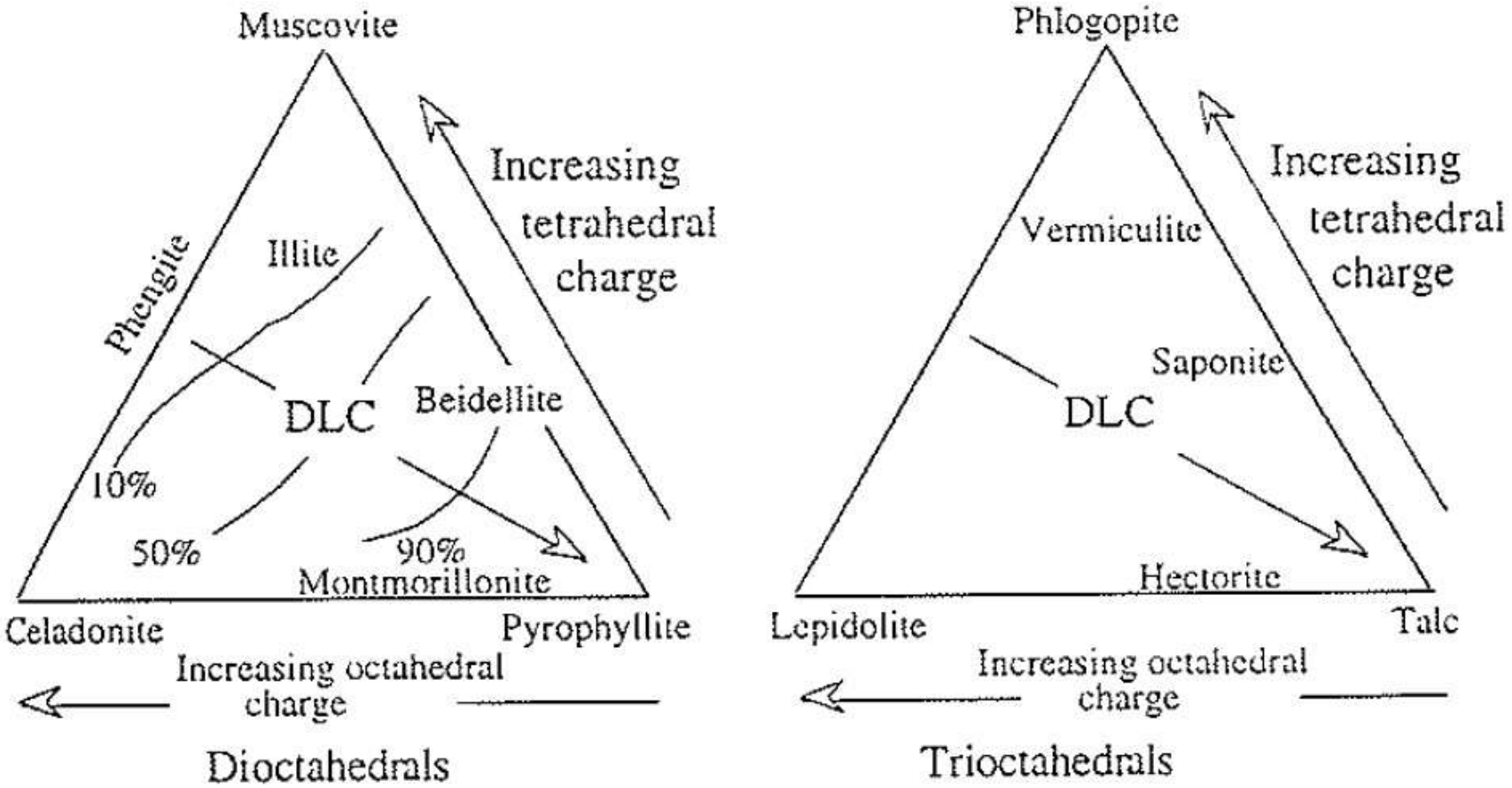

Fig. 5.13. Generalized chemical relations for the dioctahedral and trioctahedral clay minerals in relation to their macroscopic counterparts. 10, 50, and 90% label lines of equal expandable layer content in illite/smectite. DLC = decreasing layer charge.

...o que se encontra normalmente...

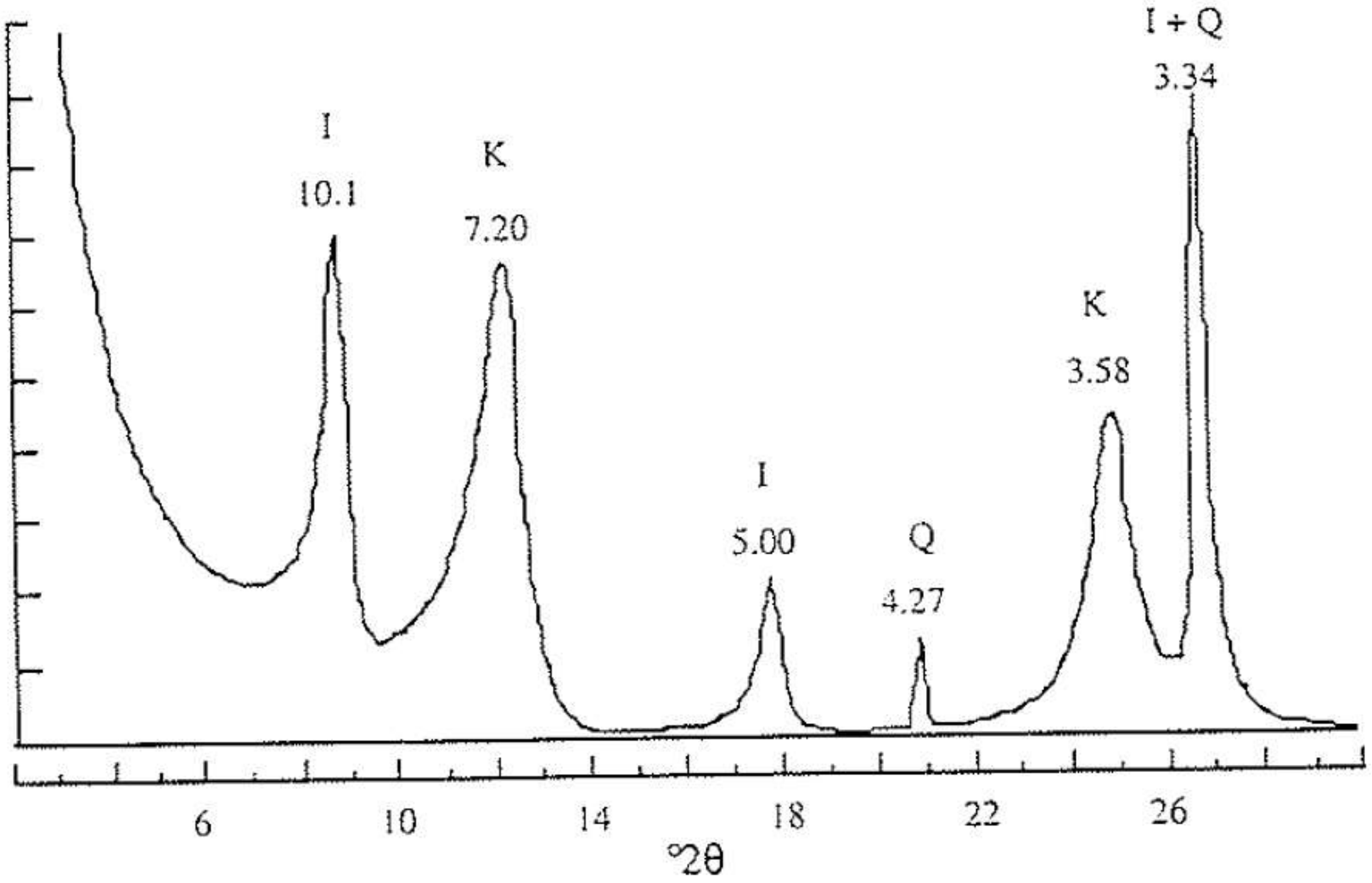

Fig. 7.2. A mixture of illite, kaolinite, and quartz.

Argilominerais 10-12Å
Grupo das "Hormitas"

~10 - 12 Å – "Hormitas"

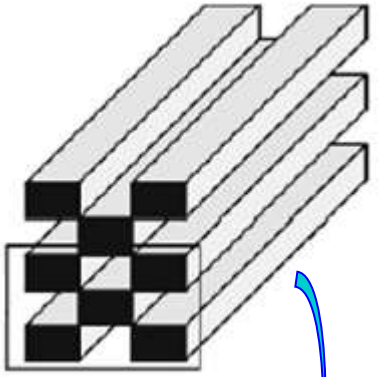

Paligorsquita

Sepiolita

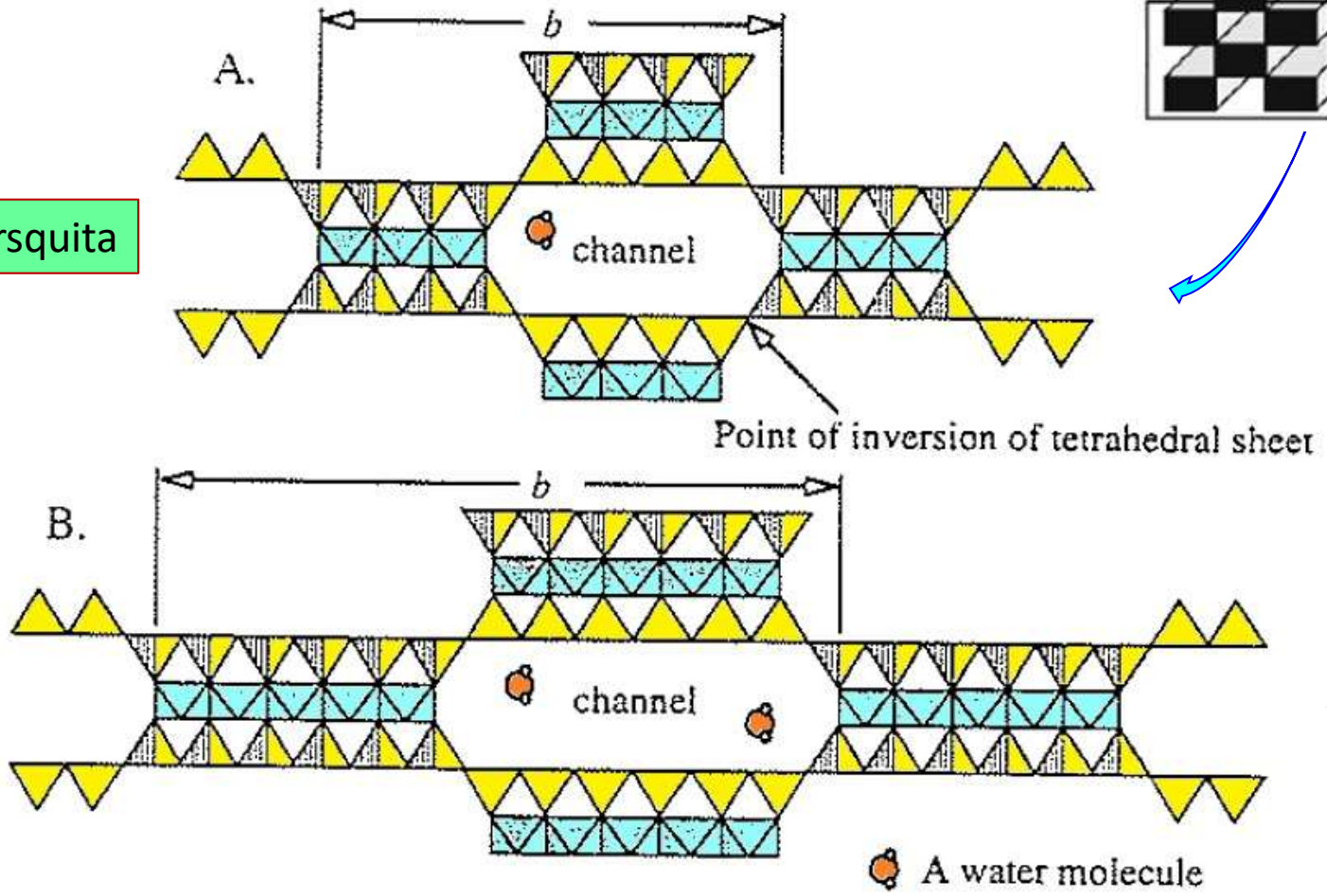

Fig. 5.12. Schematic structure diagrams: A. Palygorskite with *b* approximately 18 Å: B. Sepiolite with *b* approximately 27 Å; Note the tetrahedral sheets maintain continuity through the inversion point, whereas the octahedral sheets do not.

Paligorsquita

$(Mg,Al)_4(Si,Al)_8O_{20}(OH)_2.8H_2O$

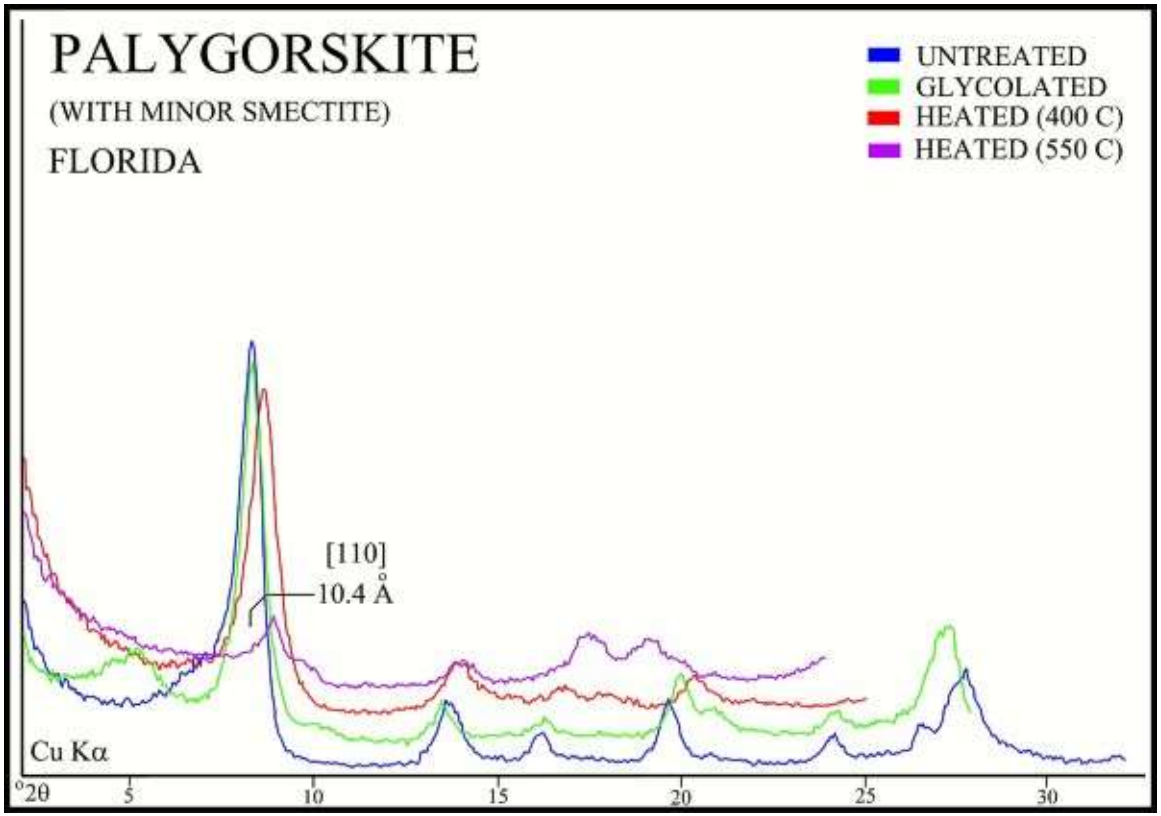

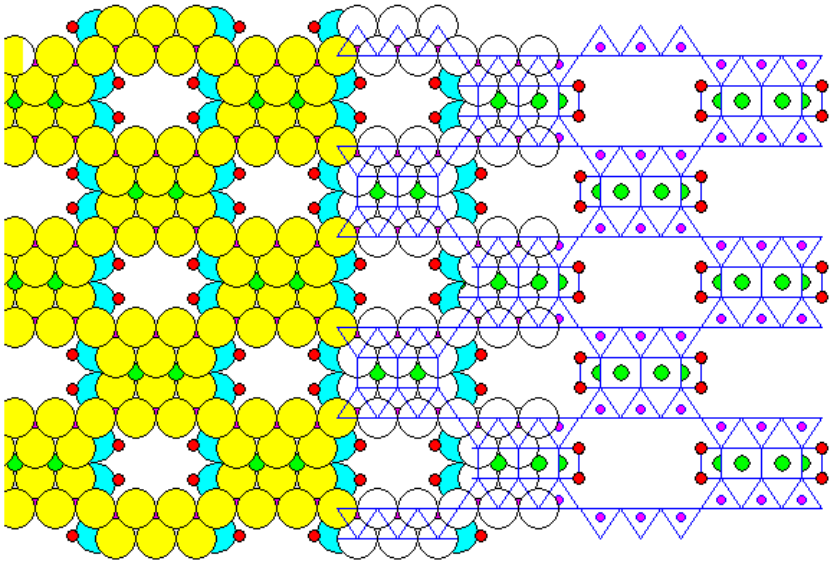

Espaçamento d_{110} = 10 Å

Sepiolita

$Mg_4Si_6O_{15}(OH)_2.6H_2O$

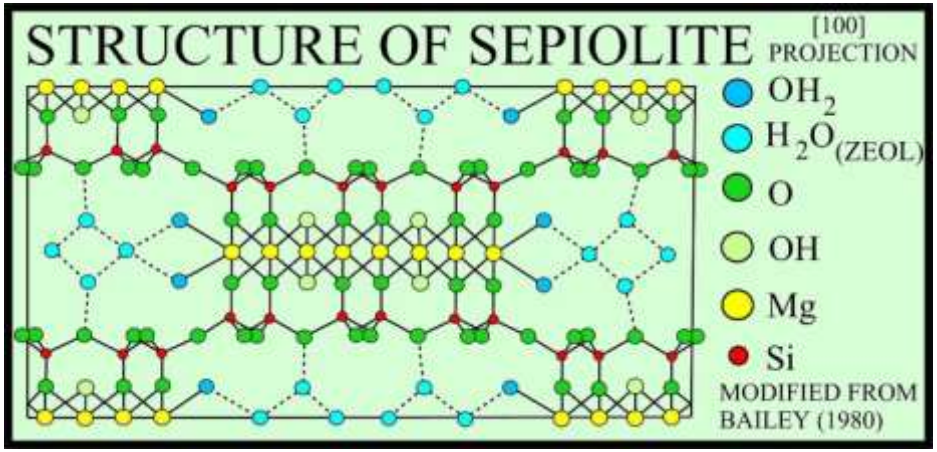

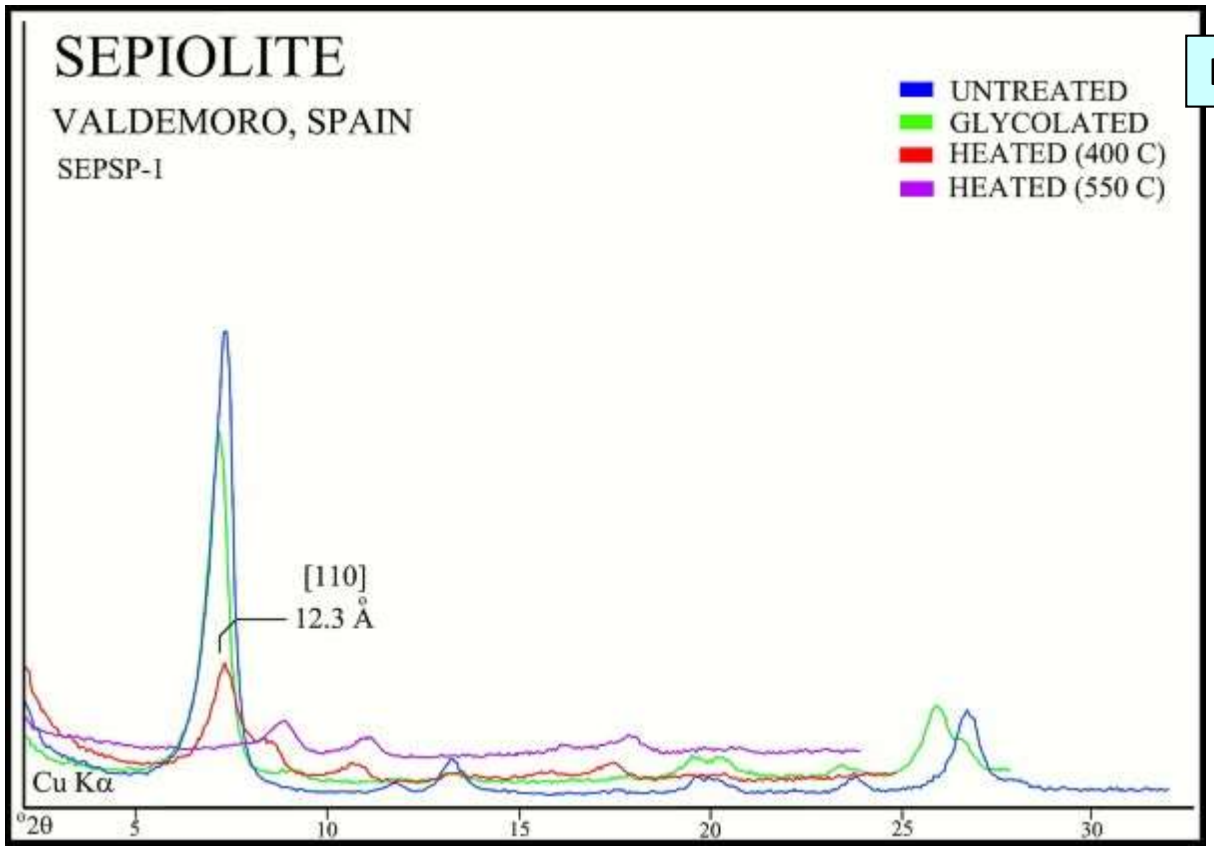

Espaçamento d_{110} = 12 Å

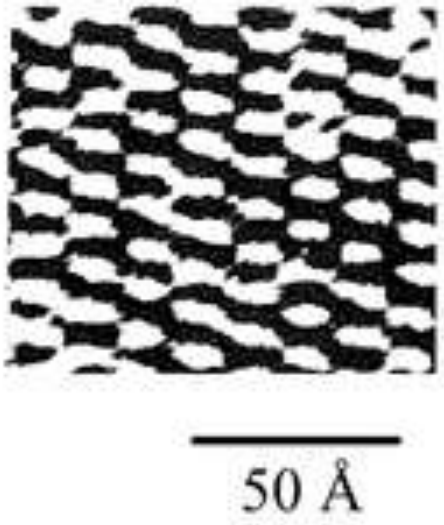

~10 - 12 Å – "Hormitas"

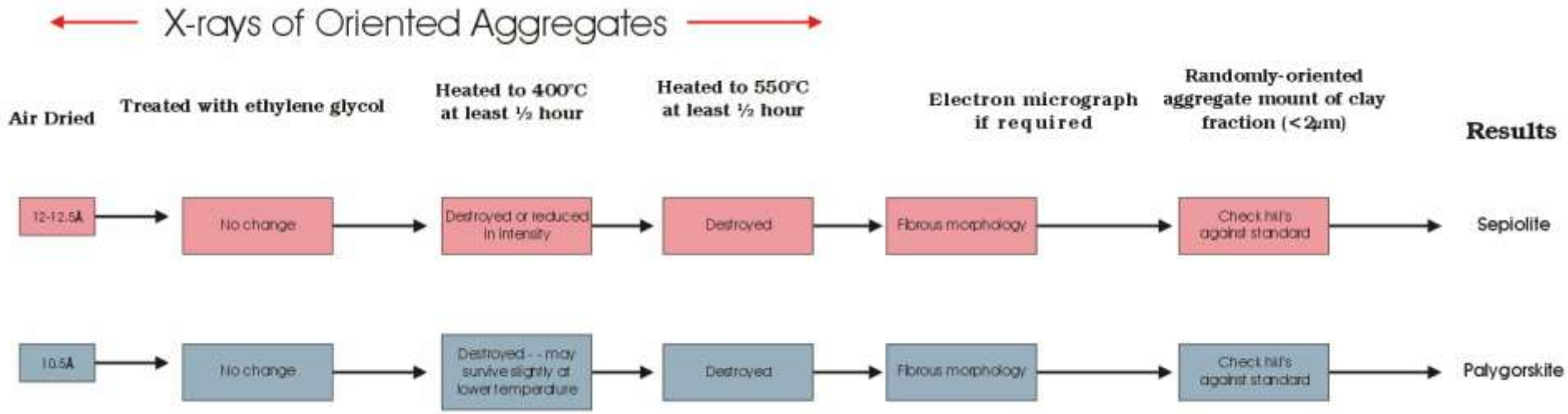

Aspectos Práticos
Preparo de Amostras

Os slides foram retirados da apresentação intitulada “Clay mineral XRD sample preparation and interpretation”, de Connie Constan, da Univesidade do Novo México, obtida por meio do site abaixo (consultado em agosto de 2014):

http://epswww.unm.edu/media/pdf/Clay-Sample-Prep-and-Interp-2012.pdf

Chemical Pretreatments

- Removal of carbonates
  - Acetic acid
- Removal of organics
  - Hydrogen peroxide
- Removal of sulfates
- Removal of iron oxides
- Cation saturation

These acids can cause burns. Wear goggles, plastic gloves, and an apron while working with these chemicals.

USGS Open-File Report 01-041

Particle Size Separation

- Methods
  - Decantation
  - Centrifugation
- Settling times
  - Stoke's Law
- Dispersant/deflocculant
  - sodium hexametaphosphate

USGS Open-File Report 01-041

USGS Open-File Report 01-041

Oriented Methods

- Why?

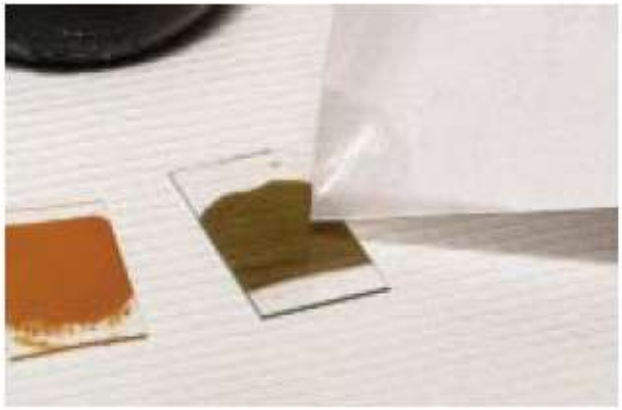

USGS Open-File Report 01-041

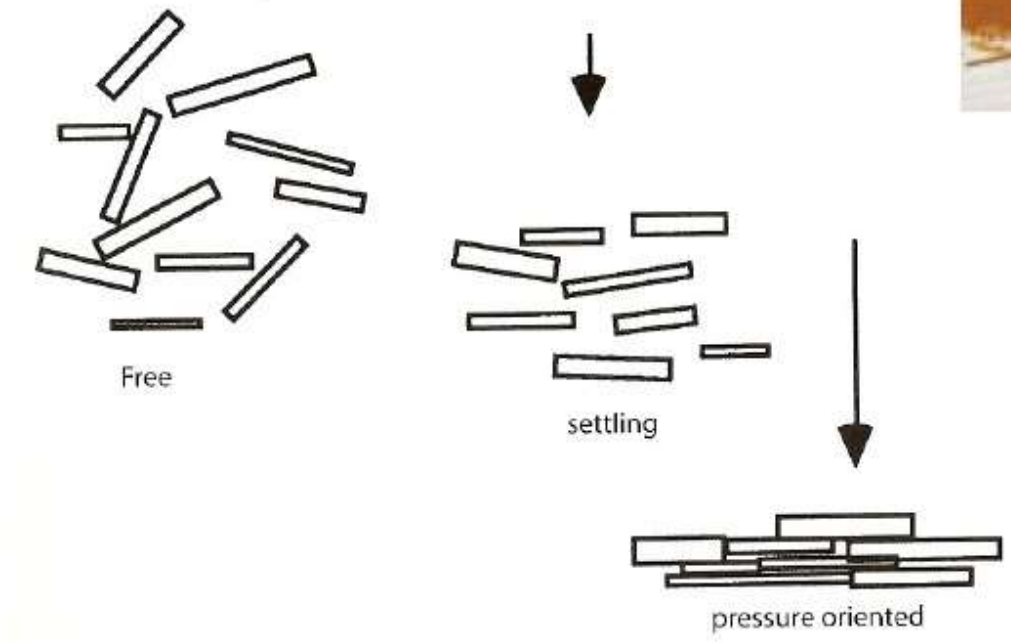

Velde and Druc 1999: Figure 3.8

Glass Slide

- Advantage
  - Quick
- Disadvantage
  - All
- Level of skill needed
  - Low
- Application
  - Qualitative analysis

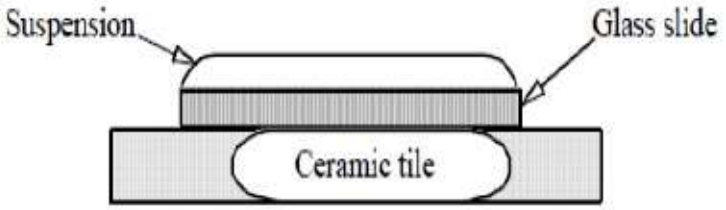

Moore and Reynolds Figure 6.1

USGS Open-File Report 01-041

Smear Mount

- Advantage
  - Quick, moderately homogenous
- Disadvantage
  - Most
- Level of skill needed
  - Moderate
- Application
  - Clay and nonclay minerals

USGS Open-File Report 01-041

USGS Open-File Report 01-041

Filter Transfer

- Advantage
  - Homogenous aggregate
- Disadvantage
  - Fair intensities
- Level of skill needed
  - Moderate
- Application
  - Quantitative representation

Images from USGS Open-File Report 01-041

Porous Plate

- Advantage
  - Best intensities
- Disadvantage
  - Inhomogeneous aggregate
- Level of skill needed
  - High
- Application
  - Crystal structure studies

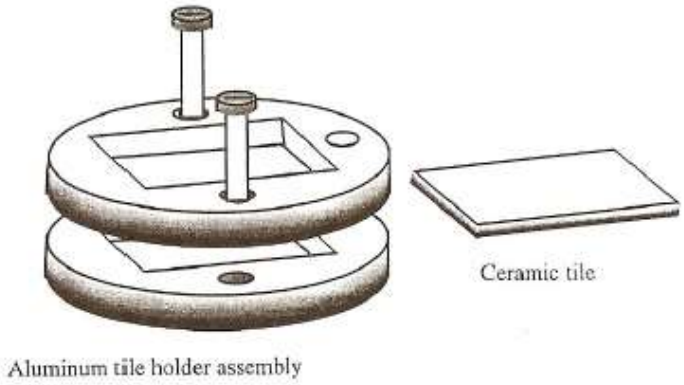

Moore and Reynolds Figure 6.4

Porous Ceramics
www.sentrotech.com

Ethylene Glycol Solvation

Images from USGS Open-File Report 01-041

Random Mount

- Why?

USGS Open-File Report 01-041

Moore and Reynolds Figure 6.5

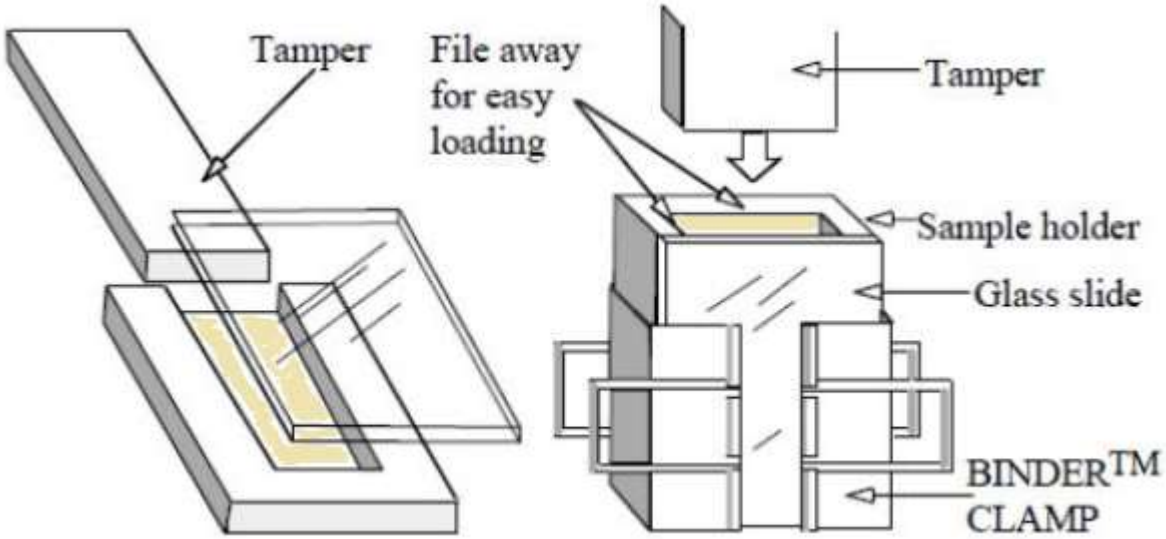

Uma proposta para obter amostras desorientadas...

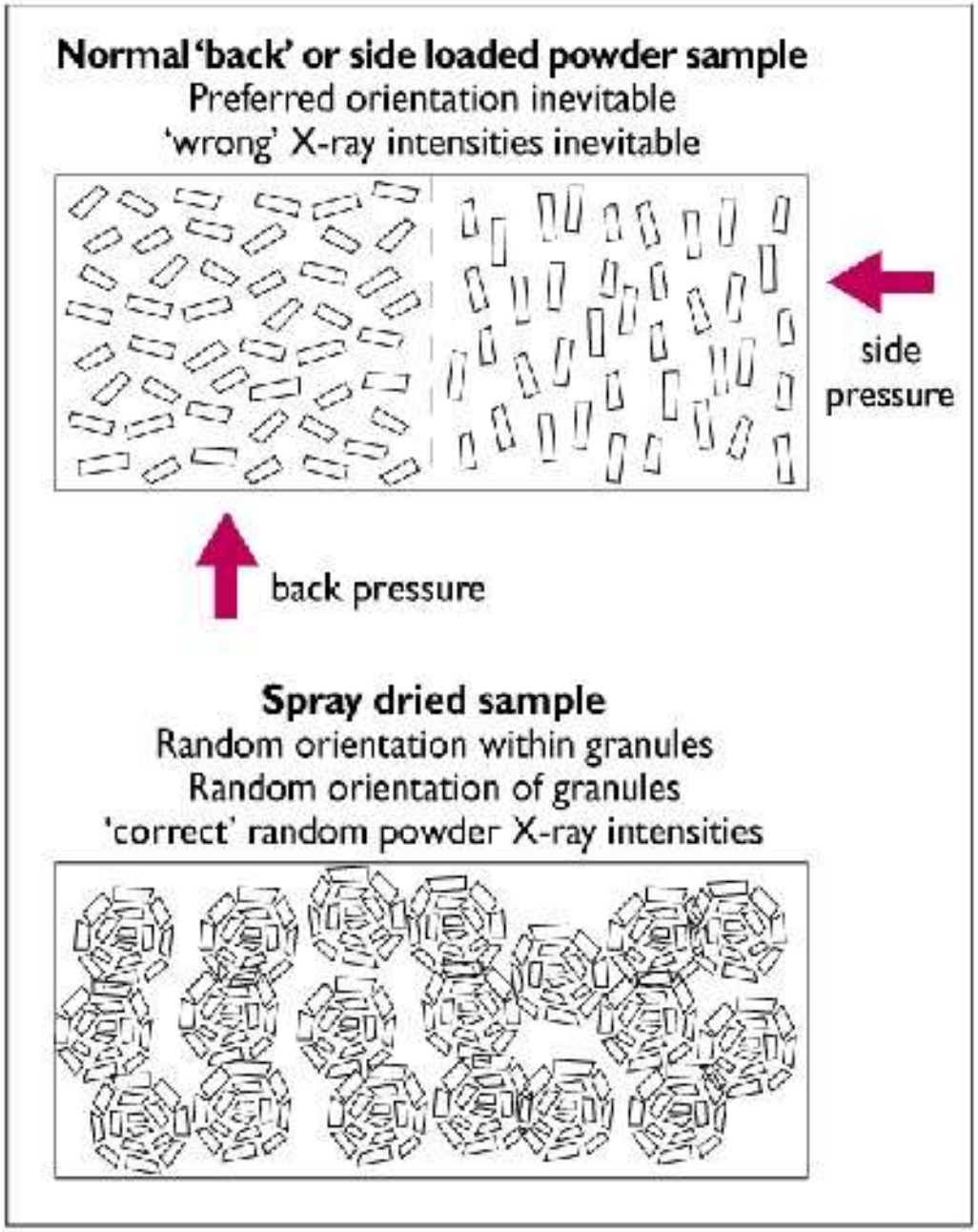

The James Hutton Institute – Escócia. Endereço: *http://www.claysandminerals.com/spraydrykit*

Examples of spray dried materials

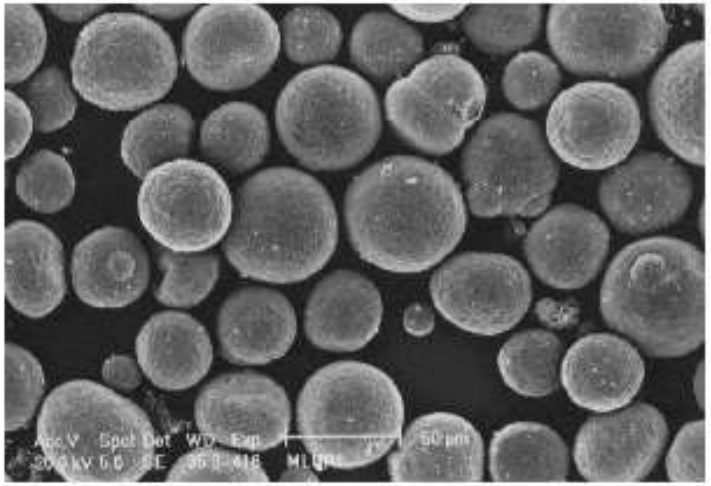

Spray dried kaolinite.

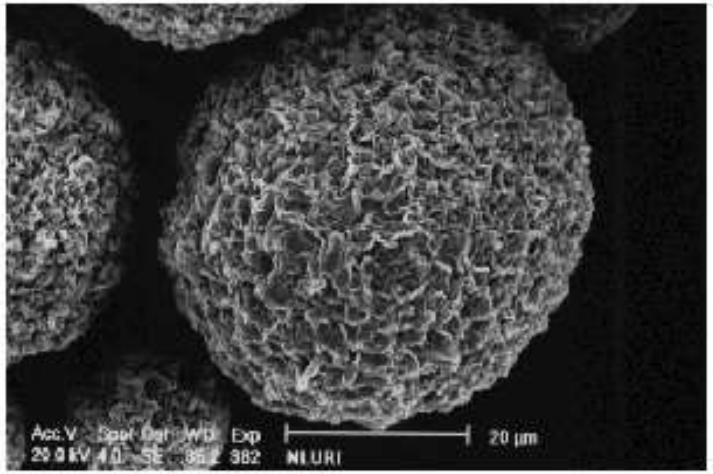

Spray dried smectite.

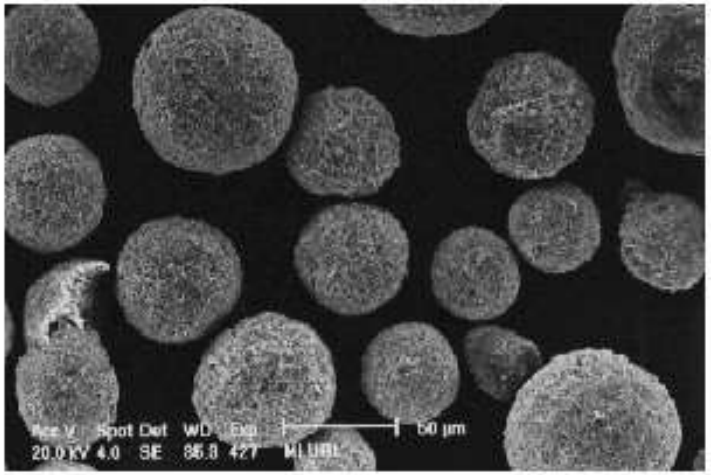

Spray dried muscovite.

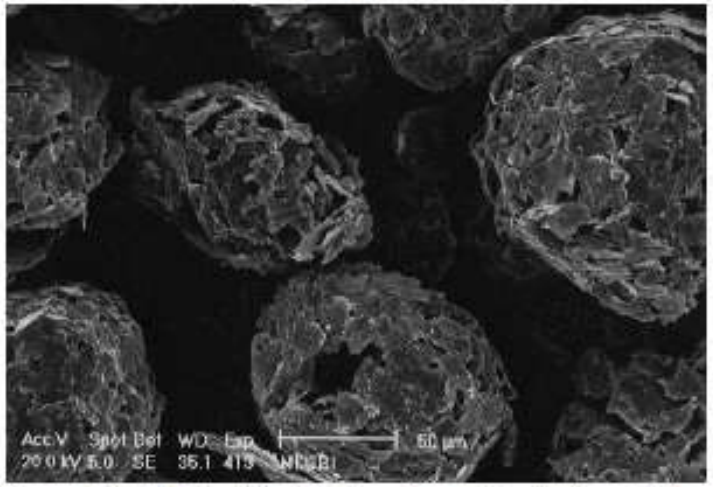

Spray dried talc, illustrating the effect of particles which are slightly too large.

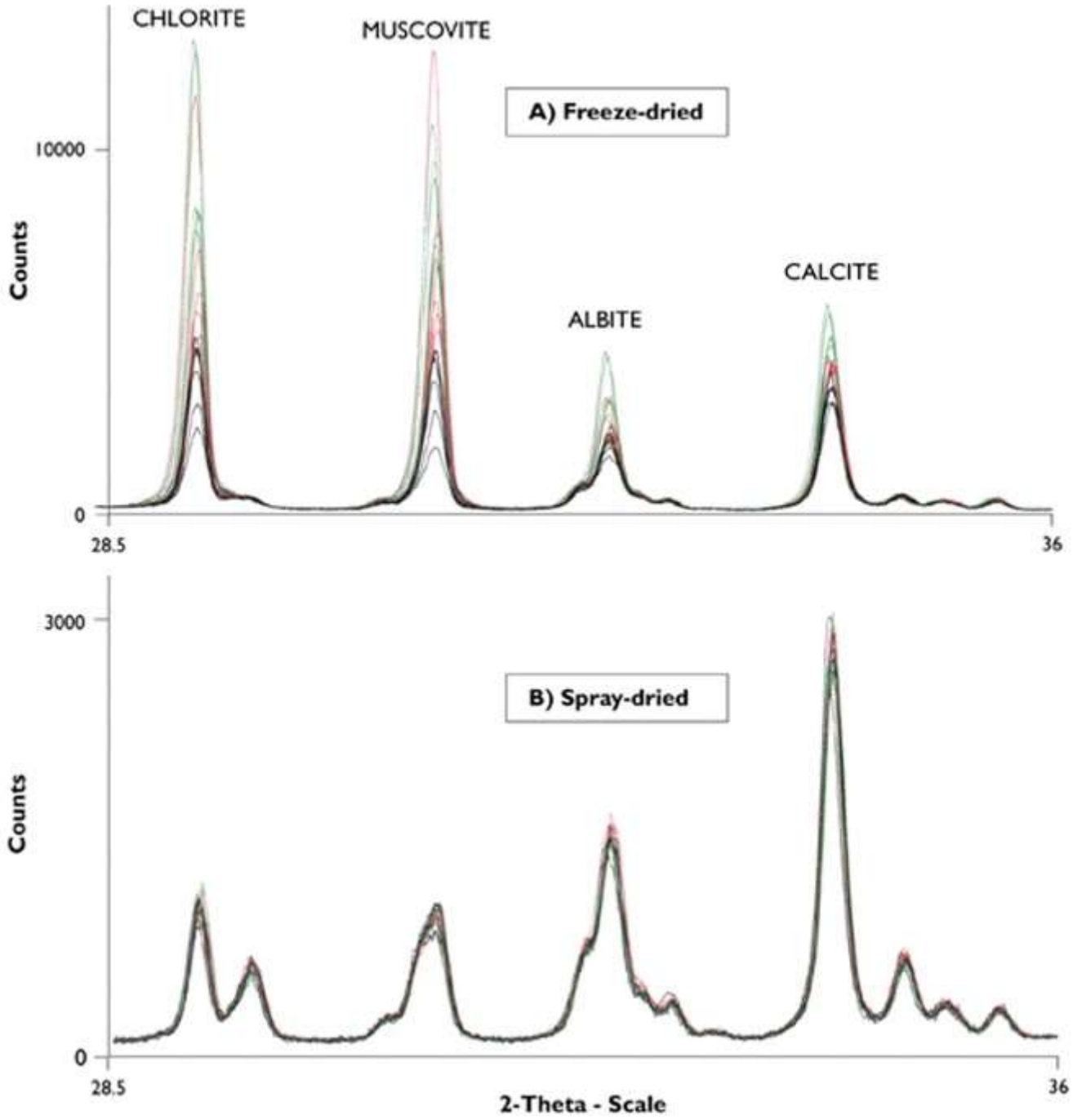
CHLORITE
MUSCOVITE
A) Freeze-dried
10000
Counts
0
28.5
36
CALCITE
ALBITE
3000
B) Spray-dried
Counts
0
28.5
36
2-Theta - Scale

Referências

- Moore, D.M.; Reynolds, Jr., R.C. – X-ray Diffraction and the Identification and Analysis of Clay Minerals. 2nd edition, Oxford University Press, New York. 1997.
- Brindley, G.W.; Brown, G. (eds) - Crystal Structures of Clay Minerals and their X-Ray Identification. Mineralogical Society. Londres. 1st reprinting. 1984.
- USGS - A Laboratory Manual for X-Ray Powder Diffraction. U. S. Geological Survey Open-File Report 01-041. Site web: http://pubs.usgs.gov/of/2001/of01-041/htmldocs/methods.htm
- Bergaya, F.; Lagaly, G. (Eds.) – Handbook of Clay Science. 2ª Ed. Elsevier. Amsterdam. Developments in Clay Science vol.5B. Cap. 2.2, pgs.25-49. 2013.
- Velde, B.; Meunier, A. – The Origin of Clay Minerals in Soils and Whethered Rocks. Springer-Verlag. Berlim. 2008. Cap. 1.
- Souza Santos, P. – Ciência e Tecnologia de Argilas. 2ª Ed. Edgard Blucher. São Paulo. 1989. Cap. 12.
- Gomes, C.S.F. – Argilas, o Que São e Para Que Servem. Fundação Calouste Gulbenkian. Lisboa. 1988. Cap. XIII.